Hannah Greiner, BSc

Development of a continuous glucose monitoring system for humans combining intravenous microdialysis, glucose sensors and ionic reference technique

MASTER THESIS

Supervisors:
Dipl.-Ing. Dr.techn. Lukas Schaupp
(Medical University of Graz)

Dipl.-Ing. Dr.techn. Roland Schaller-Ammann
(JOANNEUM RESEARCH Forschungsgesellschaft mbH)

Evaluator:
Assoc.Prof. Mag.rer.nat. Dr.rer.nat. Juliane Gertrude Bogner-Strauß

Institute for Genomics and Bioinformatics
Graz University of Technology
Petersgasse 14, A - 8010 Graz
Head: Univ.-Prof. Dipl.-Ing. Dr.techn. Rudolf Stollberger

Graz, March 2013

STATUTORY DECLARATION

I declare that I have authored this thesis independently, that I have not used other than the declared sources / resources and that I have explicitly marked all material which has been quoted either literally or by content from the used sources.

. . . . . .

Place, date

. . . . . .

Signature

EIDESSTATTLICHE ERKLÄRUNG

Ich erkläre an Eides statt, dass ich die vorliegende Arbeit selbstständig verfasst, andere als die angegebenen Quellen/Hilfsmittel nicht benutzt, und die den benutzten Quellen wörtlich und inhaltlich entnommenen Stellen als solche kenntlich gemacht habe.

. . . . . .

Ort, Datum

. . . . . .

Unterschrift

ABSTRACT

A new system, comprising intravenous microdialysis and glucose sensors, enables continuous blood glucose monitoring and provides the basis for an automated glucose clamp device. The aim of this thesis was to combine intravenous microdialysis and glucose sensors to investigate the system's overall monitoring performance during a clinical trial.

5 microdialysis probes (PME011, Probe Scientific, UK) were investigated in 5 subjects (31.2 ± 4.8 years, BMI: 24.6 ± 2.9 kg/m²). The subjects were clamped to different glucose levels (90/180/130/90mg/dl) for 24 hours. The dialysate was analysed online with an electrochemical glucose sensor (AC1.GOD, BVT, CZ) and sampled for additional offline measurement regarding glucose and ions. Blood glucose concentrations were calculated from the relative recovery using the ionic reference technique (IRT) and various calibration procedures. Sensor data suffered from strong noise artefacts and needed to be filtered before evaluation. The mean coefficients of correlation for IRT-corrected, 1 point-calibrated and filtered data were (mean value ± standard deviation) $r_{dialysate\text{-}sensor} = 0.94 \pm 0.02$, $r_{blood\text{-}dialysate} = 0.91 \pm 0.13$ and $r_{blood\text{-}sensor} = 0.83 \pm 0.20$. The overall absolute value of the system error, between blood and sensor, was 13.38 ± 7.94% and the mean absolute relative difference (MARD) was 17.34 ± 7.25%. A regression analysis further showed that a calibration interval of 30 minutes is needed to fulfil the acceptance criteria according to ISO 15197:2003. Intravenous microdialysis in combination with glucose sensors has the potential to be an attractive alternative to frequent manual blood sampling if the measurement range of the glucose sensor comprises physiological blood glucose concentrations to allow relative recoveries up to 100%.

Keywords: continuous glucose monitoring system, intravenous microdialysis, glucose sensors, ionic reference technique, automated clamp device

ZUSAMMENFASSUNG

Ein neues System, das intravaskuläre Mikrodialysetechnik und Sensortechnik kombiniert, soll die kontinuierliche Blutglukosemessung ermöglichen und die Grundlage für ein automatisiertes Glukose-Clamp-Gerät darstellen. Das Ziel dieser Arbeit war es, diese beiden Techniken miteinander zu verbinden und die Gesamtleistung des Systems während einer klinischen Studie zu untersuchen. 5 Mikrodialysesonden (PME011, Probe Scientific, UK) wurden in 5 Probanden (31,2 ± 4,8 Jahre, BMI: 24,6 ± 2,9 kg/m²) untersucht. Dabei wurde der Glukosespiegel der Probanden über einen Zeitraum von 24 Stunden auf verschiedenen Glukoseniveaus (90/180/130/90mg/dl) konstant gehalten. Das Dialysat wurde mit einem elektrochemischen Glukosesensor (AC1.GOD, BVT, CZ) online analysiert und anschließend gesammelt, um zusätzliche offline Messungen von Glukose und Ionen vorzunehmen. Die tatsächlichen Blutglukosekonzentrationen wurden mittels Wiederfindungsrate und Ionen-Referenztechnik (IRT) unter Anwendung verschiedener Kalibrierungen berechnet. Die Sensordaten zeigten starke Rauschartefakte und mussten deshalb vor der Auswertung gefiltert werden. Die mittleren Korrelationskoeffizienten für IRT-korrigierte, 1-Punkt kalibrierte und gefilterte Datensätze waren (Mittelwert ± Standardabweichung) $r_{Blut\text{-}Dialysat}$ = 0,94 ± 0,02, $r_{Dialysat\text{-}Sensor}$ = 0,91 ± 0,13 und $r_{Blut\text{-}Sensor}$ = 0,83 ± 0,20. Der Absolutbetrag des Gesamtsystemfehlers zwischen Blut und Sensorstrom war 13,38 ± 7,94% und die mittlere absolute relative Differenz (MARD) war 17,34 ± 7,25%. Eine Regressionsanalyse zeigte ferner, dass ein Kalibrierintervall von 30 Minuten benötigt wird, um die Kriterien nach ISO 15197:2003 zu erfüllen.

Intravenöse Mikrodialyse in Kombination mit Glukose-Sensoren hat das Potenzial, eine attraktive Alternative für die üblichen manuellen Blutabnahme zu bieten, falls der Messbereich des Glukosesensors den gesamten physiologischen Blutglukosebereich umfasst, um Wiederfindungsraten bis zu 100% zu ermöglichen.

Schlüsselwörter: kontinuierliches Glukose Messsystem, intravenöse Mikrodialyse, Glukose Sensoren, Ionen Referenztechnik, automatisiertes Clamp-Gerät

TABLE OF CONTENTS

LIST OF ABBREVIATIONS

AGES	Austrian Agency of Health and Food Safety
CCU	Coronary Care Unit
CGM	Continuous Glucose Monitoring
CRF	Case Report Form
CV	Coefficient of Variation
EGA	Error Grid Analysis
EMA	European Medicines Agency
EU-CLAMP	Euglycemic Clinical Application for Metabolic Profiling
FMEA	Failure Mode and Effect Analysis
FTA	Fault Tree Analysis
GIR	Glucose Infusion Rate
GOD	Glucose Oxidase
ICU	Intensive Care Unit
ISF	Interstitial Fluid
IRT	Ionic Reference Technique
iv	Intravenous
LLOQ	Lower Limit of Quantification
M2ARD	Median Absolute Relative Difference
MARD	Mean Absolute Relative Difference
MD	Microdialysis
ME	Medical Electrical
MV	Mean Value
PC	Protection Class
PE	Protective Earth
PRESS	Predicted Error Sum of Squares
SOP	Standard Operating Procedure
SD	Standard Deviation
WE	Working Electrode
WHO	World Health Organisation

LIST OF FIGURES

LIST OF TABLES

1 INTRODUCTION

1.1 Background

Glucose and Insulin Homeostasis

The monosaccharide glucose is a central molecule of carbohydrate metabolism and the most important energy source in humans. The glucose concentration in the circulating blood is the control parameter concerning the supply of glucose to human cells. This concentration is controlled by hormones where insulin plays a key role as it can decrease the blood glucose concentration.

Insulin itself is a protein that is synthesized in the β-cells of the pancreas. It increases the permeability of cell membranes to glucose and the enzymatic digestion of glucose within the cell.

During fasting condition, insulin is secreted at a low, but continuous rate, which immediately increases with food intake. The secretion maximum lasts for a few minutes and is then adapted based on the carbohydrate intake. As a result, the blood glucose concentration stays within certain tolerance levels. A high blood glucose concentration is called hyperglycemia whereas a low concentration is called hypoglycemia. [1]

Diabetes Mellitus

A dysfunction of the insulin household leads to the chronic, incurable but treatable metabolic disorders Diabetes Mellitus type 1 and 2. Diabetes type 1 is associated with an insufficient insulin secretion and mostly diagnosed in young people. Diabetes type 2 is linked to overshooting insulin secretion and insulin resistance or even insulin shortage causing clinical insulin-dependency. It is mostly associated with an unhealthy lifestyle and diagnosed in elderly people. Nevertheless an increasing number of young people develop diabetes type 2. [2] According to the International Diabetes Federation the number of patients with diabetes will increase from 366 million worldwide in 2011 by around 50% until 2030 [3].

Diabetes Mellitus type 1 and 2 are furthermore associated with more severe health effects, e.g. coronary heart disease, nephropathies or retinopathies which can even lead to blindness. The World Health Organisation (WHO) assumes that deaths caused by diabetes will increase by two thirds from 2008 to 2030. Reasons might be the occurrence of cardiovascular diseases or kidney failure. [4] To improve the health and quality of life of patients with diabetes treatment

of diabetes is obvious. Strict monitoring of blood glucose and an associated insulin therapy can reduce vascular disease and morbidity as well as onset and progression of severe complications during medical treatment [5].

Treatment of diabetes – Diet and insulin substitution therapy

About 80% of all patients with type 2 diabetes can be successfully treated with a balanced diet and exercises and do not need any oral antidiabetic drugs or insulin substitution therapy. Contrarily, patients with type 1 diabetes are dependent on an insulin substitution therapy. Insulin was discovered by Frederick Banting and Charles H. Best in 1922 [6] and Elliot Joslin already stated that patients with diabetes need to measure their urine glucose concentration to inject and adequate amount of insulin in 1922/23. Insulin substitution therapy was advanced and since the 1980s the standard therapy includes blood glucose concentration measurement and injection of different types of insulin. Basal or long-acting insulin is combined with an adjustable dose of normal or short-acting insulin which is injected during meals. This dose is calculated based on the amount of carbohydrate intake and the measured blood glucose concentration. [2]

Development of new types of insulin – Hyperinsulinemic eugylcemic insulin clamp

Various types of insulin and their blood-glucose lowering effects (time-action profiles) have to be characterized before being released to the market. The European Medicines Agency (EMA) recommends the so called “Hyperinsulinemic euglycemic glucose clamps” as gold standard for investigating the pharmacodynamics of new insulins. [7] [8] [9]

During a hyperinsulinemic euglycemic glucose clamp (refer to Figure 1) subjects receive a insulin infusion through a venous catheter to increase the plasma insulin concentration which would cause a drop of the blood glucose concentration. To keep this blood glucose concentration at a constant level (clamp level) a variable dose of glucose, based on repeatedly measured plasma glucose concentrations, is infused using another catheter. This variable dose of glucose, also called glucose infusion rate (GIR), provides information about the subject’s insulin sensitivity. An increased GIR is related to an increased glucose uptake into the tissue and is therefore associated with an increased sensitivity to insulin. [9] [10]

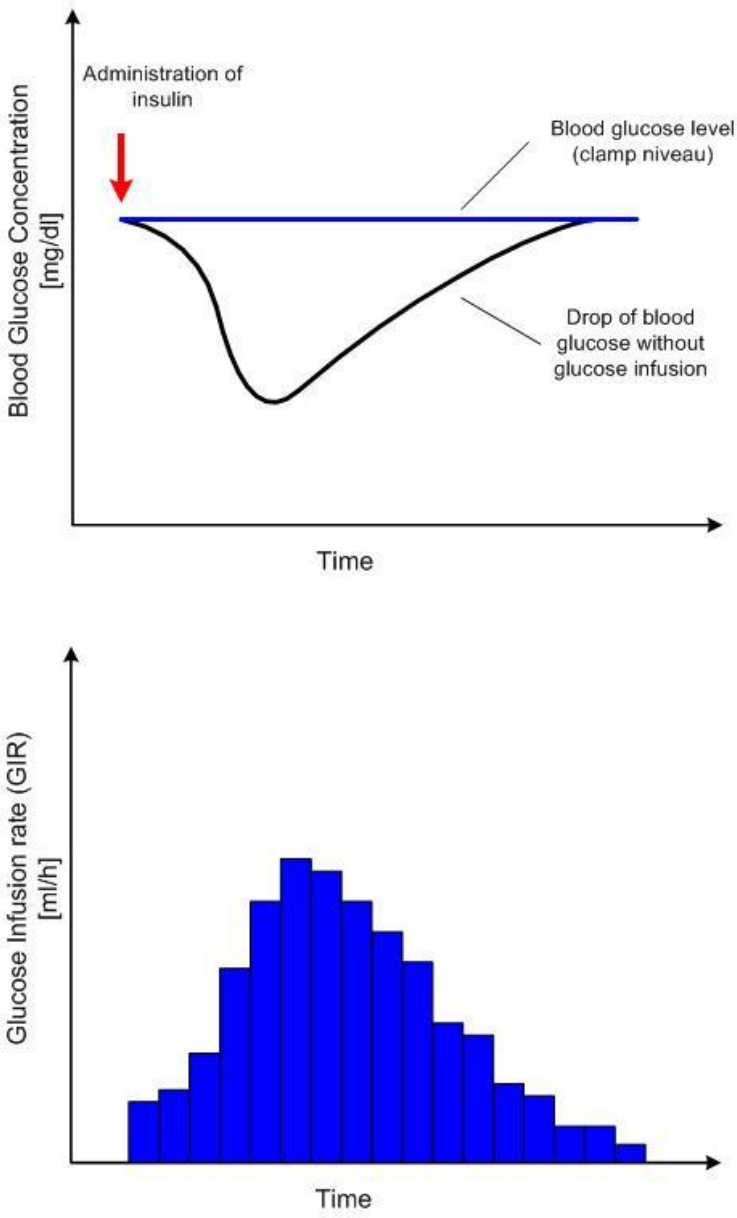

Figure 1: Schematic of a glucose clamp procedure. Top: A glucose infusion is needed to keep the clamp level stable if insulin has been applied. Bottom: The glucose infusion rate varies over time to keep the clamp level stable. **[11]**

Clamp procedures are very complex and need well-trained personnel leading to high labour costs. As a result, attempts have been made to automate this process.

An automated clamp device combines an automated continuous blood glucose monitoring unit with an automated algorithm-controlled insulin infusion.

Such an automated continuous blood glucose monitoring (CGM) unit was described in 1960 by Weller et al. [12]. This automated CGM device used two sets of tubing, inserted into a

vein, to infuse a heparin solution and to automatically withdraw 0.48ml blood per minute (28.8ml/h) which was then measured for glucose based on a colorimetric system.
Currently there are three automated glucose clamp devices on the market. The Biostator was developed by Dr. Ernst F. Pfeiffer from the Institut für Diabetes-Technologie GmbH in Ulm, DE. It consists of an analyser pump to control the withdrawal of blood, a glucose analyser for online analysis, a computer with a set of algorithms calculating the blood glucose dependent insulin infusion, a computer-controlled infusion pump to infuse insulin or glucose and a printer/plotter (see Figure 2). The glucose analyser is based on an electrochemical sensor and a membrane with immobilised glucose oxidase. A modified Clark-type electrode is used to measure hydrogen peroxide that is generated through the reaction of glucose with glucose oxidase (details see *2.3 Glucose Oxidase Biosensors*) and yields a current that is proportional to the glucose concentration. The Biostator consumes about 50ml blood per day which is currently limiting its application. [13]

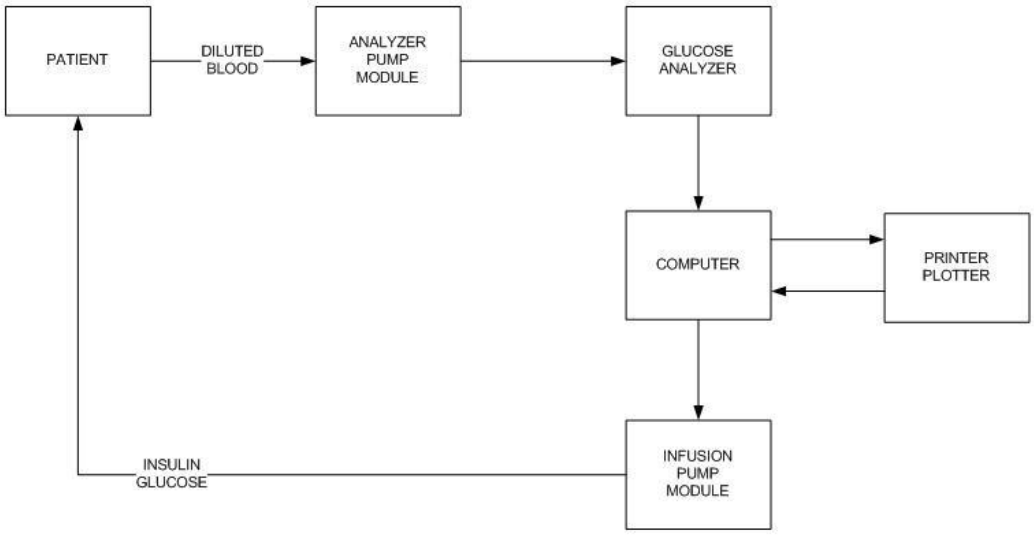

Figure 2: Block diagram of the automated CGM Biostator **[13]**.

An improvement of the Biostator is the Glucostator from mtb diabetes service GmbH, Luizhausen, DE which only needs about 1ml blood per hour [14]. The third automated clamp device is the Nikkiso STG-55 from Nikkiso Co., Ltd. in Tokyo, JP which is not available on the European market.

The Profil Institute for Metabolic Research GmbH in Neuss, DE, which is active in the area of automated clamp devices, accuses the currently available devices of unreliable glucose measurement, inaccurate pumps, unchangeable and insufficient algorithms, considerable

blood loss and frequent technical failures. They therefore put their focus on the development of a new automated clamp device using continuous glucose monitoring techniques and reducing blood loss.

Continuous glucose monitoring in interstitial fluid

One possibility for minimally invasive, continuous glucose monitoring (CGM) is to access the interstitial fluid (ISF) for glucose measurement [5]. This approach, however, suffers from the inevitable physiological lag time between blood glucose- and ISF glucose concentrations, which is around 5 – 10 minutes [5] [15]. The total lag time, including sensor reaction time and signal-processing delays for the devices available on the U.S. market (CGMS Gold, Guardian RT and Guardian REAL-Time with real-time display from Medtronic, FreeStyle Navigator system from Abbott Diabetes Care and SEVEN from DexCom which are all subcutaneously inserted in the abdominal area), is therefore 8 – 15 minutes. Furthermore, these sensor signals are noisy and often need to be filtered which can additionally increase the total lag time [5]. The magnitude of glucose concentrations in the blood and the ISF also differs, even if values are shifted for the lag time. These differences appear most obviously at large blood glucose concentrations, where ISF values are up to 40% below blood values. [15]
Moreover, critically ill patients often show variable tissue perfusion and tissue water content which can lead to further inaccuracies in ISF glucose measurements [16].

Continuous glucose monitoring using intravascular microdialysis

The above mentioned physiological lag time and the influence of the tissue can only be avoided if a CGM device is applied intravascularly. Introduced by Delgado [17] and Ungerstedt [18], intravenous microdialysis (ivMD) provides the advantage of measuring blood glucose concentrations without any loss of blood.
A MD probe is inserted into the peripheral vein via catheter and is perfused with a solution (perfusate). A semipermeable membrane at the probe’s tip allows the diffusion of glucose and ions from the blood into the perfusate which is now named dialysate. This dialysate is collected at the probe’s outlet and can then be measured for glucose. Lower flow rates of the perfusate enable more glucose molecules and ions to overcome the membrane, and at a diffusion rate of 100%, the dialysate concentration reflects the real blood concentration without applying any calibration. However, by achieving this, these low flow rates increase the time delay between reference blood glucose and dialysate glucose concentration. Finding an adequate balance between these two parameters – flow rate and so-called recovery of

glucose – is the main problem in ivMD (detailed information about ivMD can be found in 2.1 *Intravenous Microdialysis*).

In 2010, Hage et al. investigated the glucose monitoring potential of ivMD catheters in coronary care unit (CCU) patients. Although results were promising, as a reasonable congruence between ivMD and conventional venous plasma glucose concentration measurement did exist, a further improvement of the technique was recommended. [19] Another recent study investigated the feasibility and accuracy of ivMDs in intensive care unit (ICU) patients and healthy volunteers in 2010. Rooyackers et al. claimed that feasibility was outstanding, as all MD catheters functioned throughout the experiments, but accuracy needed to be improved, probably due to an insufficient perfusion process or missing calibration procedures. [16]

Based on the good results of ivMD CGM, the EU-CLAMP (EUglycemic CLinical Application for Metabolic Profiling) project, funded by the European Union, was launched in 2011. Four small and medium enterprises (SME) and three research and technical development (RTD) performers participated to develop an automated clamp device based on the technology of ivMD. This clamp device shall measure the blood glucose concentration gained via ivMD with an online glucose sensor. Processing the sensor signal yields the blood glucose concentration that is used as input for an algorithm calculating the required insulin dose. To avoid large delay times a small recovery is tolerated if MD values can be sufficiently corrected using a calibration procedure based on reference blood samples and the ionic reference technique.

1.2 Objectives

Based on the work of Andreas Huber [11] where optimal use of the ivMD probes, adequate anticoagulation of the probes, sampling and offline measurement of the MD dialysate and application of the ionic reference technique to avoid frequent calibrations was described, the current diploma thesis focuses on the characterisation of the sensor unit, the combination of the MD with the sensor unit and the performance evaluation of the combined system during a clinical trial.
The outstanding part of the project would comprise the addition of the algorithm calculating the required insulin dose to finish the closed loop of an automated clamp device.

The following features and parameters were taken from the EU-CLAMP user requirements:

1.2.1 In Vitro

In vitro user requirements included the characterization of the BVT sensor in un-buffered solution concerning linearity, ion dependency, drift, response time and the optimization of the sensor's run-in behaviour, as well as the combination of the MD and sensor unit by defining the setup, optimal flow rates, perfusate composition, measures avoiding air bubble artefacts, risk analysis and electrical safety check, to enable a clinical trial in 5 subjects.

1.2.2 In Vivo

In vivo user requirements included finding the optimal balance between flow rate and glucose recovery, defining accuracy (system error) of the monitoring unit (MD + sensor unit), calculating the number of required recalibration points to fulfil the acceptance criteria according to ISO 15197:2003, as well as estimating the correlation between sensor current and blood glucose, blood glucose and dialysate glucose and dialysate glucose and sensor current.

2 RESEARCH DESIGN AND METHODS

2.1 Intravenous Microdialysis

The method of microdialysis was developed and introduced in the 1970s by Delgado [17] and Ungerstedt [18]. Based upon diffusion effects over a semipermeable membrane, various types of microdialysis probes for the quantitative analysis of analytes in tissues like brain, subcutaneous fat and blood are available nowadays [20].

The intravenous microdialysis probe is inserted into a venous catheter that is placed in a vein, and an artificial solution (perfusate) is pumped through the probe. The length of the venous catheter allows the tip of the probe to be placed outside the catheter in direct contact with the blood. A semipermeable membrane is located at the probe's tip and analytes smaller than the membrane's molecular weight cut-off can pass through it. For intravenous microdialysis these analytes are e.g. sodium-chloride ions and glucose (see Figure 4).
Due to their concentration gradients, these analytes diffuse into the microdialysis probe and enrich the perfusate. This analyte-enriched perfusate is then named dialysate and can be collected and/or measured at the microdialysis probe's outlet.

Fick's Law is the simplest description of this diffusion process, taking into account parameters such as concentration gradients, membrane geometry and membrane characteristics, as well as the flow rate of the perfusate.
The ratio between the resulting dialysate concentration ($c_{dialysate}$) and the concentration of the surrounding medium (c_{blood}) is the relative recovery (Rec). [20]

$$Rec = \frac{c_{dialysate}}{c_{blood}} \cdot 100\% \tag{1}$$

The recovery is inversely proportional to the flow rate, meaning that low flow rates lead to high recoveries and vice versa [20]. With the flow rates chosen in our setup, a 100% recovery cannot be achieved. Thus, a mathematical correction (calibration) is needed to calculate the actual glucose concentration in the blood.

In the case of constant recovery, a 1-point calibration based on a blood reference sample is sufficient to calculate the glucose concentration in blood. In the case of changing recovery rates caused by varying flow rates, effects related to membrane swelling or agglutination, a method to monitor the changes of the recovery has to be used. One possibility is to monitor a reference substance (of constant and known concentration) such as ions, which is implemented in the “ionic reference technique”.

2.2 Ionic Reference Technique

The ionic reference technique (IRT) was introduced by Schaupp et al. [21] and explained by Andreas Huber in his diploma thesis in 2012 [11].

The IRT can be briefly explained as follows. The recovery can be calculated according to formula (1) when the glucose concentrations in dialysate and blood are known. As blood glucose concentration is the parameter of interest and glucose recovery is unknown because it cannot be directly measured and changes over time, the recovery of ions (also below the cut-off size of the MD membrane) is, therefore, an additional parameter that can be used to determine the glucose concentration in the blood (see 2.1 *Intravenous Microdialysis*). The sodium chloride concentration in the blood is assumed to be constant (100%) and the recovery of ions is assumed to be linearly proportional to the recovery of glucose in a simplified manner [21]:

$$Rec_{glucose} = f(Rec_{ions}) = k \cdot Rec_{ions} \tag{2}$$

Therefore, the blood glucose concentration ($Gluc_{blood}$) can be calculated as

$$Gluc_{blood} = \frac{Gluc_{dialysate}}{Rec_{glucose}} = \frac{Gluc_{dialysate}}{Rec_{ions}} \cdot \frac{1}{k} \tag{3}$$

with

$$Rec_{ions} = \frac{Ions_{dialysate}}{Ions_{blood}} \tag{4}$$

leading to

$$Gluc_{blood} = \frac{Gluc_{dialysate} \cdot Ions_{blood}}{Ions_{dialysate}} \cdot \frac{1}{k} \tag{5}$$

2.3 Glucose Oxidase Biosensors

Biosensors based on the enzyme electrode technique use a miniature chemical transducer, or enzyme electrode, that combines electrochemical procedures with immobilized enzyme layers. A membrane of immobilized enzyme (e.g. GOD) is, therefore, placed over the working electrode. [22]
If the sensor is then exposed to glucose, the glucose oxidase (GOD) catalyses the following reaction [23]:

$$Glucose + O_2 \xrightarrow{GOD} Gluconic\ Acid + H_2O_2 \tag{6}$$

Afterwards, a second reaction on the working electrode takes place generating a current that can be recorded via potentiostat. Hydrogen peroxide from (6) is oxidized due to a polarisation voltage applied to the working electrode with respect to the reference electrode. Formula (7) shows this oxidation which leads to an anodic electron flow that is proportional to the glucose concentration. [23] [24]

$$H_2O_2 \xrightarrow{WE\ (Anode)} O_2 + 2H^+ + 2e^- \tag{7}$$

2.4 Analytical Methods

2.4.1 Glucose Sensing

The AC1.GOD Biosensor (BVT Technologies, a.s., Brno, CZ) depicted in Figure 3A was used to measure glucose during the *in vitro* and *in vivo* investigations.
It is based on a corundum ceramic base on which working, reference and auxiliary electrodes are placed. The working electrode consists of pure platinum and the reference electrode is made of silver. The Glucose Oxidase (GOD) from Aspergillus Niger is immobilized over a 1mm radius on the working electrode of the sensor. The manufacturer's datasheet (refer to www.bvt.cz) proposes a linear measurement range of 0 – 20mg/dl for this sensor. [25]

The sensor was placed in a FC2.S flow cell (see Figure 3B, BVT Technologies, a.s., Brno, CZ). The flow cell's cable was soldered to a T01-0550-P05 plug (see Figure 3C, Farnell ordering no: 130746, TE Connectivity Ltd., Schaffhausen, CH) to connect it to the EmStat

potentiostat (see Figure 3D, PalmSens BV, Utrecht, NL). Data were recorded using a laptop and the software PSTrace, version 2.4 (PalmSens BV, Utrecht, NL).

As the flow cell was not designed to be used in clinical studies, some improvements had to be made before the start of the experiments. The backside of the flow cell was isolated by resin as it contained a small un-isolated circuit board (see Figure 3E) that connects the flow cell to the potentiostat. Furthermore, the flow cell can be connected to the microfluidics of the body interface via two metal tubes. These tubes were glued into the plastic housing by UV-cured glue which was not strong enough to withstand the stress when connecting and disconnecting the body interface. Therefore, these tubes were additionally glued to the housing of the flow cell using thermoplastic glue (see Figure 3F).

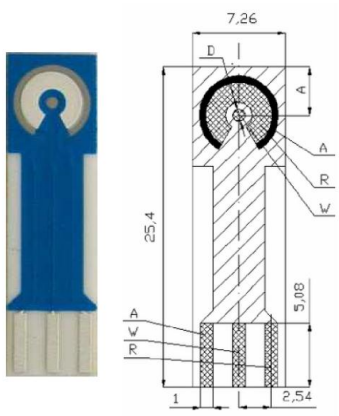

Figure 3A: AC1.GOD glucose sensor (BVT Technologies, a.s., Brno; CZ) and its geometry.

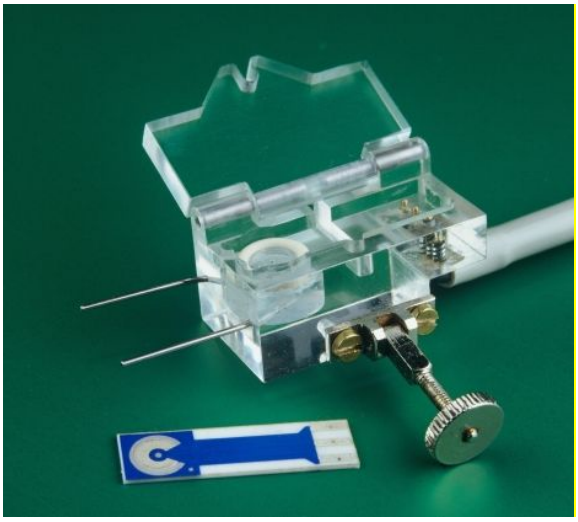

B: FC2.S flow cell (BVT Technologies, a.s., Brno, CZ)

C: T01-0550-P05 connection plug between flow cell and EmStat potentiostat (Farnell ordering no: 130746, TE Connectivity Ltd., Schaffhausen, CH).

D: EmStat potentiostat (PalmSens BV, Utrecht, NL).

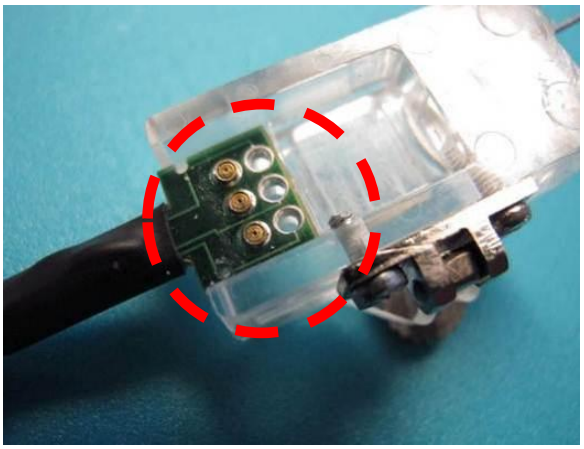

E: FC2.S flow cell – circuit board.

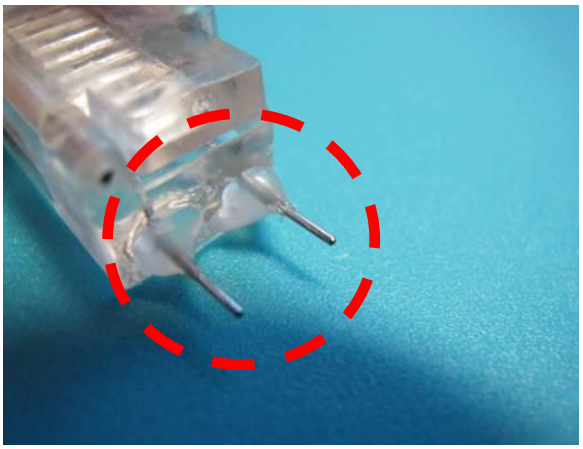

F: Connection tubing of flow cell.

The EmStat potentiostat performed the amperometric detection and the software PSTrace 2.4 was used to set the following conditions:

Technique	**Amperometric Detection**	
	Value	**Unit**
E	0.65	V
E_{cond}	-0.6	V
E_{dep}	-0.5	V
E_{stby}	0.65	V
interval	10	s
t_{run}	259200	s
t_{cond}	0	s
t_{dep}	0	s
t_{eq}	8	s

Table 1: PSTrace 2.4 settings for amperometric detection. E_{cond} and E_{dep} are default settings that were not changed as they will never be executed due to $t_{cond} = 0$ and $t_{dep} = 0$.

During *in vitro* investigations the EmStat potentiostat was grounded to avoid noisy sensor currents. During *in vivo* investigations, however, a grounding of the potentiostat was not feasible for safety reasons, as this grounding would have bypassed the isolating transformer (see Figure 20).

2.4.2 Conductivity Measurement

To enable the ionic reference technique the TraceDec® contactless conductivity detector (Innovative Sensor Technologies GmbH, Strasshof, AT) was used to determine the ion concentrations of *in vitro* and *in vivo* samples. To measure a sample's conductivity (proportional to the ion concentration) offline, a peristaltic pump (GILSON Minipuls, Gilson, Inc., Middleton, USA) draws the sample volume into a fused silica capillary that is placed in the TraceDec® sensor. The sensor itself consists of two metal electrodes that are placed around the capillary. Applying an AC voltage to the actuator electrode leads to a current flowing through the capillary wall, the detection gap inside the capillary and back to the pick-up electrode. The resulting signal is amplified, processed and displayed, but does not deliver an absolute value. The absolute value has to be calculated by applying a calibration curve. [26] The calibration curve of the TraceDec® was determined by Andreas Huber in 2012 and the formula is given in his diploma thesis [11]. y refers to the ion content in % whereas x refers to the TraceDec® output:

$$y = 10^{-6}x^3 - 0.003x^2 + 0.1503x + 0.3824 \tag{8}$$

with $r = 0.9999$. The coefficient of variation (CV) of this formula was reported as less than 2% [11].

Due to a basic conductivity of the perfusate during *in vivo* investigations (refer to *2.7.6 Perfusate and Anticoagulation (Arixtra®)* and Figure 4) (8) was expanded to the following formula to achieve the actual ion recovery in the dialysate:

$$y = \frac{(10^{-6}x^3 - 0.003x^2 + 0.1503x + 0.3824) - \lambda_{basic}}{\lambda_{blood} - \lambda_{basic}} \cdot 100\% \tag{9}$$

Conductivities are depicted as λ in % and the conductivity of human blood is $\lambda_{blood} = 100\%$.

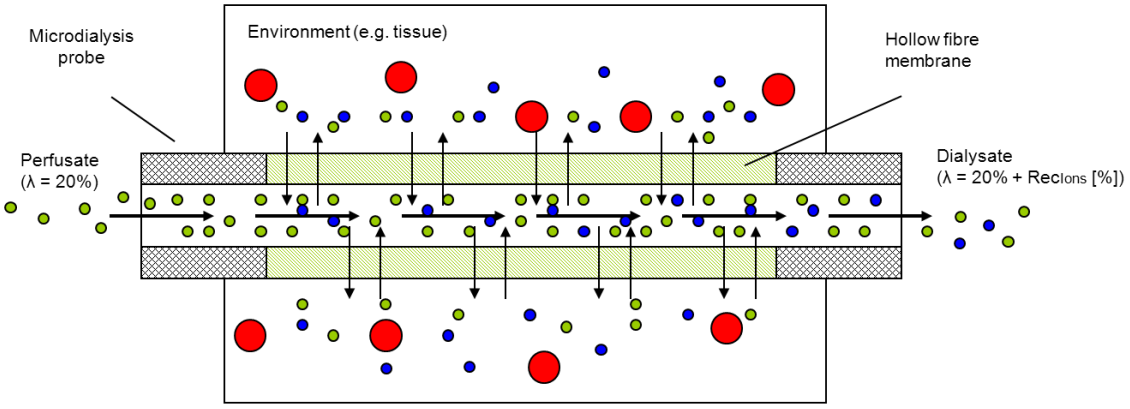

Figure 4: Recovery of ions in a microdialysis probe using a perfusate with basic conductivity λ= 20%. Ions are shown as green, glucose as blue and substances larger than the cut-off of the microdialysis probe as red circles. The dialysate shows the basic conductivity (ion content) of the perfusate plus the amount of ions that passed the membrane due to the recovery rate ($\lambda = 20\% + Rec_{Ions}$).

2.4.3 Glucose Measurement

The bench top glucose analyzer Super GL2 (Dr. Müller Gerätebau GmbH, Freital, DE) was used to measure the glucose concentrations of *in vitro* glucose standards and *in vivo* dialysate and reference blood samples. The measurement range of the Super GL2 is 9 - 910mg/dl with a coefficient of variation below 1.5% [27]. A prerequisite to achieve such a good CV is to perform an initial 2-point calibration followed by automated 1-point calibrations every hour or stable calibrations before each measurement.

To measure glucose in *in vitro* standards and dialysate samples, 20µl of the sample volume are normally spiked into vials filled with buffer solution (Glucocapil caps, 1000µl) and analyzed with the Super GL2.
Before a blood sample can have its glucose level measured it has to be centrifuged, after which, 20µl of its supernatant can be spiked into Glucocapil caps.

During *in vitro* and *in vivo* investigations dialysate samples were generated with a glucose concentration below the lower limit of quantification (LLOQ = 9mg/dl) of the Super GL2. To allow a reliable quantification of these samples, more sample volume was spiked into the Glucocapil caps and the results were mathematically corrected afterwards according to the following formula:

$$c_{corr\ spiking} = c_{sample} \cdot \frac{V_{spike\ standard}}{V_{spike\ sample}} \cdot \frac{V_{Glucocapil} + V_{spike\ sample}}{V_{Glucocapil} + V_{spike\ standard}} \tag{10}$$

with $V_{spike\ standard} = 20\mu l$, $V_{Glucocapil} = 1000\mu l$ and $V_{spike\ sample} = x \cdot V_{spike\ standard}$

The correction term in (10) was validated through an *in vitro* investigation where different volumes (20 - 400 µl) of glucose standards were pipetted into Glucocapil caps and the results were corrected afterwards. CV values of this investigation were found to be smaller than 1.28% (see Appendix Figure 54). [11]

Furthermore, an ion dependency of the Super GL2 was observed during *in vitro* investigations. Within glucose-free samples with ion concentrations below 15%, glucose concentrations up to 3mg/dl were mistakenly found. This effect was demonstrated on different days with different samples excluding any contamination. All glucose-free samples with ion concentrations above 15% fell below the LLOQ of the Super GL2 (see Table 2).

		28.06.2012			
		200µl			
Ion Concentration	**Glucose Concentration**	**1. Measurement**	**2. Measurement**	**Mean Value**	**Corrected Mean Value**
0%	**0 mg/dl**	21.3	21.5	21.4	2.5
	2 mg/dl	25.1	25.2	25.2	3.0
	10 mg/dl	84.1	83.4	83.8	9.9
	20 mg/dl	166.0	167.0	166.5	19.6
5%	**0 mg/dl**	19.0	19.3	19.2	2.3
	2 mg/dl	22.4	22.3	22.4	2.6
	10 mg/dl	82.9	82.9	82.9	9.8
	20 mg/dl	166.0	166.0	166.0	19.5
15%	**0 mg/dl**	12.7	13.7	13.2	1.6
	2 mg/dl	17.4	17.1	17.3	2.0
	10 mg/dl	83.8	83.5	83.7	9.8
	20 mg/dl	167.0	165.0	166.0	19.5
25%	**0 mg/dl**	<LLOQ	<LLOQ	<LLOQ	<LLOQ
	2 mg/dl	17.7	17.5	17.6	2.1
	10 mg/dl	85.2	84.5	84.9	10.0
	20 mg/dl	168	167.0	167.5	19.7

Table 2: Ion dependency of the Super GL2.

2.4.4 Flow Rate

To achieve a constant recovery rate of glucose and ions, as well as a stable sensor signal, a constant flow rate has to be assured during *in vivo* investigations. As there was no *in vivo*, CE-certified and sterile online flow sensor available, the flow rate was indirectly quantified by determining the weight of the dialysate samples during a sample interval (15 minutes). Weight was determined with a laboratory scale assuming a density of perfusate and dialysate of 1g/ml. The flow was calculated as:

$$flow\ [\mu l/min] = \frac{weight_{full}[g] - weight_{empty}[g]}{time_{sampling\ interval}[min]} \cdot 10^3 \qquad (11)$$

2.5 Data Acquisition and Analysis

During the clinical study various data were determined and recorded after each sampling interval:

- Start- and end-time of the sampling interval [hh:mm:ss]
- Weight of the empty and full dialysate sample container [g]
- Conductivity (ion concentration) of a calibration standard [% of 0.9% NaCl]
- Conductivity of the dialysate sample [% of 0.9% NaCl]
- Reference blood plasma glucose concentration [mg/dl]
- Dialysate sample glucose concentration [mg/dl]
- Volume of the dialysate sample that was spiked into the Glucocapil cap for glucose measurement with the Super GL2

Furthermore, the start-time of the sensor and all relevant events during the clinical trial (e.g. toilet break, flushing of the sensor flow cell, change of the sensor, etc.) were recorded.
The data were stored in printed and handwritten case report forms (CRFs) and Microsoft Excel worksheets (Microsoft Corporation, Redmond, WA).
Sample containers, CRFs and Microsoft Excel worksheets were all colour coded to minimize the risk of mixing up samples when two systems were investigated in parallel.

2.5.1 Filter Function for Sensor Current

Problems with noisy sensor currents arose, especially during the clinical trial (*see 3.2.3 Overview Clinical Study,* Figure 38 - Figure 42). With these data a point-to-point comparison between reference blood glucose and sensor glucose would have led to an extremely bad correlation. Therefore, a filter was applied to reduce the noise and allow a reasonable data evaluation.
Before applying the filter the raw sensor current was corrected by the ion recovery and 1-point-calibrated to obtain glucose concentration values (mg/dl) instead of current values (nA).

In the first step, the filter algorithm defines the first sampling interval (15 minutes) as start interval. The user can predefine how many points within this interval should be averaged to obtain a stable starting point for the filter. For all proximate values the filter then calculates the slope between the current data point and the data point before. If this slope exceeds a positive or negative slope predefined by the user, the current data point is replaced by a selectable mean value interval of prior data points. If the slope lies within the positive and negative threshold (e.g. ±0.1nA per sample interval for the *in vivo* investigations) the original value of the data point is retained (see Figure 5).
Positive and negative slope, as well as strength of the averaging, can be predefined individually (see Figure 6).

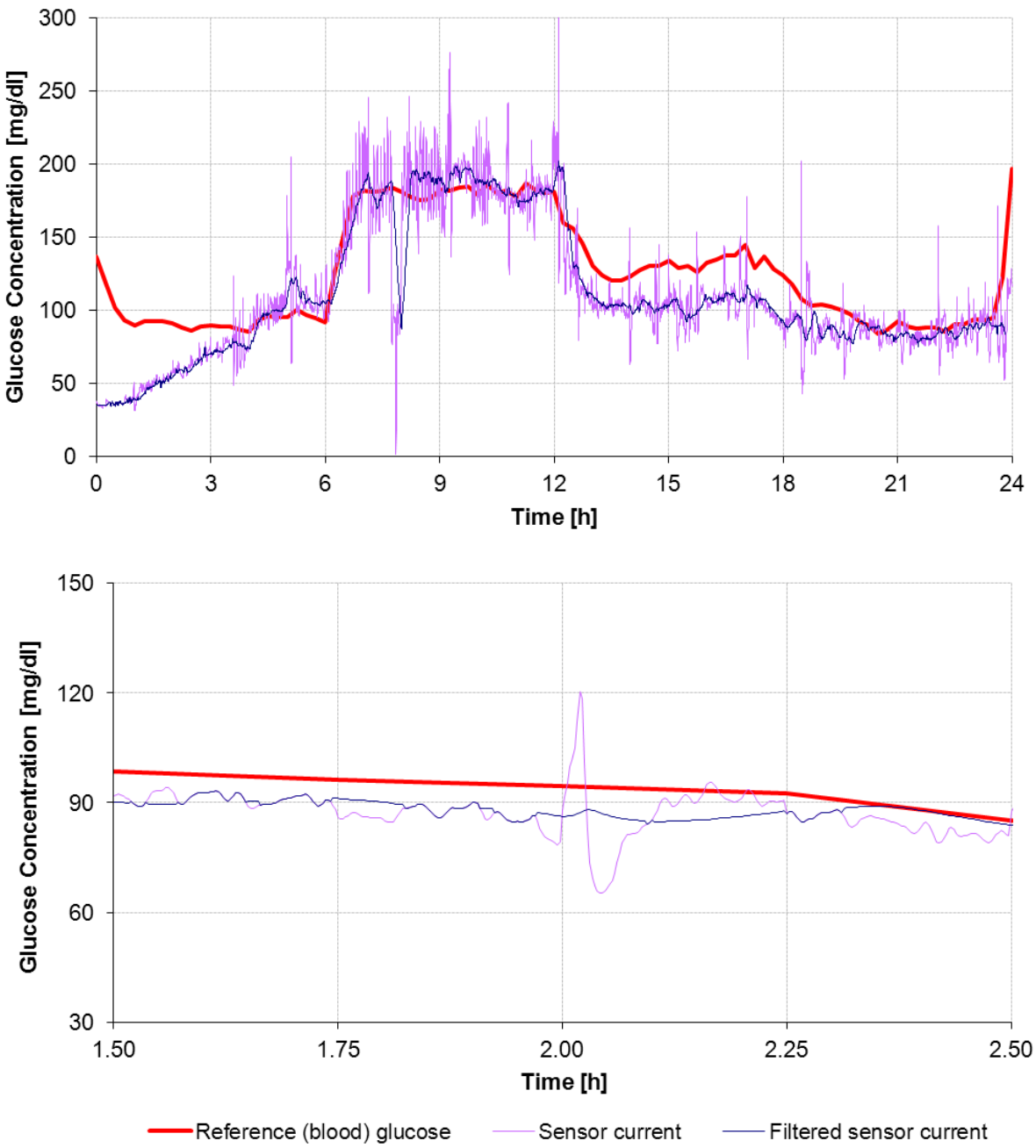

Figure 5: Filter function exemplarily applied to the *in vivo* data of subject 021 and 023. Reference blood is depicted as a red line, sensor current is depicted as a purple line and the filtered sensor current is depicted as a blue line.

stable start interval #P	positive threshold	negative threshold	sensor interval	MV interval
0 - 90 pts (0 = no interval; first value)	*nA/interval*	*nA/interval*	*s*	*0 - 90 pts (0 = no interval)*
90	0.1	-0.1	10	90

Figure 6: Individually adjustable filter parameters.

2.5.2 Correction of Fluidic Delay Time

A 5cm tubing was placed between the MD probe's outlet and the flow cell of the sensor to allow free movement of the subject's arm and to avoid a backflow from the unsterile flow cell to the body interface and thus a contamination possibly causing an infection (see *3.2.1 Risk Management*). However, the internal volume of this tubing, together with the low flow rate of the perfusate and the reaction time of the sensor itself, caused an undesired time delay between reference blood and sensor measurements.

In the final setup the flow cell should be directly connected to the body interface to at least eliminate the delay time caused by this 5cm tubing. A prerequisite for this would be a passed safety test with this changed setup and a sterile flow cell. This could not be realised within the EU-Clamp project due to time and cost issues.

Nevertheless, this time delay worsened the correlation between blood glucose and sensor signal and needed to be compensated. I*n vitro* investigations (see *3.1.3 Response Time*) discovered a general delay time of approximately 1.8 minutes between changing of the test solution and first reaction of the sensor, at a flow rate of 20µl/min. However, this delay time also included the diffusion process at the MD membrane and the sensor's reaction time itself, and a shifting by 1.8 minutes would, therefore, overestimate the improvement of an integrated system without the 5cm tubing. Because of this, the sensor current was only shifted by 1.5 minutes for flow rates of 20µl/min and 3 minutes for flow rates of 10µl/min.

2.5.3 Calibration of In Vivo Data

The ionic reference technique improves the correlation between dialysate and blood glucose but cannot compensate the absolute difference between these two values. Thus the dialysate concentrations and the sensor results need to be calibrated as well. As the sampling process and the mathematical correction of the dialysate concentrations had already been investigated and optimized by Andreas Huber, the calibration protocol mentioned in [11] was used for the calibration of the sensor signal as well.

In short, the calibration is done by linear regression with the following formula:

$$c_{blood} = c_{dialysate} \cdot \mathrm{k} + \mathrm{d} \tag{12}$$

where k is the slope and d the intercept of this regression line.

A calibration with more than one point is only required if different reference blood values are available. Because of the rather constant blood glucose concentrations during a glucose clamp, a 1-point-calibration with d = 0 is sufficient. (12) changes and k can then be determined as follows:

$$k = \frac{c_{blood}}{c_{dialysate}} \tag{13}$$

All subsequent data are corrected with (13) until the next calibration is performed, depending on the length of the calibration interval. If one value is not available (reference value or value that should be corrected) the next complete pair of values is used for calibration.
A restrictive fact for this calibration is that the dialysate concentration is a time-integrated value (15min) whereas the reference value is a point-measurement. Comparing the sensor value with the reference value has the advantage that both are point-measurements. A limiting factor of this comparison, however, is that the sensor value corresponds to a reference value taken a few minutes earlier due to the fluidic delay of the combined system. This delay can be partly corrected as described in *2.5.2 Correction of Fluidic Delay Time*.

Calibration based on a Limit of the System Error (|SE|<10%)

A special calibration procedure avoiding rigid calibration intervals was implemented by Andreas Huber [11]. This protocol only applies a calibration if the relative error (system error) between the reference and the dialysate or sensor value exceeds ±10%.
The average calibration interval was used for evaluation and calculated as follows:

$$Average\ Calibr.Interval\ [min] = \frac{Data\ Points}{Calibr.Points} \cdot\ Sampling\ Interval\ [min] \tag{14}$$

2.5.4 Statistical Methods

Coefficient of Correlation (r)

The Coefficient of Correlation (r) shows the linear agreement between the estimated glucose value of the new method and the reference glucose value. It can be calculated as follows:

$$r = \frac{\sum_{n=1}^{N}(Estimate_n - \overline{Estimate_n}) \cdot (Reference_n - \overline{Reference_n})}{\sqrt{\sum_{n=1}^{N}(Estimate_n - \overline{Estimate_n})^2} \cdot \sqrt{\sum_{n=1}^{N}(Reference_n - \overline{Reference_n})^2}} \tag{15}$$

The Correlation Coefficient can take values between -1 (anti-correlation) and 1 (correlation). A value of 0 indicates uncorrelated data.

Mean Absolute Relative Difference (MARD)

The Mean Absolute Relative Difference (MARD) shows the average absolute difference between the estimate value of the new method and the value of the reference method divided by the reference value in %.

$$MARD[\%] = 100 \cdot \frac{1}{N} \cdot \sum_{n=1}^{N} \left| \frac{Estimate_n - Reference_n}{Reference_n} \right| \tag{16}$$

A large MARD indicates a large disagreement between these two methods. [28]

Median Absolute Relative Difference (M2ARD)

The Median Absolute Relative Difference (M2ARD) shows the median absolute difference between the estimate value of the new method and the value of the reference method divided by the reference value in %.

$$M2ARD\ [\%] = 100 \cdot Median \left| \frac{Estimate_n - Reference_n}{Reference_n} \right| \tag{17}$$

A large M2ARD indicates a large disagreement between these two methods. The M2ARD usually gives a lower value than the MARD and is statistically more accurate, but still, the MARD is more widely used and accepted. [28]

Clark Error Grid Analysis (EGA)

In 1987 the Clark EGA was developed to analyse the clinical consequences of a treatment based on a new glucose measurement method. The values of the new method are displayed on the y-axis and the reference values are displayed on the x-axis. Figure 7 shows the error grid which is divided into 5 different zones (A, B, C, D and E) which allow the evaluation of the treatment proposed by the new method. [28]

Zone A encloses glucose values that lie within ±20% of the reference value or values that fall below 70mg/dl (hypoglycemic range) when the reference is also below 70mg/dl. Zone B encloses values with a deviation larger than ±20% that would still lead to an inoffensive or no treatment. Contrarily, zones C, D and E would lead to inacceptable, wrong treatment. [29]

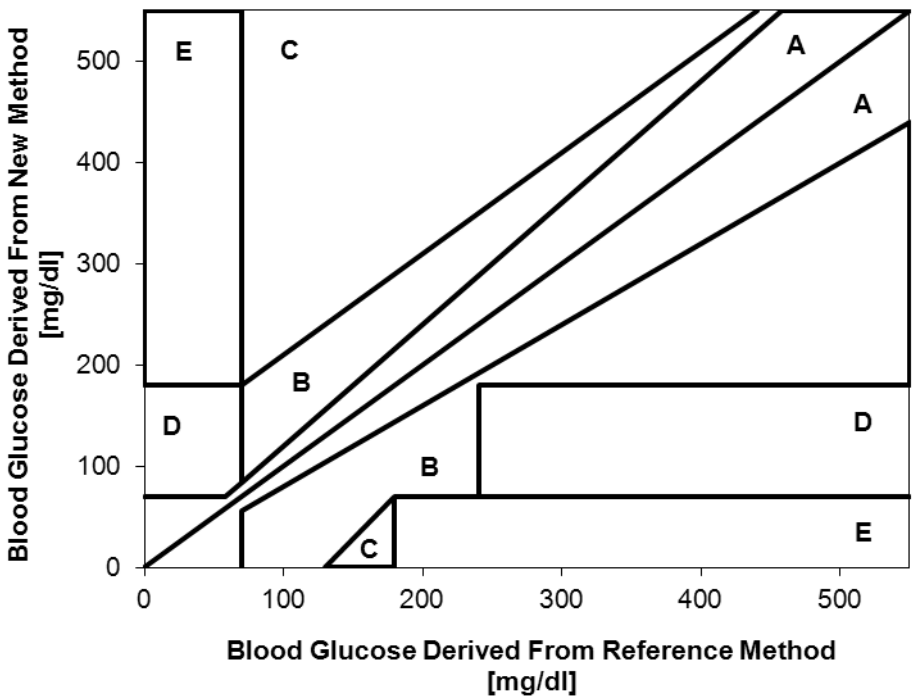

Figure 7: Clark Error Grid Analysis. Blood glucose derived from new method versus reference method **[29]**.

Predicted Error Sum of Squares in % (%PRESS)

The Predicted Error Sum of Squares compares the estimated glucose values with the reference values. It can be calculated as follows:

$$\%PRESS\ [\%] = 100 \cdot \sqrt{\frac{\sum_{n=1}^{N}(Estimate_n\text{-}Reference_n)^2}{\sum_{n=1}^{N}(Reference_n)^2}} \tag{18}$$

A low %PRESS indicates a good agreement between estimated and reference value. Although the %PRESS is sensitive to outliers, it neglects the influence of algebraic signs.

Regression Analysis

In accordance with ISO 15197:2003 [30] the accuracy of a glucose monitoring unit can be evaluated with a regression analysis.

The regression analysis plots the tested continuous glucose measurement method (new method) on the y-axis versus the reference method (well-known method) on the x-axis. A straight line at 45° is depicted in the plot and represents the line of identity between reference and new method (see Figure 8). The regression analysis thereby implies that the reference method is without error and deviations only occur vertically to this straight line. [28]

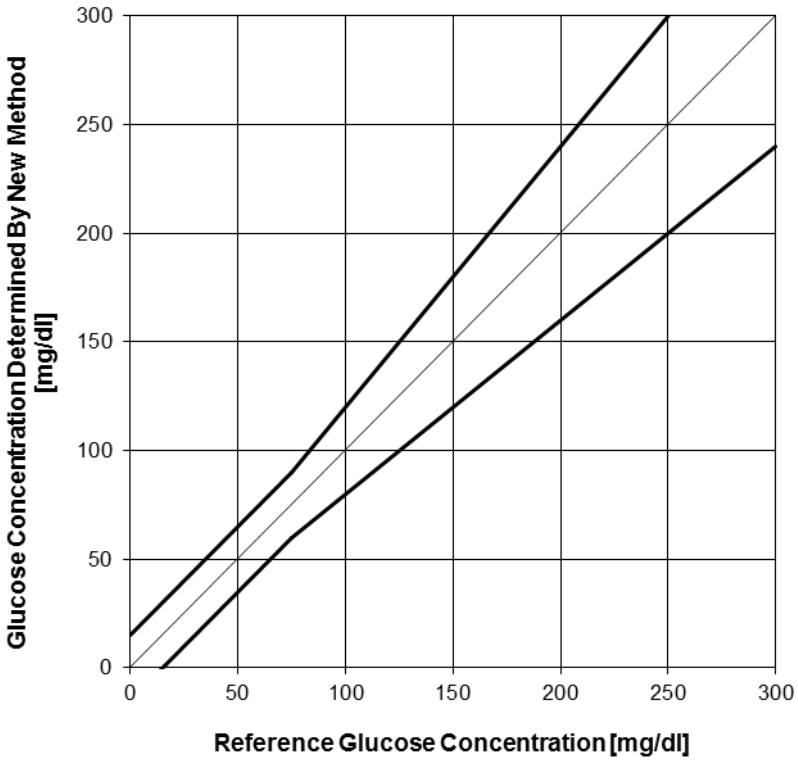

Figure 8: Regression diagram according to ISO15197:2003 **[30]**.

According to ISO 15197:2003 a glucose measurement device must fulfil the following minimum acceptance criteria: 95% of all individual glucose measurement values must fall in a region defined within ±15mg/dl compared to the reference method (blood measurements determined on Super GL2) for glucose concentrations <75mg/dl and ±20% for reference values with a glucose concentration ≥ 75mg/dl. [30]

2.6 In Vitro Investigations

According to the user requirements of the EU-CLAMP project the sensor was characterized *in vitro* before developing the optimal combined setup for the clinical trial.

2.6.1 Cup Experiments

The first *in vitro* setups with sensor and flow cell suffered from severe air bubble problems which led to noisy sensor currents and artefacts that made any evaluation impossible (see Appendix, Figure 55). Thus, cup experiments without flow cell were performed to characterize the sensor without its fluidics.

Adapted Flow Cell

The original connectors of the BVT flow cell were used to avoid loose contacts by using other pin connecters. Figure 9 shows the adapted BVT flow cell without flow channel which allows a direct immersion of the sensor in a cup with test solution.

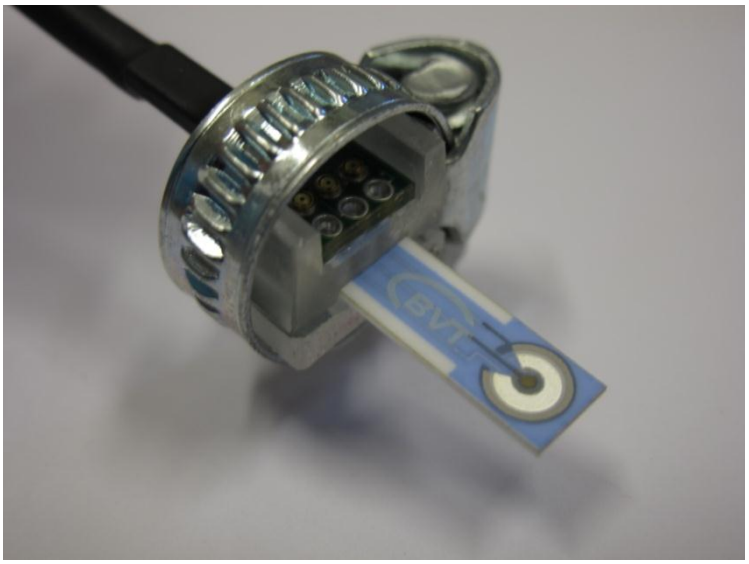

Figure 9: Adapted BVT flow cell for cup experiments containing original pin connectors.

Setup of Cup Experiments

Figure 10 shows a sensor (AC1.GOD, BVT Technologies, a.s., Brno; CZ) with adapted flow cell (FC2.S, BVT Technologies, a.s., Brno, CZ) that was directly immersed in a cup with test solution. This test solution could be changed manually to record calibration curves. The solution was stirred with a magnetic stir bar[4] on a magnetic stirrer (MR1000, Heidolph Instruments GmbH & Co. KG, Schwabach, DE) and room temperature was recorded using a USB temperature logger (Voltcraft DL-100 T).

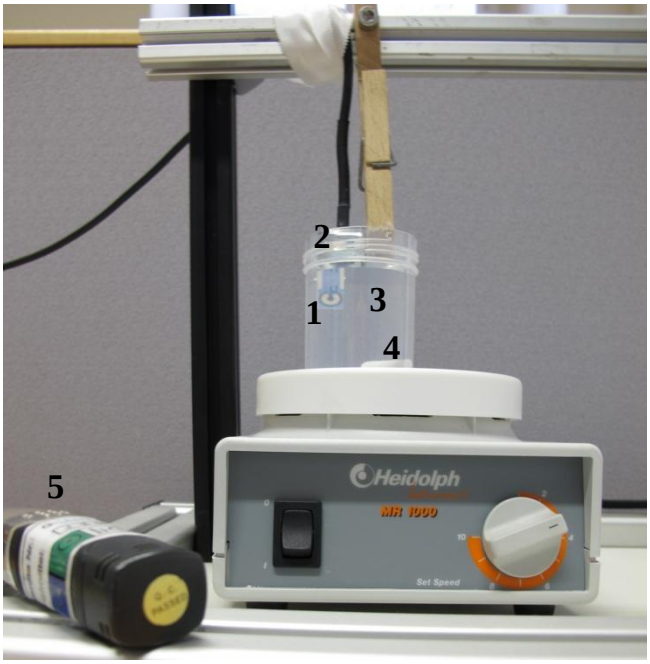

Figure 10: Setup of cup experiments: The BVT sensor[1] was operated through the contacts of an adapted flow cell[2]. It was directly immersed into a cup with test solution[3] that was stirred with a magnetic stir bar[4]. Room temperature was monitored using a USB temperature logger[5].

Un-Buffered *In Vitro* Test Solutions

The test solutions' matrix consisted of 5% Mannitol solution (dilution of 15% Mannitol, FRESENIUS-KABI, Z.Nr.: 1-20984 with double distilled water) and sodium chloride (SIGMA-ALDRICH, Pcode: 101010725, CAS: 7647-14-5) that was spiked with different amounts of D-glucose (D-glucose, SIGMA-ALDRICH, Pcode: 101038207, CAS: 50-99-7) creating *in vivo* like un-buffered standard solutions (perfusate composition see *2.7.6 Perfusate and Anticoagulation (Arixtra®)*). All test solutions were prepared at least 24 hours prior to the experiments, stored in the refrigerator and warmed to room-temperature before being used. Their actual glucose content was verified with the glucose analyser Super GL2 after the experiment.

The cup experiments were used to evaluate the sensor's calibration curve and to examine the influence of ions on the sensor signal.

Calibration Curve Characterisation in Un-Buffered Solution

The sensor was immersed in the following glucose concentrations in ascending and descending order: 0, 2.5, 5, 7.5, 10, 12.5, 15, 17.5 and 20mg/dl. The non-linear range was characterised by exposing the sensor to 30, 40, 50 and 75mg/dl in ascending order afterwards (see red line in Figure 27).

The calibration curve was determined by calculating the mean value and standard deviation of the sensor current for each glucose step.

Due to delayed delivery of the EmStat potentiostat from PalmInstruments these investigations were alternatively performed with the Gamry G300 potentiostat and the software Gamry Framework 5 from Gamry Instruments, Warminster, USA.

Ion Dependency Investigations in Un-Buffered Solution

During *in vivo* investigation changing recoveries lead to changing ion concentrations in the dialysate. The influence of different ion concentrations on the sensor signal had not been investigated by the manufacturer. Thus, eight sensors were characterised using sixteen different test solutions: 5% Mannitol with 0, 5, 15 and 25% NaCl with glucose concentrations of 0, 2, 10 and 20mg/dl, respectively.

Initial experiments (data not shown) revealed that the sensor needed an increased time to stabilize when the glucose and ion concentrations were changed simultaneously.

Therefore, four different glucose concentrations with the same ion concentration were tested before this procedure was repeated for the other ion concentrations (details of the protocol see Figure 11).

The length of the glucose steps was 15 minutes for the 0 and 2mg/dl solutions, but as the sensor needed an increased time to stabilize when higher glucose concentration differences were applied, the time was expanded to 20 minutes for the 10 and 20mg/dl solutions. For data analysis, only the second half of the signal of each glucose step (7.5-15 and 10-20 minutes, respectively) was considered.

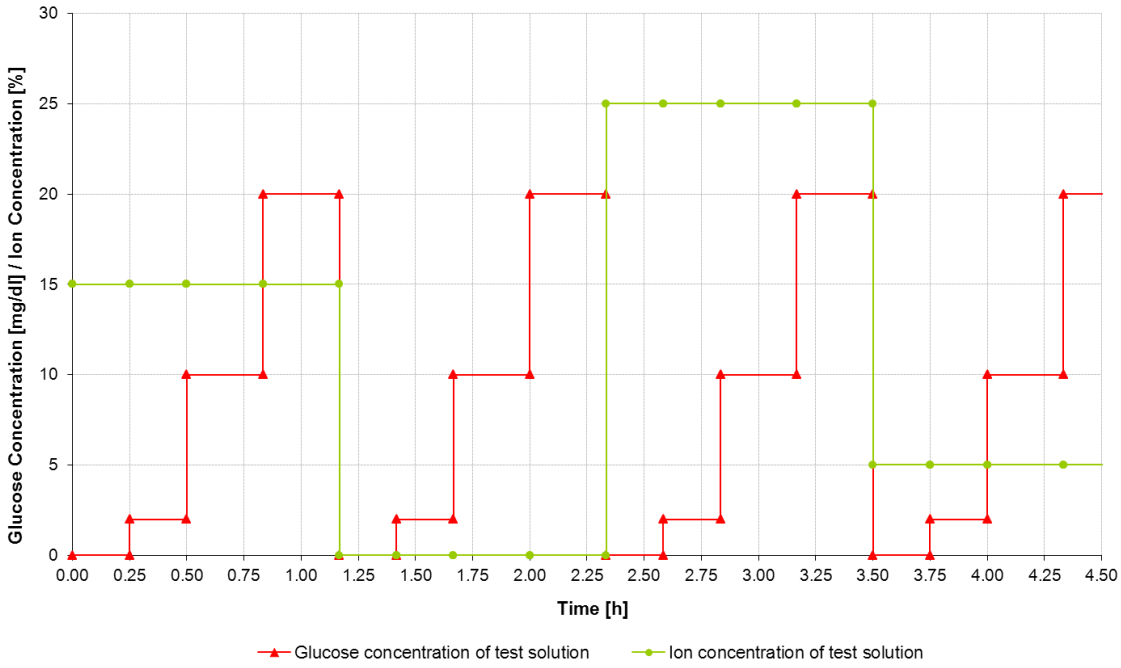

Figure 11: Exemplary protocol of ion dependency investigations.

All data were evaluated by calculating the mean value and standard deviation of the calibration curves.

2.6.2 Air Bubble Free Combined Setup

During former *in vitro* experiments, air bubbles present in the perfusate or being generated within the fluidics (e.g. changes of flow, pressure and temperature), accumulated within the flow channel around the sensor's active area and thus influenced the sensor signal.

Therefore, the aim of these experiments was to avoid the occurrence of any air bubbles within the combined system operated with an *in vivo* like protocol. The term "combined system" describes the combination of the body interface connected via a PHARMED BPT tubing from COLE PARMER to the flow cell containing the sensor, with the EmStat potentiostat (see Figure 13), a pump and additional tubing.

A syringe pump (BBRAUN Perfusor fm, Ref: 8713820) with an inserted BBRAUN Perfusor syringe (OPS 50ml, Ref: 8728810F) and the dedicated extension tubing (CODAN E87-P Tubing, Ref: 71.4310) perfused the body interface with a 5% Mannitol solution (with and without the anticoagulant Arixtra®). The body interfaces were immersed into heated NaCl-

glucose standard solutions imitating the human blood. The perfusate was enriched with glucose and sodium chloride ions and then measured online by the BVT sensor for glucose, and offline by the TraceDec for conductivity (see Figure 12).
Before the experiments the sensors were run in overnight either in a 5% Mannitol (sensors 1-1 and 1-2) or a 0.9% NaCl solution (sensors 1-3, 1-4, 1-5, 1-6, 1-7 , 1-8, 1-9, 1-10, 1-11, 1-12, 1-13, 1-14, 1-15, 1-16 and 1-17) instead of the NaCl-glucose standard solutions.

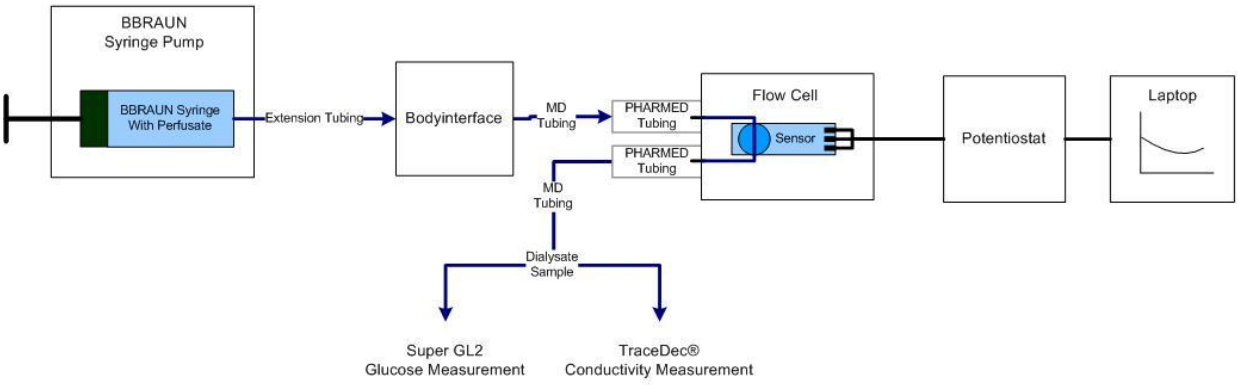

Figure 12: Schematic setup of the combined system.

The blood glucose levels that have to be measured during the clamp trials are 90, 130 and 180mg/dl (see *2.7.3 Protocol*). As the glucose sensor has a limited linear range of 20mg/dl (see *3.1.1 Calibration Curve*) the maximum allowed *in vivo* recovery rate of the body interface would therefore be around 10%. Prior investigations showed that this recovery rate can be achieved with an approximate flow rate of 20µl/min (data not shown). Missing agglutination effects in pure physiological NaCl solution lead to a better recovery rate than those found in whole blood. Thus, to operate the sensor at the same flow rate as planned to be used during *in vivo* studies, the concentration of the 3 *in vitro* glucose-NaCl solutions had to be decreased to stay within the linear range of the glucose sensor. Hence, *in vitro* solutions with 20, 35 and 50mg/dl of glucose were used. The dialysate was sampled every 30 or 15 minutes to quantify flow rate, recovery rate and actual glucose concentration.

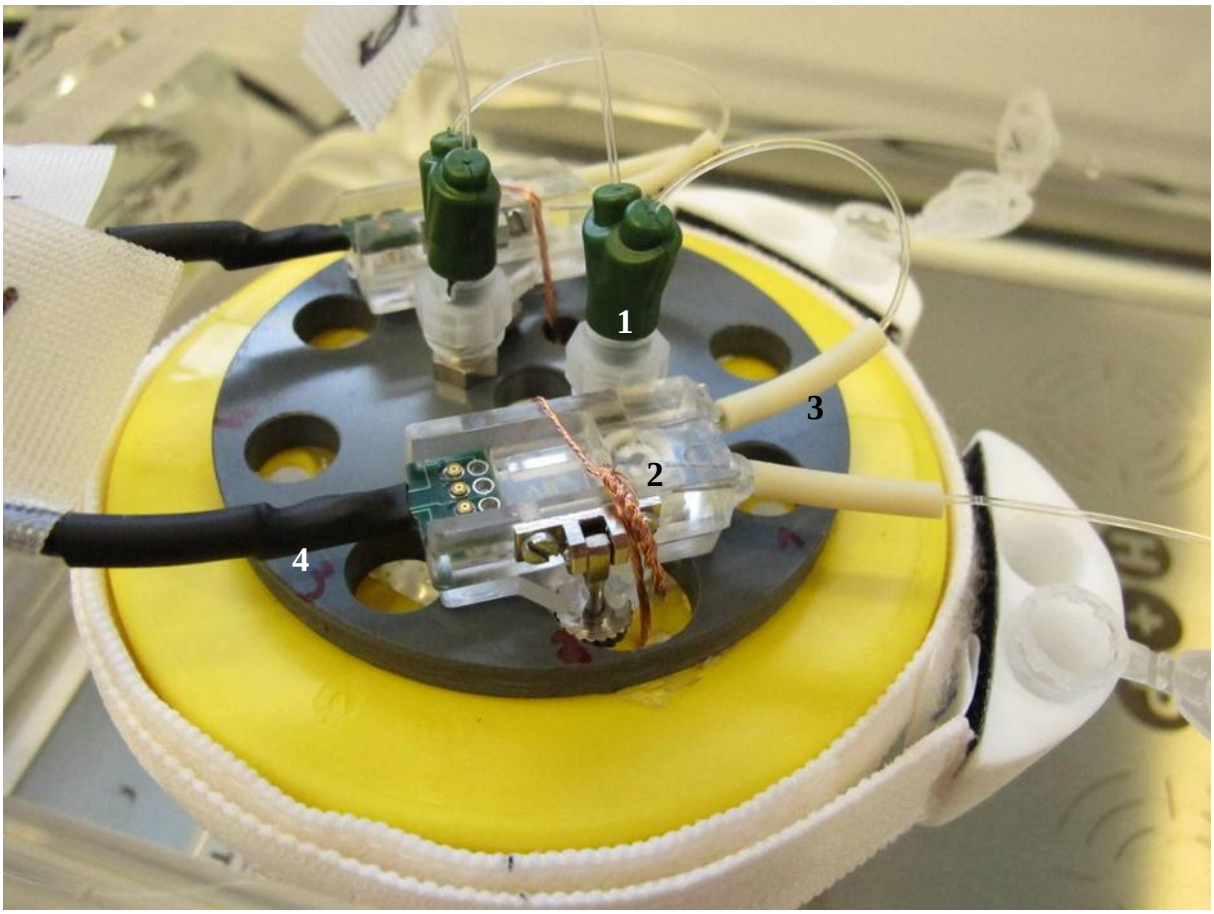

Figure 13: Combination of body interface and flow cell with sensor. The body interfaces[1] were directly immersed in the glucose solution cup. The cup itself was placed within a water bath (36.5 - 40°C) on a magnetic stirrer and stirred with an individual magnetic stir bar at 200rpm. The body interface was connected to the flow cell with the sensor[2] with a PHARMED BPT tubing[3]. To record the data the sensor was connected to the EmStat potentiostat[4].

Nine experiments with changing setups and conditions were investigated (see Appendix, Table 11) to overcome problems with noisy sensor currents caused by air bubbles. Most of the air bubbles resulted from out-gassing effects (see *3.1.6 Air Bubble Free Setup* and Appendix, Figure 55) when the temperature of the perfusate was increased in the body interface. Two setups allowing air bubble free investigations were found before the combined system could be operated with the *in vivo* like protocol as mentioned above:

Combined system with an integrated Belmont® Buddy fluid warmer (Belmont Instrument Corporation, Billerica, USA) and a syringe filter

Figure 14 shows a schematic setup of a combined system with integrated Belmont® Buddy fluid warmer (see Figure 15).

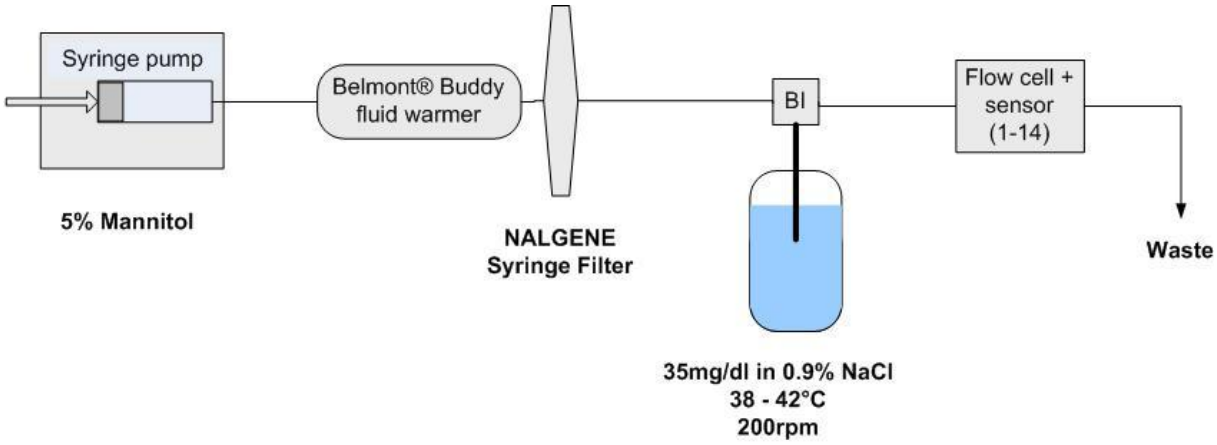

Figure 14: Schematic setup of the combined system with integrated Belmont® Buddy fluid warmer.

Figure 15: Belmont® Buddy fluid warmer with syringe filter.

To achieve the air bubble free system two additional parts were integrated: the Belmont® Buddy fluid warmer and a syringe filter (NALGENE, 0.2µm, Cat.No. 190-2520). The fluid warmer heated the perfusate to 38°C causing out-gassing of the perfusate. The adjacent syringe filter then held back all resulting air bubbles before they reached the body interface and flow cell.

For the run-in period a 5% Mannitol solution was used as perfusate and the body interfaces were immersed in pure 0.9% NaCl solution. On the next day they were immersed in a 35mg/dl glucose solution and remained in this solution for 47 hours. During the experiment the temperature of the water bath was changed stepwise from 38 to 42°C to investigate any air

bubble development caused by increasing temperature differences (temperature of perfusate in syringe vs. temperature of perfusate/dialysate in body interface).

Combined system with degassed perfusate

Based on experiments with the fluid warmer (Appendix, *Air bubble investigations*) it was concluded that degassing of the perfusate is essential to avoid out-gassing in the body interface and air bubble accumulation within the flow cell. To further avoid increased costs, complexity and additional training of the staff, a setup without the Belmont® Buddy fluid warmer was preferred.

As a consequence the perfusate in the syringe was degassed manually by applying under pressure (for detailed instructions see Appendix, *Degassing of the perfusate within a syringe applying underpressure*). To remove air bubbles caused by improper filling of the syringe a subsequent syringe filter can be used. Additional treatment of the perfusate within a heated ultra sound bath did not improve the degassing effect.

The schematic setups of the two experiments are shown in Figure 16 and Figure 17.

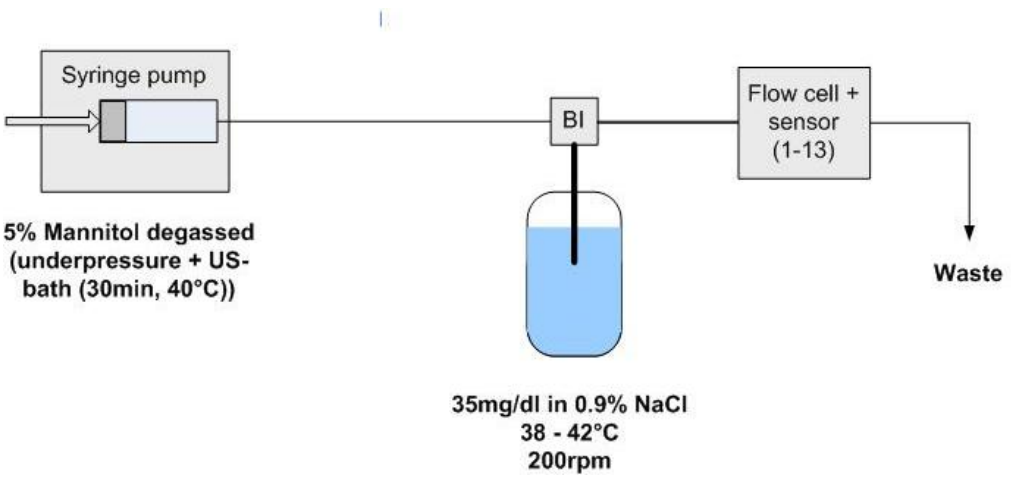

Figure 16: Schematic setup of the combined system with a degassed perfusate. The body interface (BI) was immersed into the heated test solution and the dialysate was withdrawn through the flow cell (FC) containing the BVT sensor into a waste container.

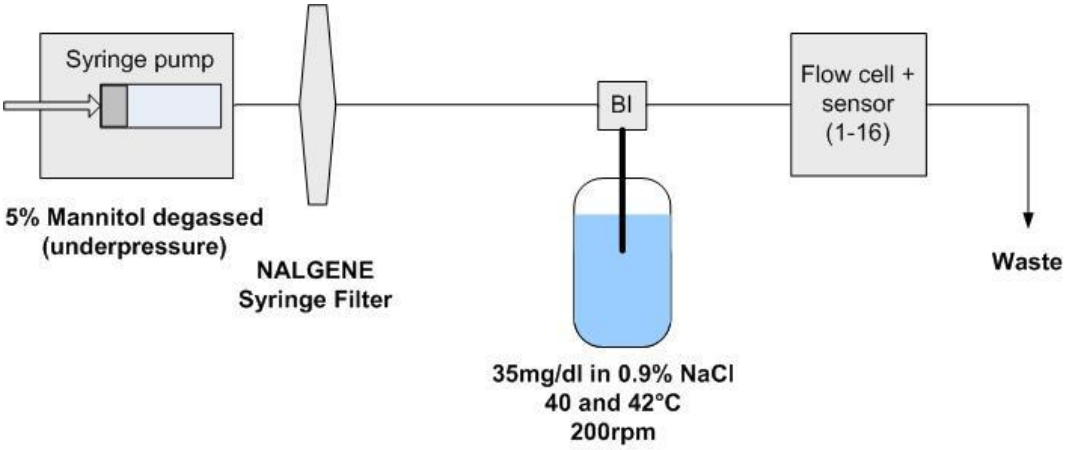

Figure 17: Schematic setup of the combined system with degassed perfusate and syringe filter. The body interface (BI) was immersed into the heated test solution and the dialysate was withdrawn through the flow cell (FC) containing the BVT sensor into a waste container.

The protocol of the setup in Figure 16 is the same as described in *Combined system with an integrated Belmont® Buddy fluid warmer (Belmont Instrument Corporation, Billerica, USA) and a syringe filter*.

The protocol for the setup in Figure 17 differed from the above as the body interfaces were immersed in a 35mg/dl NaCl-glucose solution for 91 hours and the temperature of the water bath was only changed from 40 to 42°C. In parallel to this setup a reference system was operated using normal perfusate and no filter, but the same protocol, to clearly prove that the degassing and filtering of the perfusate avoids air bubble formation.

As *3.1.6 Air Bubble Free Setup* revealed that Figure 16 and Figure 17 are the most suitable setups for the *in vivo* investigations, a setup like in Figure 17 was performed once again with the following protocol: the sensor was perfused with a 5% Mannitol solution with 2.5mg Arixtra added. During the run in period, the body interfaces were immersed in 0.9% NaCl and, on the next day, exposed to three different glucose-NaCl solutions (20, 35 and 50mg/dl) in ascending order. The body interfaces remained in the 20mg/dl solution overnight and were exposed to the same three glucose-NaCl solutions on the third day. Dialysate samples were collected and measured as described in *2.7.3 Protocol*.

2.7 In Vivo Investigations

The aim of the clinical feasibility trial was to test the combined system in 5 subjects. The main focus was to establish a stable and air bubble free microdialysis process and to record the sensor signal over 24 hours.
Moreover, the differences between reference values, dialysate values and filtered and shifted sensor current values as well as the differences between dialysate values and processed sensor values were analysed. Dialysate and sensor values were corrected applying the IRT (see *2.2 Ionic Reference Technique*).

2.7.1 Risk Management

To find the optimal setup for the clinical trial a risk management according to ISO14971:2007 [31] was introduced to manage the potential risks for patient, operator, other persons, other equipment and the environment. The risk management process focuses on four main elements: risk analysis, risk evaluation, risk control and production and post-production information (see Figure 18).

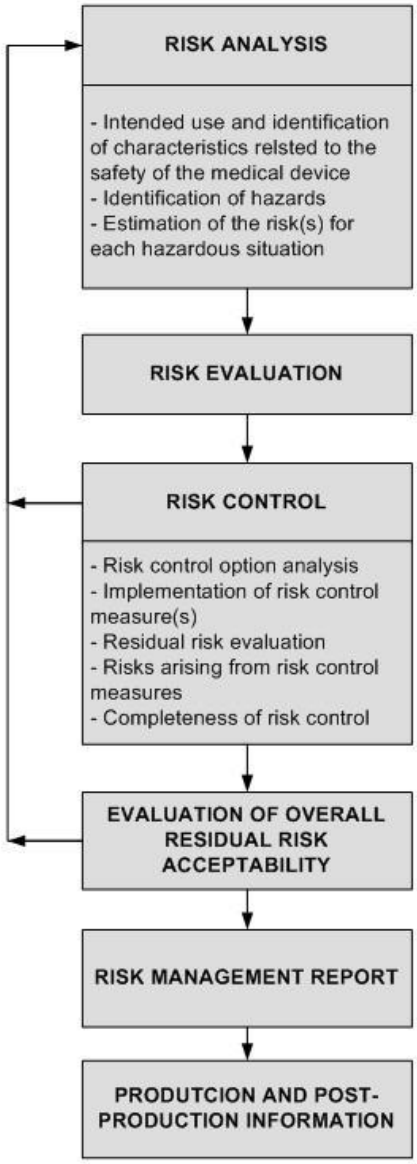

Figure 18: Risk management process according to ISO 14971:2007 **[31]**.

In two workshops, engineers, physicians, researchers, quality managers and outsiders identified as many risks as possible. These risks were then illustrated, reordered and analysed in a Fault Tree Analysis (FTA) according to ÖVE/ÖNORM EN 61025:2006 [32]. Two more workshops were organized for subsequent risk evaluation and risk control. The detailed information of the identified risks (e.g. failure mode, cause, effect, etc.), the risk evaluation (likelihood and consequence) and possible measures that could trigger new risks were recorded in a Failure Mode and Effects Analysis (FMEA) according to ÖVE/ÖNORM EN31010:2009 [33]. This data was then filled into two risk matrices (with and without measures) and evaluated regarding likelihood and severity. The risk matrix therefore clusters

risks into three different areas: acceptable area (green), ALARP-area (as low as reasonable possible, orange) and inacceptable area (red) shown in Figure 19 (details see Appendix, Figure 63).

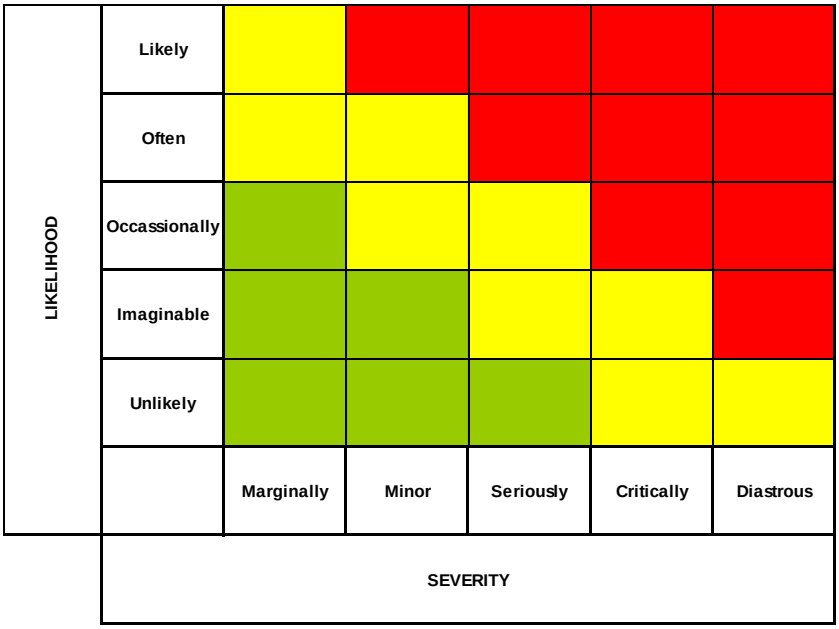

Figure 19: Risk matrix template.

The aim of the risk management process was to eliminate all inacceptable risks by inherent safe design, protective measures in the device itself or the manufacturing process or safety information as a last possible opportunity. [31]
Required measures identified during the risk management process or the subsequent safety check were integrated in the final *in vivo* setup.

2.7.2 Safety Check

During the risk management process, electrical, thermal and biological hazards were identified as major risks.

To perform the safety check, the combined system (see Figure 24) was classified according to IEC 60601-1 [34] to ensure a safe application in humans.
The classification defines the limits for the essential electrical safety parameters (leakage currents) of the safety check as shown in Table 3:

Current in microamperes

CURRENT	TYPE B APPLIED PART		TYPE BF APPLIED PART		TYPE CF APPLIED PART	
	NORMAL CONDITION	SINGLE FAULT CONDITION	NORMAL CONDITION	SINGLE FAULT CONDITION	NORMAL CONDITION	SINGLE FAULT CONDITION
PATIENT LEAKAGE CURRENT and PATIENT AUXILIARY CURRENT d.c.	10	50	10	50	10	50
PATIENT LEAKAGE CURRENT and PATIENT AUXILIARY CURRENT a.c.	100	500	100	500	10	50
Total PATIENT LEAKAGE CURRENT d.c.	50	100	50	100	50	100
Total PATIENT LEAKAGE CURRENT a.c.	500	1000	500	1000	50	100
PATIENT LEAKAGE CURRENT with MAXIMUM MAINS VOLTAGE on non-PROTECTIVELY EARTHED ACCESSIBLE PART	500		500		Note 4	
Total PATIENT LEAKAGE CURRENT with MAXIMUM MAINS VOLTAGE on unearthed ACCESSIBLE PART	1000		1000		Note 4	
PATIENT LEAKAGE CURRENT with MAXIMUM MAINS VOLTAGE on APPLIED PART	—		5000		50	
Total PATIENT LEAKAGE CURRENT with MAXIMUM MAINS VOLTAGE on APPLIED PART	—		5000		100	

NOTE 1 For EARTH LEAKAGE CURRENT see 8.7.3 *d)*.

NOTE 2 For TOUCH CURRENT see 8.7.3 *c)*.

NOTE 3 The condition referred to in Table IV of the 2nd edition as "MAINS VOLTAGE on APPLIED PART", and treated in that edition as a SINGLE FAULT CONDITION, is treated in this edition as a special test condition. The test with MAXIMUM MAINS VOLTAGE on a non-PROTECTIVELY EARTHED ACCESSIBLE PART is also a special test condition, but the allowable values are the same as for SINGLE FAULT CONDITION. See also the rationales for 8.5.2.2 and 8.7.4.7 *d)*.

NOTE 4 This condition is not tested with TYPE CF APPLIED PARTS because it is covered by the test with MAXIMUM MAINS VOLTAGE on the APPLIED PART. See also the rationale for 8.7.4.7 *d)*.

Table 3: Limits of the electrical safety parameters for applied parts TYPE B, BF and C according to IEC 60601-1 **[34]**.

The following safety parameters were tested for electrical safety with the BENDER safety tester (BENTRON, Type Unimet 1100ST): Protective earth (PE) resistance, PE measuring current, load current operating voltage, power consumption, earth leakage current, patient leakage current, patient auxiliary current, and enclosure current (equivalent to the touch current). Detailed information about the definition and related test procedures of these safety parameters can be found in the Appendix, *Electrical Safety Check*. Furthermore, the allowed thresholds are shown in the protocols. The schematic setup for the safety check of the final system is shown in Figure 20:

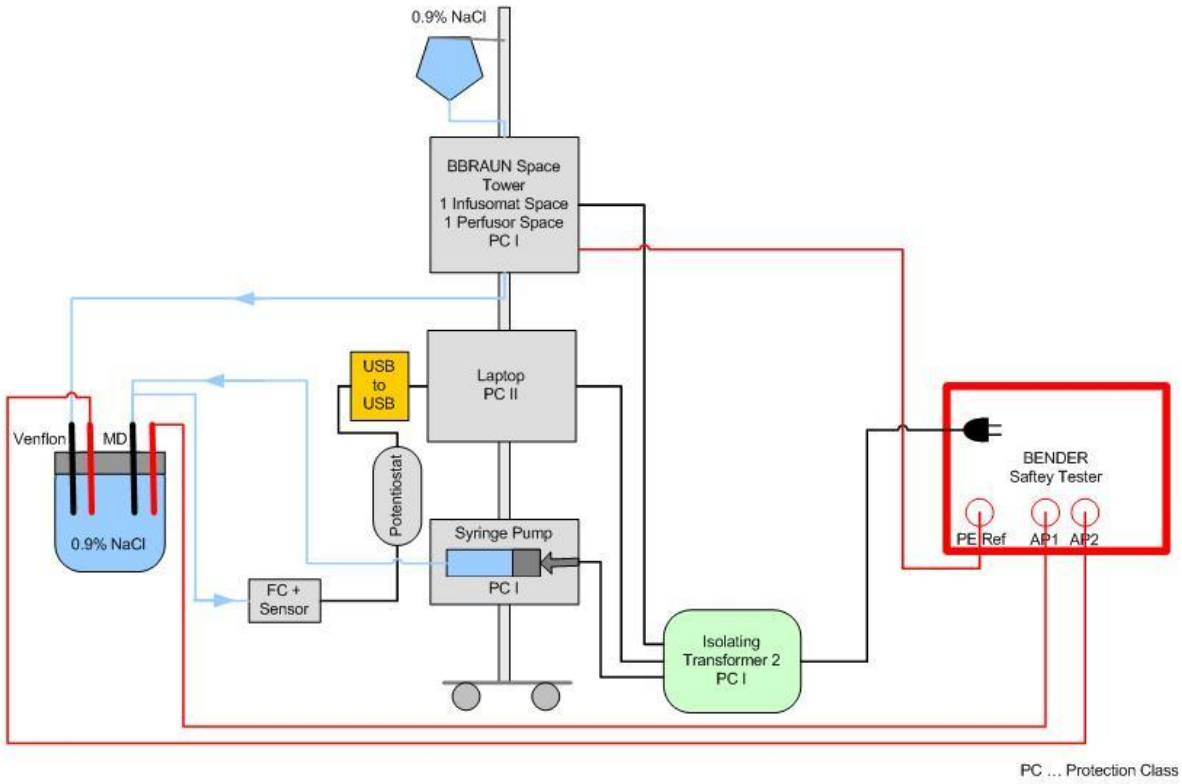

Figure 20: Schematic setup of the electrical safety check of the final combined system with the BENDER safety tester.

To avoid any hazard caused by hot applied parts, the temperature limitations according to IEC 60601-1 (listed in Table 4) were taken into consideration.

APPLIED PARTS of ME EQUIPMENT		Maximum Temperature, °C [b) c)]		
		Metal and Liquids	Glass, Porcelain, Vitreous Material	Moulded Material, Plastic, Rubber, Wood
APPLIED PART having contact with the PATIENT for a time "*t*".	$t < 1$ min	51	56	60
	1 min $\leq t <$ 10 min	48	48	48
	10 min $\leq t$	43	43	43

a) The likelihood (probability) of contact and of the duration of contact shall be determined and documented in the RISK MANAGEMENT FILE.

b) These temperature limit values are applicable for the healthy skin of adults. They are not applicable when large areas of the skin (10% of total body surface or more) can be in contact with a hot surface. They are not applicable in the case of skin contact with over 10% of the head surface.

c) Where it is necessary for APPLIED PARTS to exceed the temperature limits of Table 20 in order to provide clinical benefit, the RISK MANAGEMENT FILE shall contain documentation showing that the resulting benefit exceeds any associated increase in RISK.

Table 4: Temperature limitations for ME equipment according to IEC 60601-1 **[34]**.

The maximum occurring temperature was evaluated by calculating the maximum power that can be delivered by the potentiostat and, thus, generated within the applied part. Therefore a resistance of 33Ω (three 100Ω resistors in parallel) was operated at maximum voltage of 2V

and current of 60mA to simulate the maximum occurring power of 120mW. Temperature was then recorded using the TESTO temperature logger (177-T3, Testo GmbH, Wien, AT).

Biological hazards could not be evaluated in a sufficient manner as the BVT sensor and flow cell, as well as the PHARMED BPT tubing, were unsterile. Thus these hazards had to be avoided in construction by using a 5cm tubing between body interface and flow cell, and by employing trained personnel using standard operating procedures, to avoid any backflow of the possibly contaminated dialysate from the flow cell to the subject.

2.7.3 Protocol

The clinical trial to test the combined system was designed as a 24 hour open mono-centre clinical feasibility trial in 5 diabetic subjects. It was approved by the local Ethics Committee of the Medical University of Graz and the Austrian Agency of Health and Food Safety (AGES) and performed according to the GCP guidelines [35]. Subjects were treated according to the declaration of Helsinki [36]. All subjects signed an informed consent before any trial specific actions were taken.

The five subjects were manually clamped to four glucose levels for six hours by using glucose and insulin infusions. Figure 21 illustrates the schematic process.
Blood and dialysate samples were collected every 15 minutes and analysed offline for glucose (see *2.4.3 Glucose Measurement*). The dialysate samples were further analysed offline for conductivity (see *2.4.2 Conductivity Measurement*). The current of the BVT glucose sensor was recorded every 10 seconds and represented an online measurement of the dialysate.
The aim of this trial was to evaluate sampling process, impact of the added anticoagulant Arixtra® (added to the perfusate or added to the perfusate and injected subcutaneously), performance of the glucose sensor and adequate monitoring of the blood glucose.

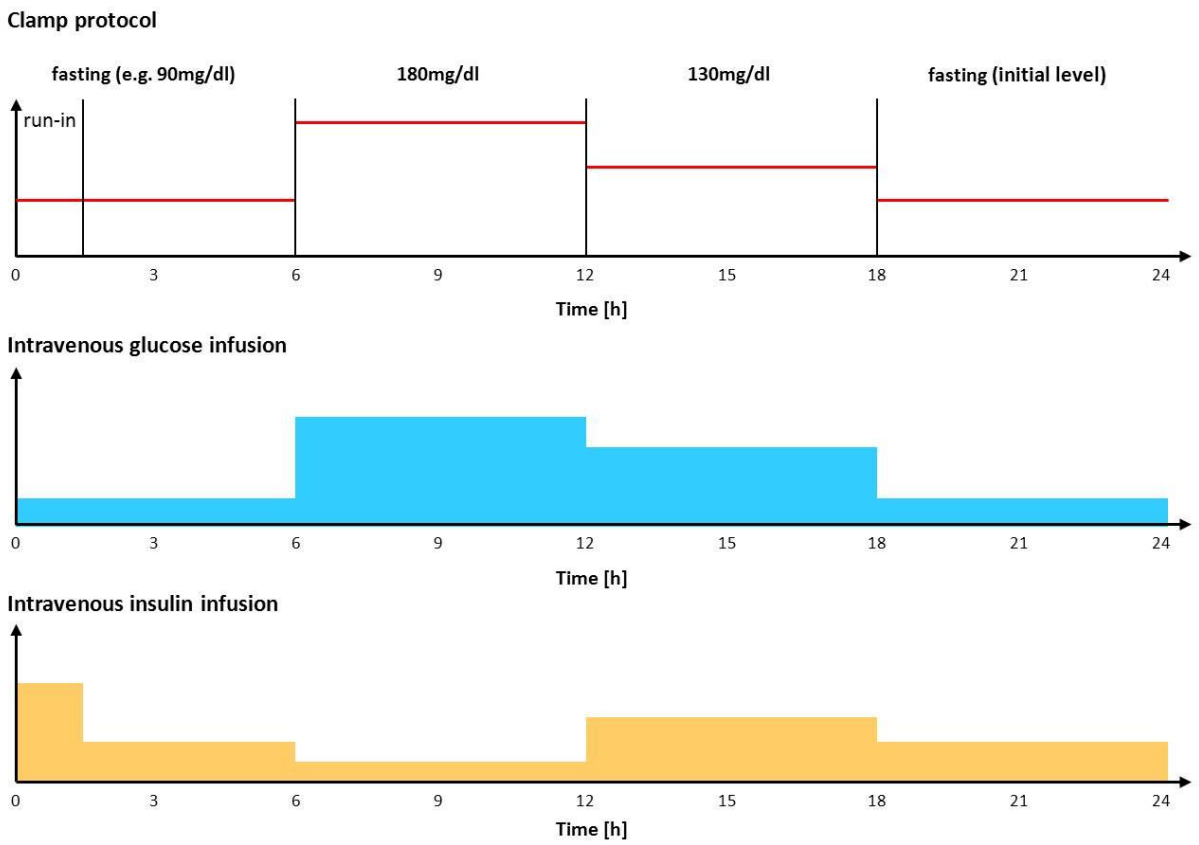

Figure 21: Protocol of the clinical trial. Profiles for glucose and insulin infusions are exemplarily.

Preconditioning of Sensor and MD Probe

The BVT sensors were run in overnight with an external syringe pump (BBRAUN Perfusor fm, Ref: 8713820) that pumped a 5% Mannitol – 0.9% NaCl (4:1) solution through a CODAN extension tubing (E87, Ref: 71.4473, 15cm, Ø = 0.9/2.0mm). This extension tubing was connected to a Nordson Precsion tip (Ref: 7018314, TIP 23GA. 013X.5 orange) to further connect to a PHARMED BPT tubing which could then be attached to the flow cell containing the BVT sensor. PHARMED BPT tubing, a tip and extension tubing with a male luer to luer adapter (COLE PARMER, Ref: AAQ13050) were used to withdraw the perfusate from the flow cell's outlet into a waste container (see Figure 22). The run in data was recorded with the laptop and the EmStat potentiostat that were then also used for the *in vivo* investigation.
Two sensors per subject were run in to allow an exchange of flow cell and sensor during the trial if problems with the sensor unit arose.

While the venous catheters were placed in the subject's arms, the MD probe was attached to the syringe pump and perfused with the perfusate. During that time the MD probe remained in the sterile package and was inserted into the venous catheter as soon as perfusate leaked from its outlet. At the same time, the extension tubing between the flow cell and the run in pump was disconnected from the syringe pump and connected to the luer to luer adapter of the flow cell's outlet tubing (see Figure 22). Therewith, the sensor could not run dry and was attached to the MD probe's outlet as soon as it was inserted into the venous catheter.

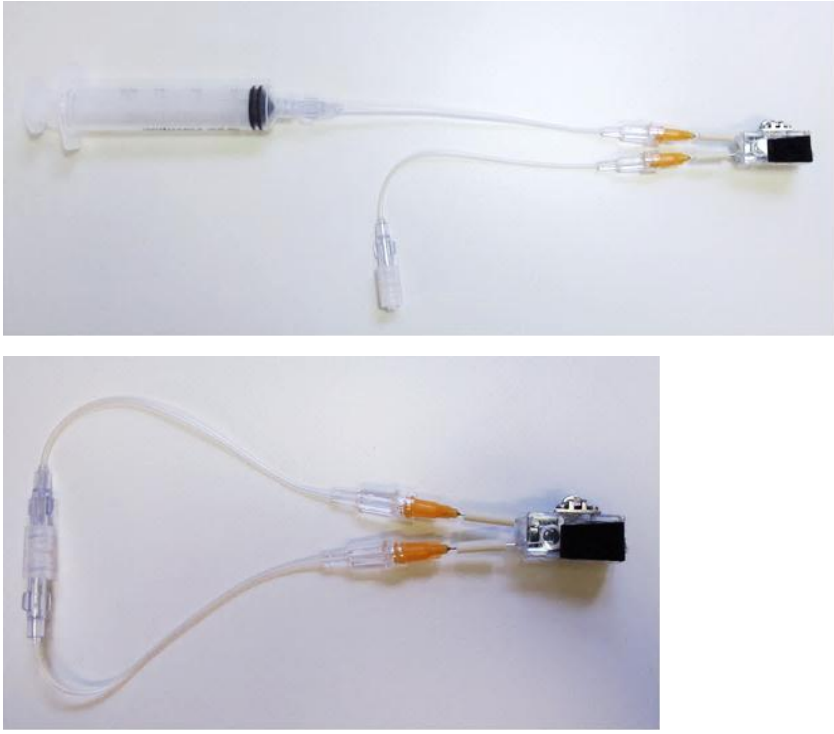

Figure 22: Run in tubing for the BVT sensor.

Clamp Procedure

All 5 subjects suffered from type 1 diabetes. Three peripheral venous catheters per subject were implanted (see Figure 20).

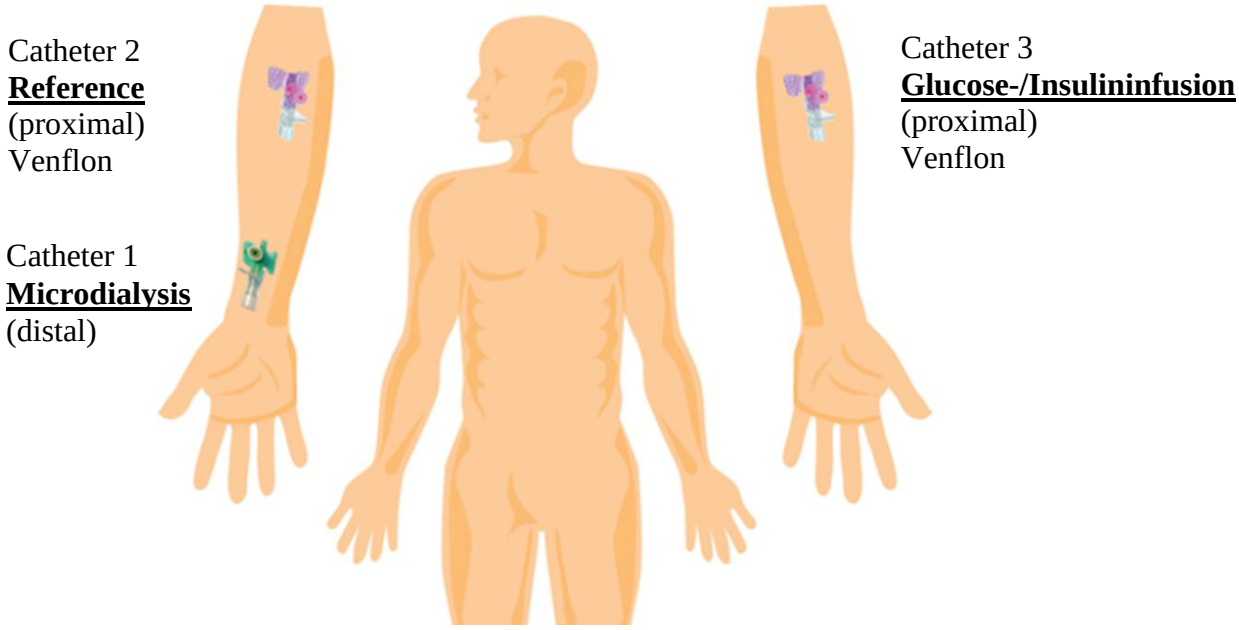

Figure 23: Position and function of the three venous catheters.

The MicroEye PME011 microdialysis probe (Figure 23, catheter 1) of the combined glucose monitoring unit was placed distally to one arm of the subject. The proximal catheter 2 was used for reference blood sampling and was always located on the same arm as the glucose monitoring unit. Furthermore, catheter 2 was placed proximally to avoid a dilution of the collected dialysate samples and, thus, an influence of infused flushing fluids on the glucose monitoring unit. Additionally, the proximal catheter 3 was used for glucose and insulin infusion and placed on the opposite arm to avoid an influence of the glucose monitoring unit by infused glucose solution.

During the first 6 hours of the clamp, the subjects were infused with insulin and glucose to obtain a euglycaemic blood glucose level of approximately 90mg/dl. After these 6 hours an intravenous glucose bolus was given to reach the 180mg/dl glucose clamp level within minutes. After the infusion of the bolus the blood glucose was clamped to a level of 180mg/dl for 6 hours and 130mg/dl for another 6 hours subsequently. Throughout the last 6 hours of the experiment the subjects were clamped to the same euglycaemic level as at the beginning of the experiment (i.e. 90mg/dl). All subjects had breakfast during the last hour of the trial and

were taken for ultrasound examination to survey the condition of the implanted microdialysis probes afterwards.

Blood Sampling Procedure

Every 15 minutes, reference blood samples of approximately 200µl were taken from the reference catheter and the Venflon was flushed with a 0.9% saline solution. These samples were immediately centrifuged to generate supernatant plasma which was measured offline for glucose with the Super GL2. Thus, these blood glucose values reflected a point measurement every 15 minutes. Furthermore, four blood samples for ion determination were taken after 9, 15 and 24 hours.

Dialysate Sampling Procedure

As the dialysate was collected in Eppendorf tubes (1500µl) for 15 minutes, it reflected a time integrated glucose and ion concentration. Ideally, 96 dialysate samples per system were collected throughout 24 hours and were analysed offline for weight, ion and glucose concentration.

Due to the high flow rate, the glucose concentration of the dialysate samples was lower than the lower limit of quantification (LLOQ) of the glucose analyser Super GL2, but, as at least 150µl of dialysate were collected, 100µl instead of the requested 20µl were pipetted into the Glucocapil caps and analysed. Consequently, results had to be corrected for volume and glucose concentration as described in *2.4.3 Glucose Measurement*.

Sensor Measurement

The glucose and ion enriched dialysate passed the BVT flow cell containing the sensor before being collected in Eppendorf tubes. The sensor's settings were described in *2.4.1 Glucose Sensing.* The values delivered by the sensor reflected point measurements every 10 seconds.

2.7.4 Setup Overview

A schematic overview of the whole *in vivo* setup is shown in Figure 24. A Venflon was placed in the subject's vein to attach the MicroEye microdialysis probe PME011 (refer to *2.7.7 Body Interface*). The microdialysis probe was operated using a syringe pump in push mode (BBRAUN, Perfusor fm). The pump was attached to the microdialysis probe using a rigid and stiff tubing (CODAN, E87-P) to avoid an influence on the flow by being unintentionally squeezed. The perfusate was pumped through the microdialysis probe, the

BVT flow cell containing the glucose sensor and collected in probe containers (Eppendorf tubes) for offline glucose and conductivity analysis (refer to sampling unit and sensor in Figure 26). In parallel, sensor currents were recorded via EmStat potentiostat using PSTrace software.

Subjects were clamped manually by infusing glucose and insulin via a BBRAUN Space Tower containing a BBRAUN Infusomat Space and a BBRAUN Perfusor Space.

As a safety measure, derived from the risk assessment procedure, an isolating transformer and an USB to USB isolator containing an optocoupler were used to reduce hazardous leakage and touch currents for the subjects. Two systems (Sys1 and Sys2) were manufactured and tested for these experiments. A list of the all components and used disposable parts can be found in the Appendix, Table 12 - Table 14.

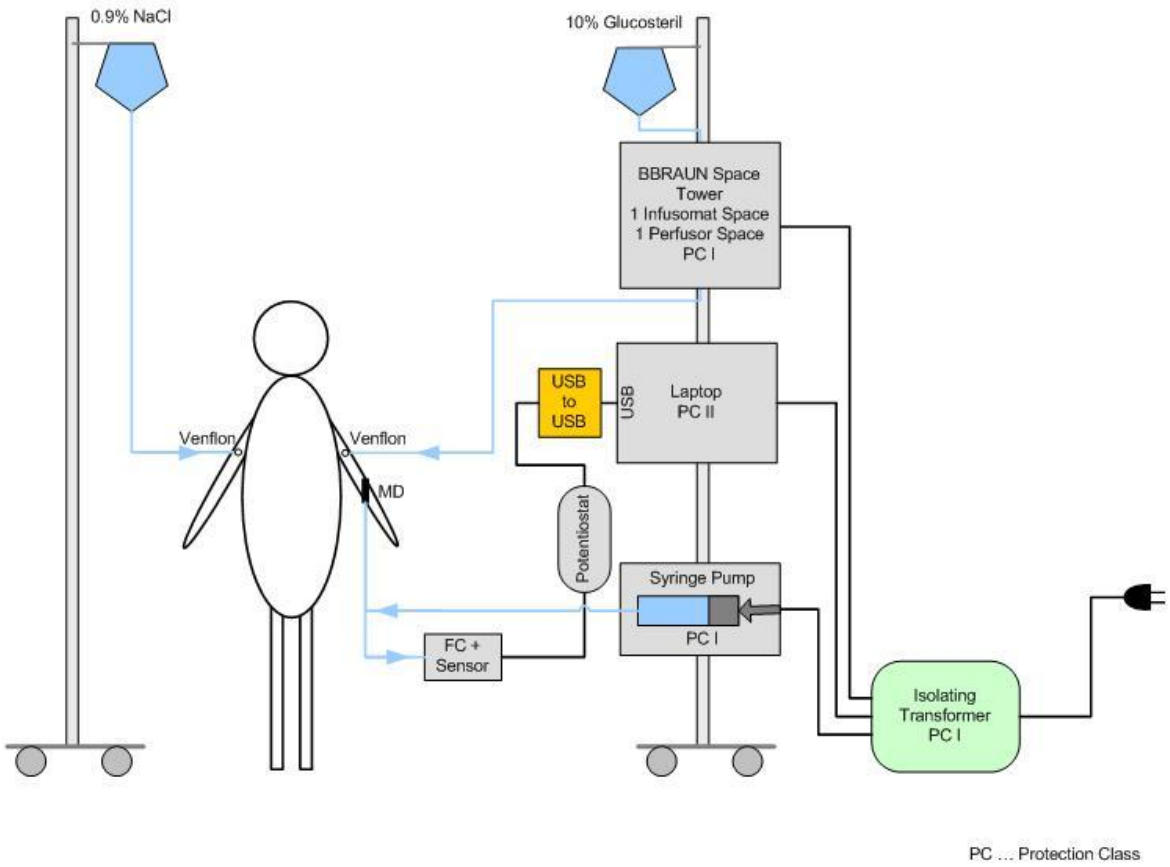

Figure 24: Schematic overview of the *in vivo* setup of the glucose monitoring unit.

2.7.5 Flow Rates

It was concluded from prior *in vivo* experiments [11] that the best correlation between blood and dialysate glucose can be achieved with recoveries higher than 10%. During the clamp phase of 180 mg/dl this would imply a concentration of at least 18 mg/dl glucose in the dialysate. The measurement range of the BVT sensor, however, is only up to 20mg/dl. This limits the applicable recovery to a maximum of 10% and therefore requires a flow rate of 20µl/min. Moreover, the recovery rate of the body interfaces changes over time and sometimes even decreases by a factor of 6 (see *3.2.5 Recovery*, Figure 44). In order to compensate for these changing recoveries, the flow rate was sometimes adjusted during the experiments. The flow rate of subject 021 was set to 10µl/min throughout the experiment. Subject 023 and 026 arrived with blood glucose levels around 200mg/dl and the flow rate was therefore set to 20µl/min at the beginning of the experiment. The flow rate of subject 023 was then reduced to 10µl/min when the dialysate glucose fell below 5mg/dl. Subjects 024 and 025 started with a flow rate of 10µl/min which was then raised to 20µl/min when the clamp phase of 180mg/dl started.

2.7.6 Perfusate and Anticoagulation (Arixtra®)

5% Mannitol, an iso-osmotic and ion-free sugar alcohol, was used as matrix for the perfusate. As, however, the sensor and the Super GL2 showed an ion dependency (see *3.1.2 Ion Dependency* and *2.4.3 Glucose Measurement*), 0.9% saline solution was added to the perfusate in a ratio of 4:1. This basic conductivity then had to be considered when calculating the ion recovery of the dialysate (details see *2.2 Ionic Reference Technique*). Effectiveness of different anticoagulants was investigated by Andreas Huber [11]. Based upon his findings the anticoagulant Arixtra® (GlaxoSmithKline, fondaparinux-sodium, 2.5mg/0.5ml) was added to the perfusate to reduce agglutination effects on the membrane of the microdialysis probe. To further reduce agglutination effects, four out of five subjects were systemically anticoagulated by receiving additional Arixtra® subcutaneously. Thus, subject 021 received 5mg Arixtra® in 45ml perfusate whereas subjects 023 – 026 received 2.5mg Arixtra® in 45ml perfusate and 2.5mgArixtra® subcutaneously.

Regarding the *in vitro* results (see *3.1.6 Air Bubble Free Setup*), the perfusate was manually degassed with underpressure to avoid air bubble formation (detailed instruction see Appendix, *Degassing of the perfusate within a syringe applying underpressure*).

2.7.7 Body Interface

During the investigations, the CE-certified, single-use and sterile microdialysis probe MicroEye PME011 from Probe Scientific, Ltd., Coventry, UK (http://www.probescientific.com/) for human use was used together with a Vasofix Safety 18G, 45mm venous catheter (see Figure 25). The MicroEye PME011 has a membrane length of 20mm, a cut-off of 10kDa and can be operated with a maximum flow of 50µl/min. After the experiment, the microdialysis probe had to be removed, together with the venous catheter, to reduce the risk of membrane breakage and scraping off potential clots which could possibly lead to embolisms.

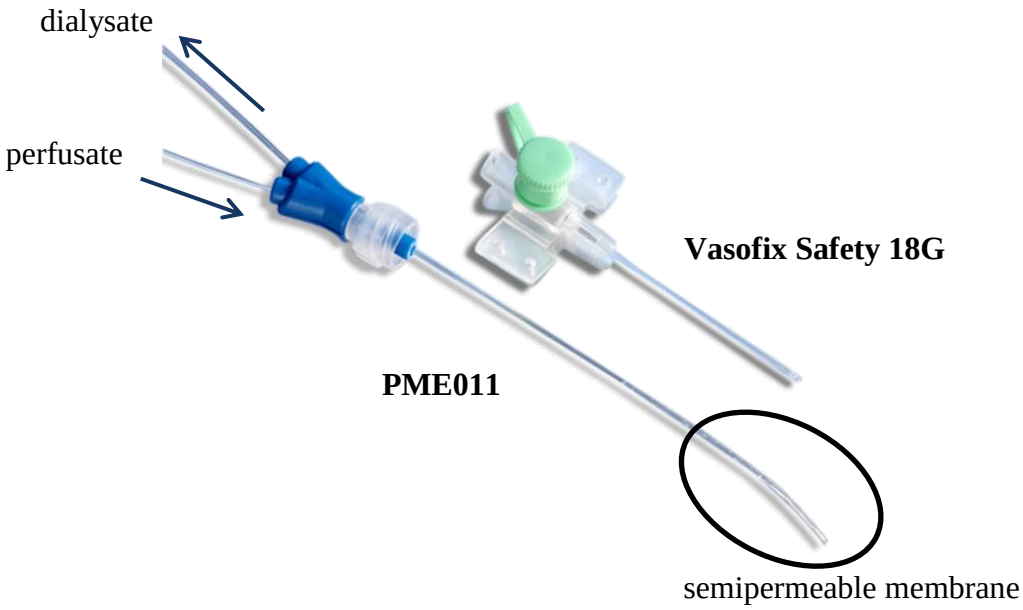

Figure 25: MicroEye PME011 and Vasofix Safety 18G venous catheter.

2.7.8 Perfusate Container, Tubing and Sampling Containers

A 50ml BBRAUN OPS Perfusor syringe was used as a perfusate container. After degassing the perfusate it was inserted into the syringe pump (BBRAUN, Perfusor fm). The syringe was connected to the microdialysis probe via a stiff and rigid extension line (CODAN, E87-P). This tubing was used to minimize flow artefacts and fluctuations resulting from unintended squeezing of the tubing.

The outlet tubing of the microdialysis probe was then shortened and connected with the flow cell through a PHARMED BPT tubing from COLE PARMER. The leftover of the MD outlet

tubing was again connected with a PHARMED BPT tubing to the flow cell's outlet to transfer the dialysate from the flow cell to the sampling containers. The end of this leftover tubing was then led through the cap of a perforated Eppendorf tube. A second perforation was used as ventilation hole to prevent increasing pressure within the tube. This cap was plugged into 1500µl Eppendorf tubes that had been labelled, colour-coded and weighed prior the experiment and were used as sampling containers (see Figure 26).

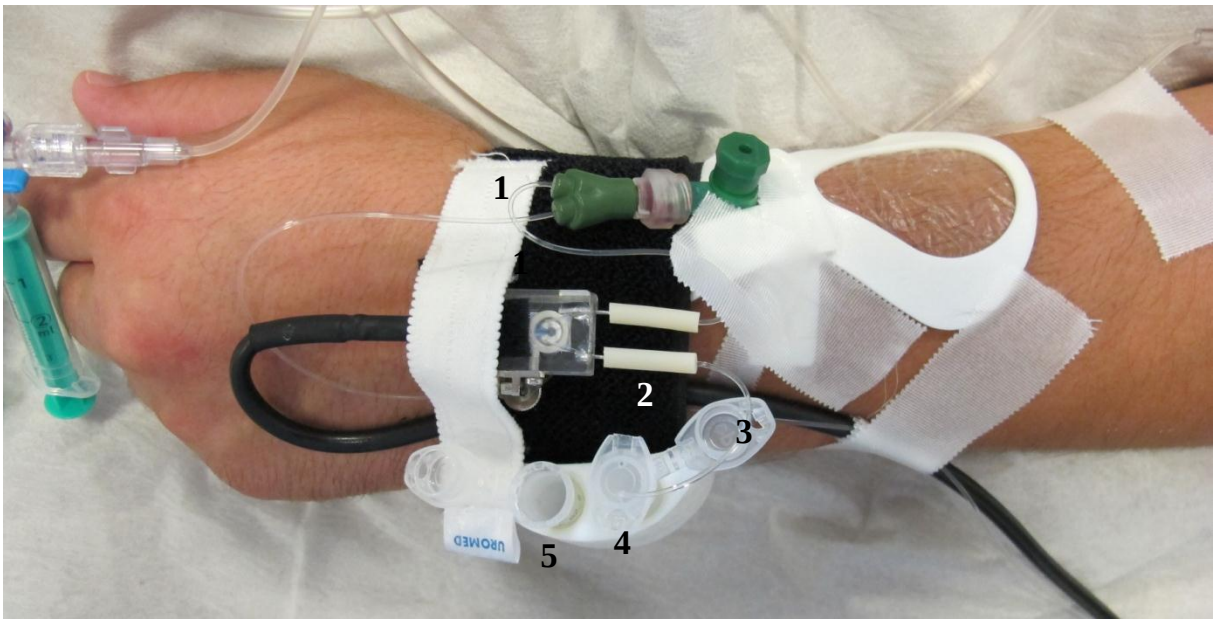

Figure 26: Tubing and sampling containers during *in vivo* investigations. The shortened MD outlet tubing[1] was connected to the flow cell via BPT PHARMED tubing[2]. The leftover of the MD outlet tubing[3] was attached to the flow cell's outlet to draw the dialysate through the cap of a perforated Eppendorf tube[4] into the sampling container[5].

3 RESULTS

3.1 In Vitro Investigations

3.1.1 Calibration Curve

The calibration curve in phosphate buffer performed by BVT Technologies, Brno, CZ indicates a linear measurement range up to 20mg/dl and is shown in Figure 56 in the Appendix.

Figure 27 shows the sensor current used for the calibration curve and linearity analysis in un-buffered 5% Mannitol – 0.9% NaCl (9:1) solution. The sensor current is plotted as a blue solid line on the first y-axis. The experimental protocol (13 different glucose solutions) is plotted as a red dashed line and the room temperature as a pink dashed line on the second y-axis. The sensor showed a zero current of approximately 5nA after about 16 hours running in in a 5% Mannitol – 0.9% NaCl solution.

When exposed to the glucose test solutions the sensor quickly responded and showed hardly any artefacts or fluctuations at the lower glucose steps, however, the higher the glucose concentrations the stronger the fluctuations. In general, the sensor current in un-buffered solution is lower compared to the experiments in phosphate buffer (see Appendix, Figure 57). No air bubbles interrupted the measurement and room temperature was constant throughout the experiment.

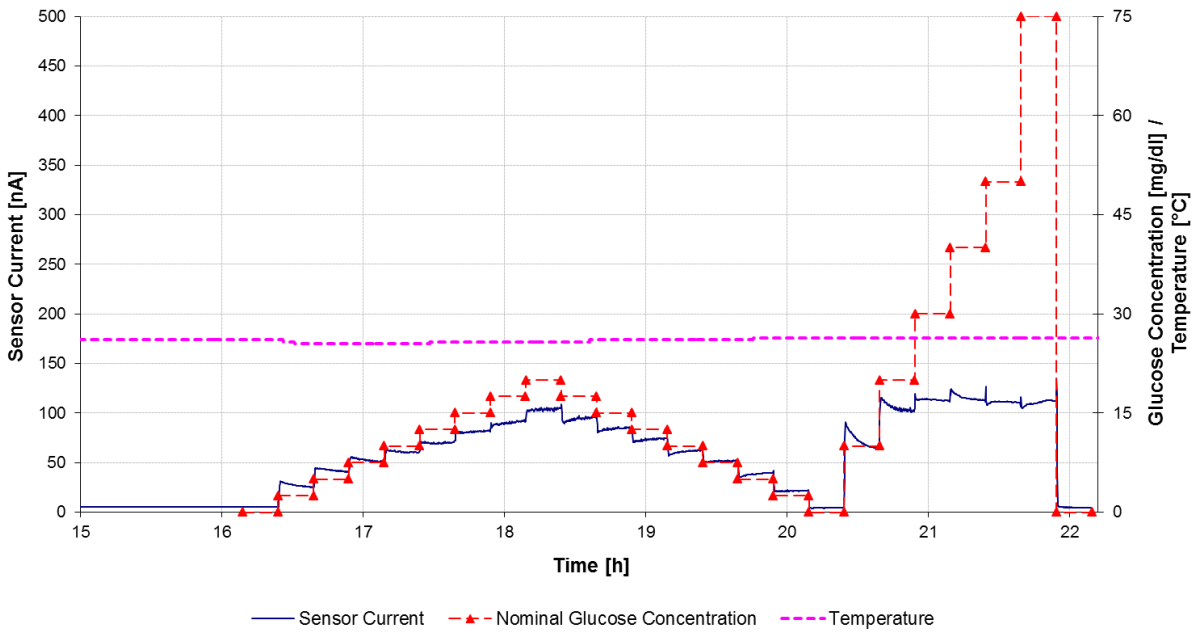

Figure 27: Blow-up of the sensor current for analysing the calibration curve and the linear behaviour of the sensor in un-buffered 5% Mannitol - 0.9% NaCl solution (ratio 9:1).

Figure 28 shows the calibration curve of the BVT sensor in un-buffered solution in a range from 0 to 75mg/dl D-glucose. The sensor shows a linear behaviour up to 10mg/dl D-glucose and a reduced linear behaviour up to 20mg/dl. Glucose concentrations above 20mg/dl unsettle the sensor and it no longer responds to increasing glucose concentrations (strong saturation effects). This experiment indicates that the sensor should only be operated in a glucose range up to 20mg/dl.

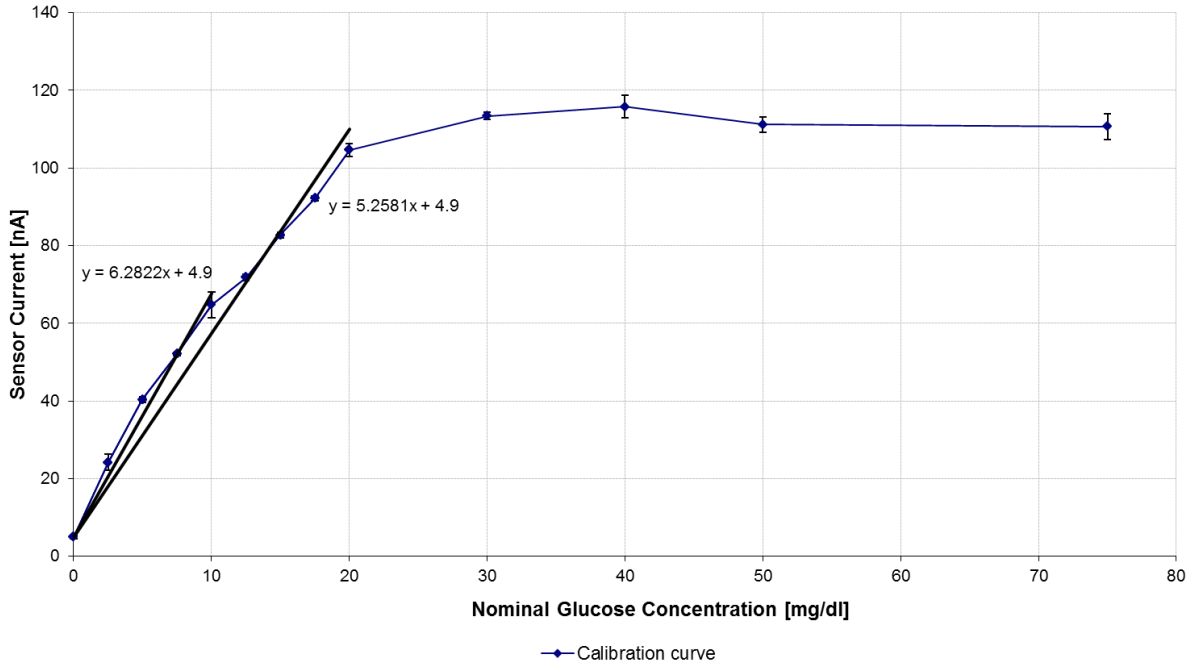

Figure 28: Calibration curve of the BVT glucose sensor in un-buffered 5% Mannitol - 0.9% NaCl (9:1) solution. The plot shows the mean values of the glucose steps in Figure 27 with their standard deviations. Moreover linear trends for 10mg/dl and 20m/dl are displayed.

3.1.2 Ion Dependency

The impact of different ion concentrations within the Mannitol-glucose test solutions yield the following calibration curves averaged over 8 sensors:

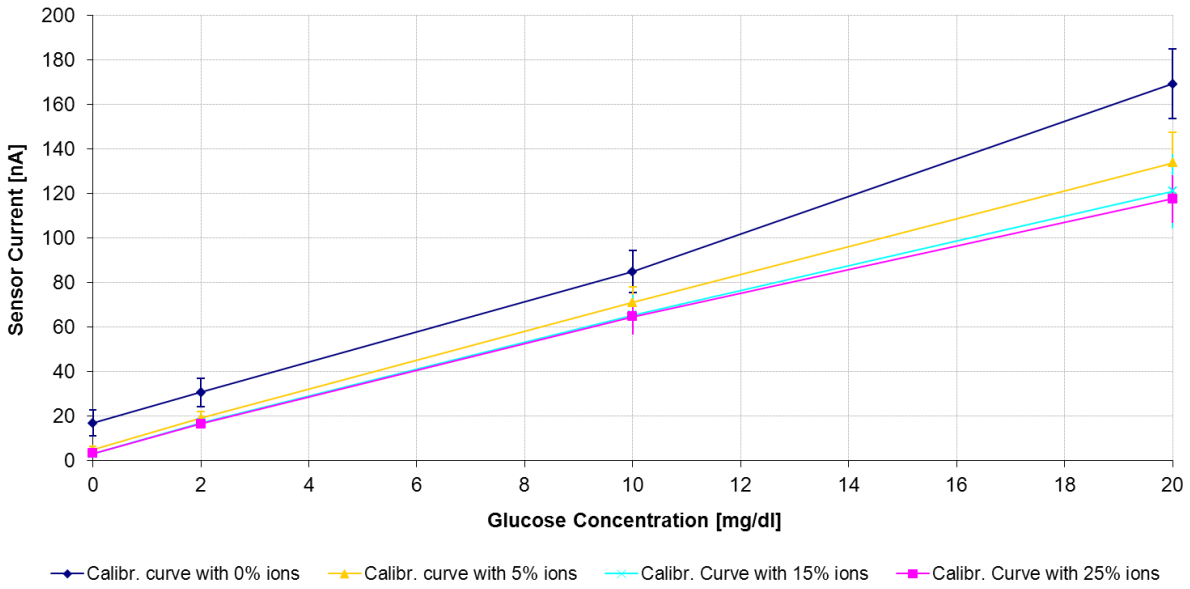

Figure 29: Mean calibration curve of 8 BVT sensors exposed to different ion and glucose concentrations to investigate the sensor's ion dependency. Shown are mean values and standard deviation of the second half of the glucose steps to exclude any stabilisation process after changing the cup with test solution.

Figure 29 shows that higher ion concentrations lead to lower sensor currents. By trend, the calibration curve for solutions without ions shows larger standard deviations even at low glucose concentrations. The calibration curves for 15 and 25% ion concentration are almost identical and therefore suggest that the sensor needs an ion concentration of at least 15% in the dialysate to deliver stable and ion independent values. As a result of this, together with the findings concerning the ion dependency of the Super GL2 in *2.4.3 Glucose Measurement*, the *in vivo* perfusate was then composed of 5% Mannitol with 20% ions (see *2.7.6 Perfusate and Anticoagulation (Arixtra®)*).

Furthermore, all calibration curves except the one for solutions without ions show good linearity up to 20mg/dl.

3.1.3 Response Time

To eliminate the time delay between reference values and sensor response, experiments with the combined system were performed (protocol and results described in the Appendix, *Response time investigations in the final combined system* and Figure 58 and Figure 59) and the time delay caused by the microdialysis process and the fluidics was thereby investigated. Figure 30 shows that the sensor needed 1.8 minutes to react when the body interface was immersed in a new glucose-NaCl solution at a flow rate of 20µl/min. The experiments once again showed that the sensor itself reacts quickly when exposed to glucose. As a result, the sensor current was shifted for data evaluation as described in *2.5.2 Correction of Fluidic Delay Time*.

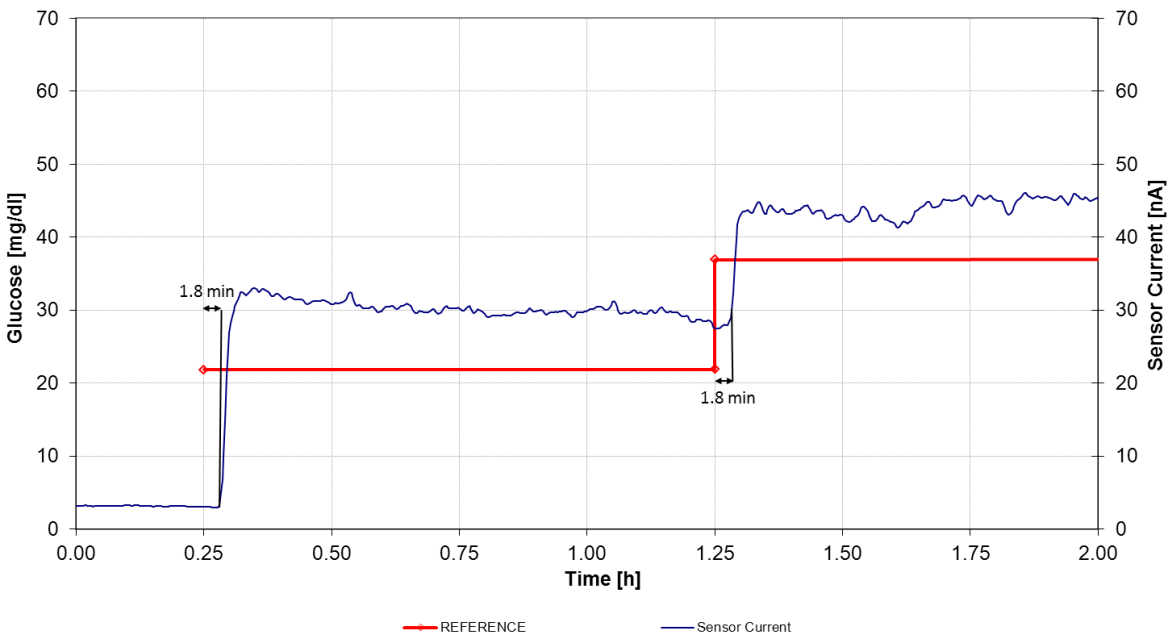

Figure 30: *In vitro* time delay of the combined system with a 5cm tubing between body interface and flow cell.

3.1.4 Long-term Stability

Figure 31 shows that the BVT sensor within the combined system drifted approximately 8mg/dl within 20 hours. This implies a drift of 0.4mg/dl per hour. Due to the short calibration interval (30min – 4h) that was applied onto the sensor data, this drift did not need to be corrected during the 24 hour trial.

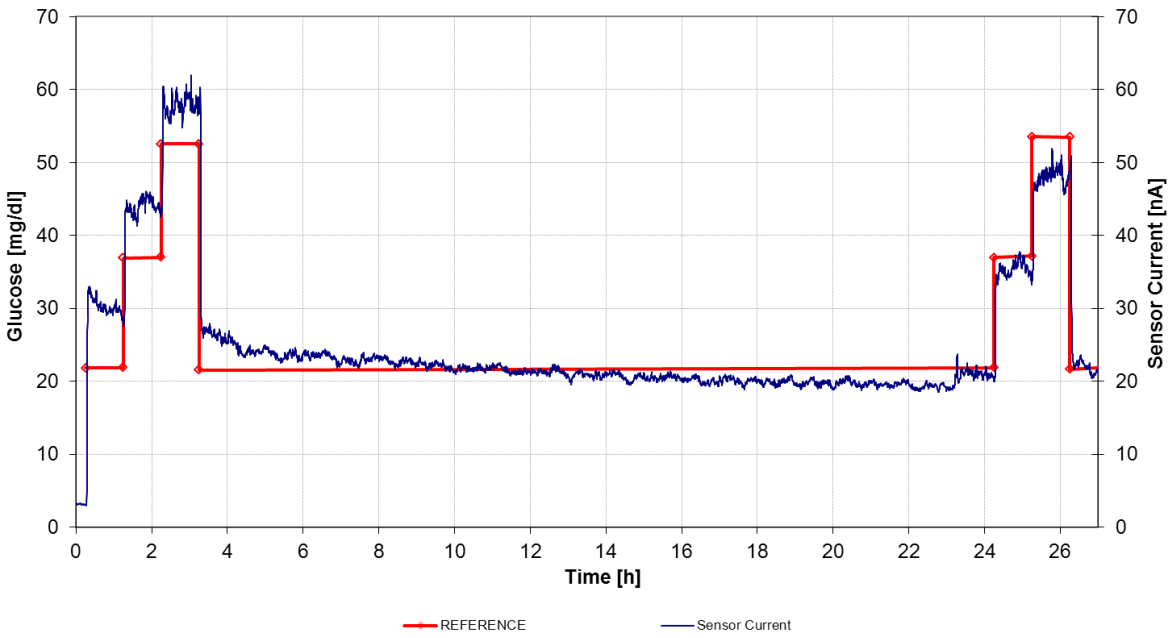

Figure 31: Long term stability and drift of the BVT sensor within the combined system.

3.1.5 Air Bubble Problems

During the *in vitro* investigations, air bubbles accumulated in the flow channel near the active area of the sensor and therefore influenced the measurement.

When filling the flow cell with test solution, air was often trapped in the narrow gap beside the flow channel of the flow cell (see Figure 32A). These air bubbles usually remained in their position throughout the experiment. They had no apparent impact on the sensor signal, but probably led to noisy sensor currents due to pulsatile movements. When air bubbles were present in the input tubing (e.g. due to improper filling of the syringe or outgassing effects in the MD probe, see Figure 32D) they most likely got stuck at the inlet of the flow channel (see Figure 32A). Additional air bubbles were accumulating at the same position and started to

cover parts of the sensor's active area (see Figure 32B) or even the whole channel (see Figure 32C). As a result, the sensor current decreased or even fell back to its zero current.

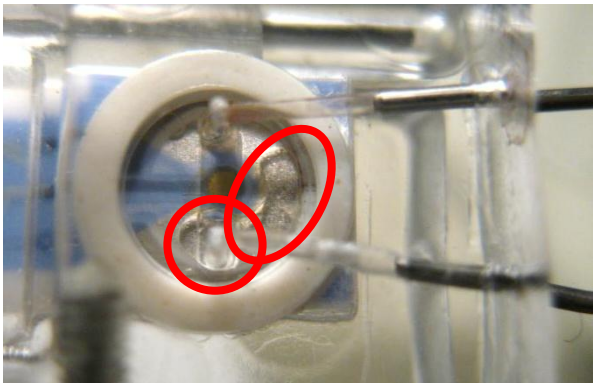

Figure 32A: Air bubbles were trapped in the narrow gap or were growing at the flow cell's inlet.

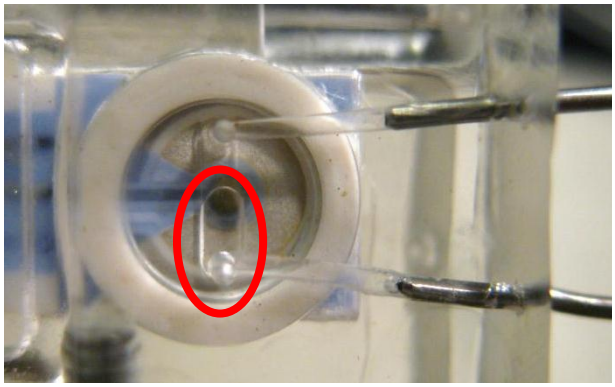

B: Air bubble growing and partly covering the working electrode.

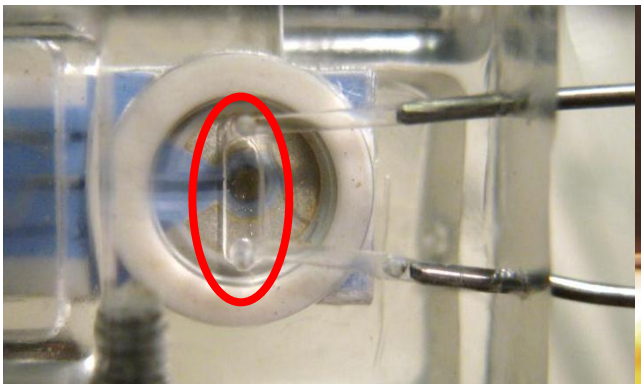

C: Air bubble totally covering the working electrode.

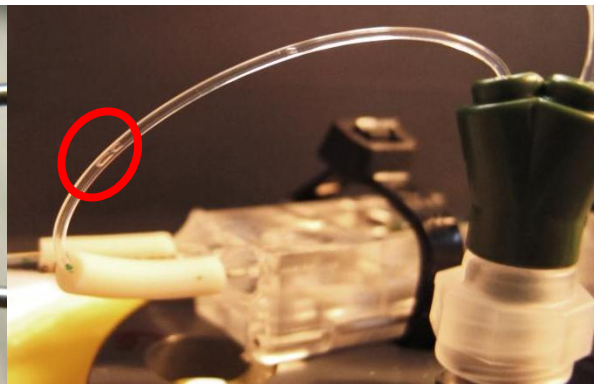

D: Air bubbles forming due to outgassing effects in the BI and flowing to the flow cell.

In general, air bubbles caught in the flow channel could not be removed by applying higher flow rates. They sometimes left the flow channel without any supporting action, or were sucked into the narrow gap. If they did not leave the flow channel they could also be manually flushed out of the flow cell by directly injecting up to 3ml of perfusate with a small syringe (detailed description see Appendix, *Flushing of the flow cell to remove accumulated air bubbles*). Nevertheless, the flushing of a flow cell did not always lead to the desired result and could disable the measurement for minutes. The accumulation of air bubbles, therefore, needed to be actively avoided by proper filling of the syringe and degassing of the perfusate.

3.1.6 Air Bubble Free Setup

Figure 33 shows the sensor current of a combined system with integrated Belmont® Buddy fluid warmer and a syringe filter, in light blue, and the sensor current of a combined system with degassed perfusate in dark blue. Although the temperature of the test solutions was increased up to 42°C, both measurements were not interrupted by air bubbles in more than 60 hours.

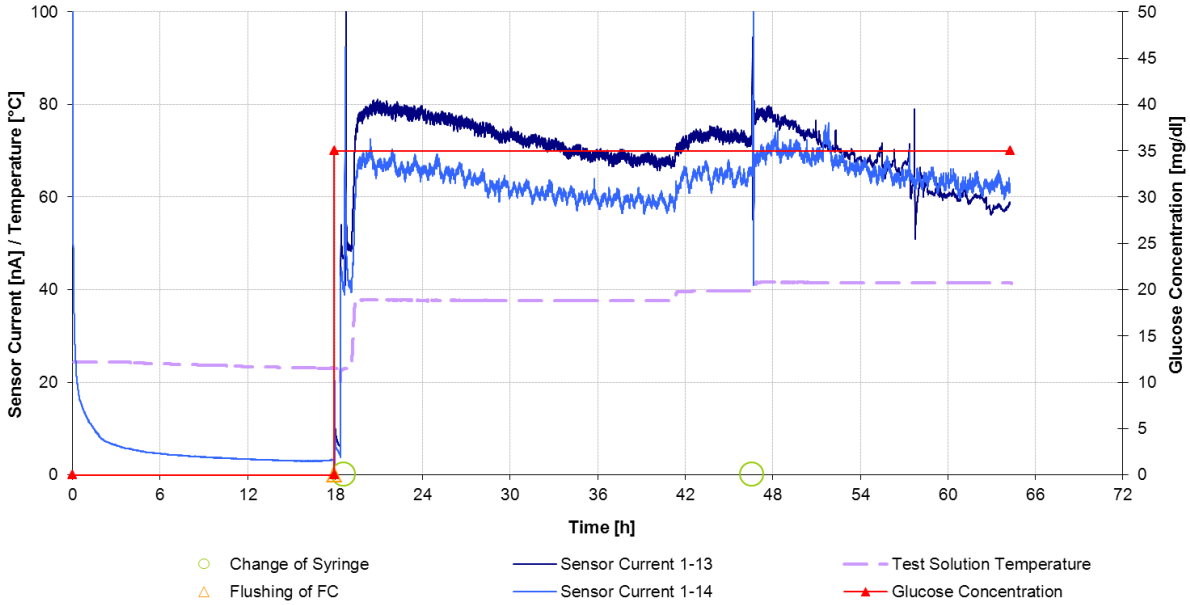

Figure 33: Sensor current of a combined system with integrated Belmont® Buddy fluid warmer and a syringe filter (light blue line) as well as the sensor current of a combined system with degassed perfusate (dark blue line).

To reference this improvement, a combined system with degassed perfusate was also compared to a combined system with normal perfusate. Figure 34 shows the sensor current of the combined system with degassed perfusate as a light blue line and the reference system with normal perfusate as a dark blue line. While the reference system suffered from severe air bubble problems, the system with the degassed perfusate did not show any artefacts for 91 hours. This proves that a degassing of the perfusate is sufficient to avoid out-gassing and air bubble accumulation in the final *in vivo* setup.

The noisy currents might be a result of pulsating micro air bubbles or interfering signals from other devices.

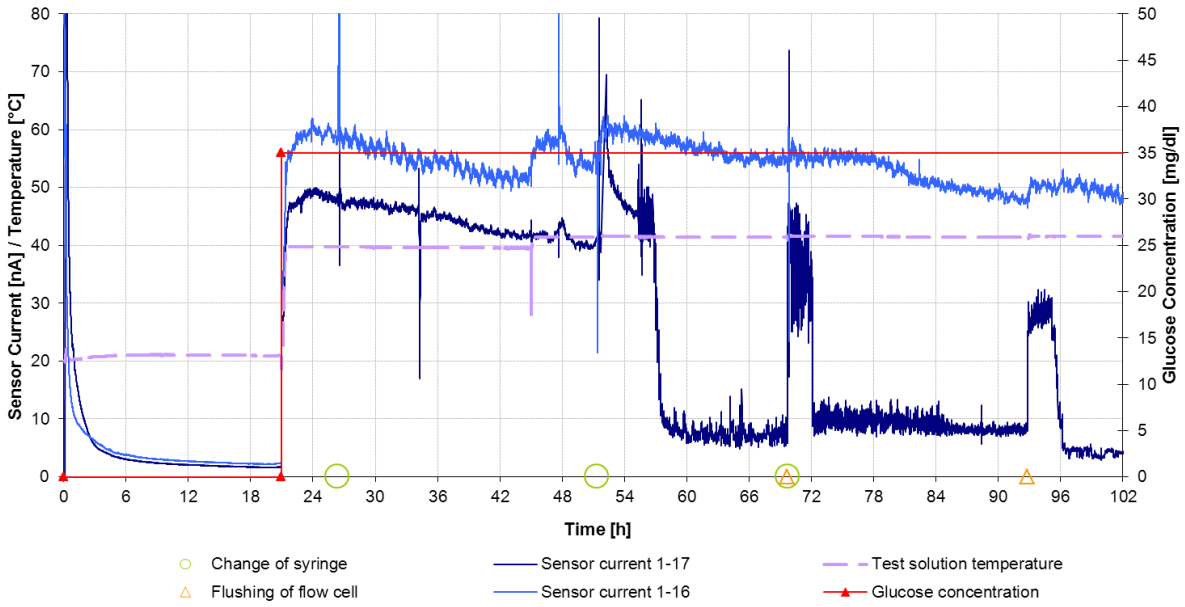

Figure 34: Sensor currents of a combined system with degassed perfusate and syringe filter and a reference combined system with normal perfusate suffering from severe air bubble artefacts.

Testing this final setup again, with an *in vivo* like protocol, revealed the sensor currents depicted in Figure 35 and Figure 36. The actual and IRT-corrected glucose concentrations in the dialysate are depicted as pink and green solid lines, respectively. An additional calibration of the IRT-corrected dialysate concentrations to the first blood reference value yielded the light blue lines which correlate quite well with the sensor current, although a drift of the current can be observed.

Once again the sensor current did not show any artefacts. As both the setup with and without syringe filter showed good results, the filter was not used in the final setup during the *in vivo* investigations due to missing experience concerning the permeability for the anticoagulant.

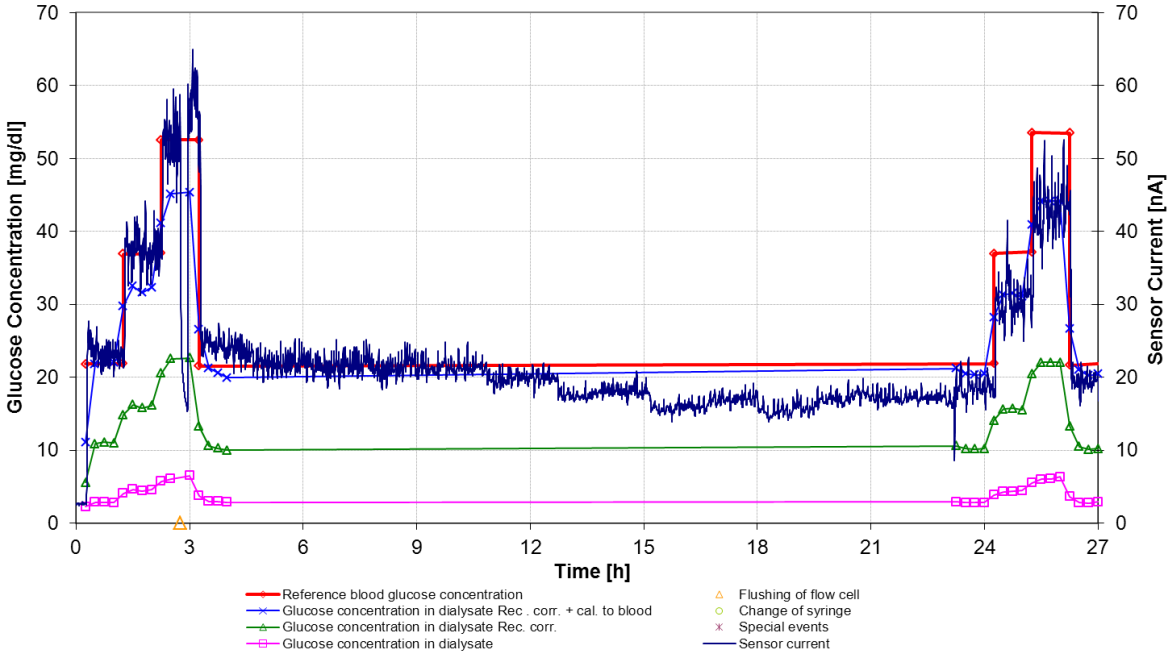

Figure 35: Final *in vitro* setup tested with an *in vivo* like protocol for Sys1 with a syringe filter. Depicted are glucose concentrations in the dialysate (pink), IRT-corrected glucose concentrations in the dialysate (green) and IRT-corrected and 1-point-calibrated glucose concentrations in the dialysate (light blue) as well as the sensor current (dark blue).

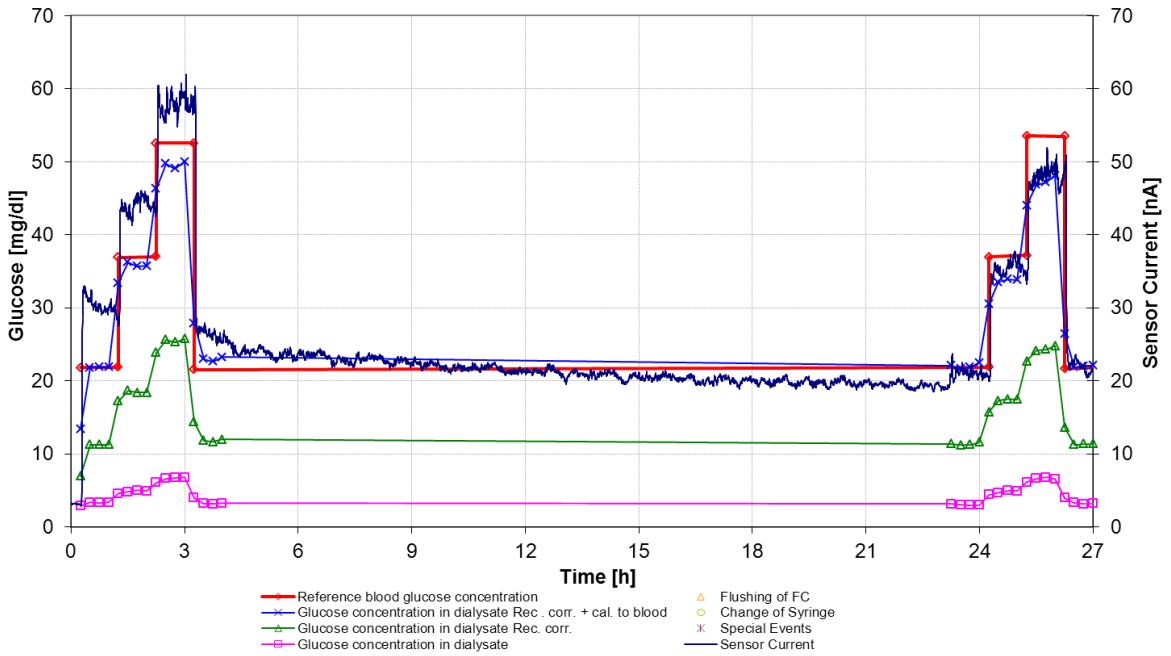

Figure 36: Final *in vitro* setup tested with an *in vivo* like protocol for Sys2. Depicted are glucose concentrations in the dialysate (pink), IRT-corrected glucose concentrations in the dialysate (green) and IRT-corrected and 1-point-calibrated glucose concentrations in the dialysate (light blue) as well as the sensor current (dark blue).

3.2 In Vivo Investigations

3.2.1 Risk Management

All identified risks were recorded in the FTA, see Appendix Figure 64. Thereby three major hazards were identified: first, electrical hazards comprising leakage currents over the subject as a result of dry electrodes (e.g. air bubbles), interactions between the system and other devices (e.g. grounding of the subjects with their personal laptops) or circuitry-wise errors (e.g. wrong electrode connections or high output values of the potentiostat); second, biological hazards leading to embolism as a result of a defect MD probe or infection due to contamination through unsterile components (e.g. flow cell and sensor); and third, thermal hazards as a consequence of a hot flow cell due to short circuits within the electronics of the sensor unit.

All these risks were transferred to the FMEA, see Appendix Figure 65, evaluated and analysed regarding possible prevention measures. Measures against electrical hazards included the evaluation of leakage currents via safety check (see *2.7.2 Safety Check and 3.2.2 Safety Check*), a potentiostat with adequate output values, prohibiting the use of any other line-powered devices (e.g. only battery-operated personal laptops were permitted) and the training of the staff for the correct handling of devices.
To avoid any biological hazards only sterile, CE-certified equipment was allowed to be used in direct contact with the subject. As flow cell and sensor were unsterile and not CE-certified a backflow from the flow cell to the body interface (subject) had to be avoided. Staff interacting with the subject were therefore trained in that particular respect according to the standard operating procedure (SOP) and the study protocol.
Measures against thermal hazards were not required as calculation and measurement of the maximum possible temperature of the sensor were below the limits of IEC 60601-1 [34] (see *3.2.2 Safety Check*).

In order to avoid inacceptable risks, measures had to be taken. Figure 37 shows the risk matrices with and without measures resulting from the FMEA. Some risks in the ALARP-area remained, but when all measures are implemented successfully the overall risk is controllable. Conclusions, evaluation and implemented measures from the complete risk management file can be found in the Appendix, Figure 66.

Risk Graph without measures

Risk Area			Severity				
			marginally	minor	serious	critical	desastrous
			1	2	3	4	5
Likelihood	likely	5	2	0	0	0	0
	often	4	2	0	0	0	1
	occasionally	3	17	4	3	0	1
	imaginable	2	12	6	11	0	1
	unlikely	1	8	0	6	0	0

Evaluated Risks:	74
Acceptable Area	49
ALARP-Area	22
Inacceptable Area	3

Risk Graph with measures

Risk Area			Severity				
			marginally	minor	serious	critical	desastrous
			1	2	3	4	5
Likelihood	likely	5	2	0	0	0	0
	often	4	0	0	0	0	0
	occasionally	3	7	0	0	0	0
	imaginable	2	19	5	8	0	0
	unlikely	1	21	0	12	0	0

Evaluated Risks	74
Acceptable Area	64
ALARP-Area	10
Inacceptable Area	0

Figure 37: Risk matrices for the combined system. Top: Without measures 3 risks were identified within the unacceptable region. Bottom: These risks were eliminated through adequate measures.

3.2.2 Safety Check

Classification of the Combined System

The combined system is an invasive and active device with a measuring function and an application time of less than 30 days. Applying the rules defined in Appendix IX from the Council Directive 93/42/EEC of 14 June 1993 [37] concerning medical devices, the system was therefore classified as a IIa device. If a glucose and/or insulin infusion is used as well it is classified as a IIb device.

According to the IEC 60601-1 [34], chapter 8.3, the applied parts of the combined system were classified as medical electrical (ME) equipment of TYPE CF (see Appendix, Figure 67). Normally, classification as BF would be sufficient but the system is in contact with the cardiovascular system and the infusion pump used, as well as most other commercially available infusion pumps, is also marked as TYPE CF.

Moreover, the combined system was classified as a 1d ME System (see Appendix, Figure 68), as it combines ME equipment and non-ME equipment.

It was furthermore identified to be of protection class I (see Appendix, *Classification of ME Systems and ME Equipment based upon the protection against electrical shock according to IEC 60601-1*) as all components, except the laptop, are of protection class I (PC I). The laptop, classified as PC II, was separately tested for the touch current.

A sticker “for clinical evaluation” was attached to the system according to Norbert Leitgeb, “Sicherheit von Medizingeräten” [38].

Electrical Safety Check

Throughout the safety check several thresholds for the leakage currents were exceeded. Thus an isolating transformer was included for practical means of compliance to decrease these leakage currents.

Three enhanced setups were tested in the safety check: a setup with an isolating transformer (see Appendix, Figure 69), a setup with two isolating transformers (see Appendix, Figure 70) and a setup with an isolating transformer and a USB to USB isolator (see final setup in Figure 20). Throughout the safety check, the infusion stand was positioned isolated for all setups.

The setup with one isolating transformer did not pass the safety check as measured leakage currents were partly above the allowed thresholds. A second isolating transformer was,

therefore, integrated into the setup to decrease these leakage currents. Although this setup passed the safety check it is not practicable for use in humans during the clinical trial as subjects are allowed to stand up for toilet breaks and the weight of two isolating transformers is too high for the portable infusion stand .

In order to decrease the total weight of the system, as well as decrease the leakage currents, a USB to USB isolator with integrated optocoupler was used to galvanic isolate laptop and sensor unit (see Figure 20).

Finally, two systems (Sys1 and Sys2), containing the USB to USB isolator as well as the BBRAUN Space Tower for glucose- and insulin infusion, were built. Both systems passed the safety check and the results are shown in Figure 76 and Figure 77 in the Appendix.
As the PC I safety check of the final setup did not consider the enclosure leakage current of the laptop, this was tested separately. The laptop connected to the sensor unit was therefore tested as a PC II system and its BENDER protocols are shown in Figure 78 and Figure 79 in the Appendix.

Devices and disposables included and tested in system 1 (Sys1) and system 2 (Sys2) are shown in Table 12 - Table 14. If used during the clinical trial the systems have to be arranged as shown in Figure 24. Integration of any other equipment is prohibited and the instructions of use of all devices have to be considered.

Furthermore, the isolating transformers must not be connected to a multiple socket but directly to a wall socket to keep the protective earth resistance low. The USB to USB isolator and the EmStat potentiostat have to be placed in a plastic enclosure to avoid any conductible parts being accessible for the subject as well as any ingress of liquid.

Thermal Hazards - Occurring power in the case of short circuit

The maximum voltage of the EmStat operational amplifiers is 12V. The maximum current that can be driven by the potentiostat is 100µA for the EmStat and 10mA for the EmStat2 [39].

The maximum occurring power is therefore:

$$P_{EmStat} = \mathrm{U} \cdot \mathrm{I} = 12\mathrm{V} \cdot 100 \cdot 10^{-6} A = 1.2mW \quad (19)$$

$$P_{EmStat2} = U \cdot I = 12V \cdot 10 \cdot 10^{-3} A = 120mW \quad (20)$$

When 120mW were applied to the 33Ω resistor there was only a mild increase in temperature. Measuring the actual temperature with a TESTO temperature sensor revealed a temperature of 27.9°C which is below limit of 43°C given by the IEC 60601-1 (see Table 4).

Moreover, this experiment only demonstrated the worst case (EmStat2 instead of the used EmStat) and the maximum heat occurring on the sensor's surface, but as it is placed in a polycarbonate housing (flow cell), the maximum occurring temperature on the subject's skin would be even lower. Nevertheless, the flow cell containing the sensor was not directly placed on the subjects' skin but on the Velcro® strip cuff that was used to support the Eppendorf vials (see Figure Figure 26).

3.2.3 Overview Clinical Study

Five healthy subjects suffering from diabetes type 1 (5 males, 0 females; age: 31.2 ± 4.8 years, BMI: 24.6 ± 2.9 kg/m²) participated in the clinical trial. Subject 022 was excluded as it did not fulfil the inclusion criteria. All subjects finished the investigations at the Clinical Research Centre located at the Medical University of Graz without any adverse events. No MD probe or BVT sensor had to be replaced during the trial.
Table 5 gives an overview of the conditions under which the five subjects were tested.

Subject	System	Flow Rate	Anticoagulation (Arixtra®)
021	1	10µl/min	perfusate: 5mg
022	subject was excluded during screening		
023	2	20µl/min t: 18.25h → 10µl/min	perfusate: 2.5mg + systemic: 2.5mg
024	2	10µl/min t: 5.25h→ 20µl/min	perfusate: 2.5mg + systemic: 2.5mg
025	1	10µl/min t: 5.25h→ 20µl/min	perfusate: 2.5mg + systemic: 2.5mg
026	1	20µl/min	perfusate: 2.5mg + systemic: 2.5mg

Table 5: Overview of all 5 systems investigated during the clinical trial.

Figure 38 - Figure 42 show the five individual glucose profiles during the 24h investigation. On the 1st y-axis the reference blood samples (Reference bood glucose concentration) are displayed as a red solid line. Red diamonds represent the glucose concentration measured within the dialysate samples that had already been corrected for volume and glucose concentration due to an increased spiking volume (Glucose concentration in dialysate). These corrected dialysate values were then further corrected by the IRT, taking into consideration the mean ion recovery rate (Glucose concentration in dialysate Rec. corr.), and are shown as pink squares. Finally, these values were 1-point-calibrated (Glucose concentration in dialysate Rec. corr. + cal. to blood) and are shown as green triangles. The sensor values that were unfiltered, unshifted, but corrected for the recovery and 1-point-calibrated to blood (Sensor current corr Rec + cal. to blood) are shown as a light blue solid line. On the 2nd y-axis, the originally recorded sensor current (Sensor current) that was unfiltered, unshifted, not IRT corrected and uncalibrated is shown as a dark blue solid line. Additionally, information concerning toilet breaks (violet crosses), flushing of the flow cell (orange triangles) and change of the perfusate syringes (green cycles) is shown as well.

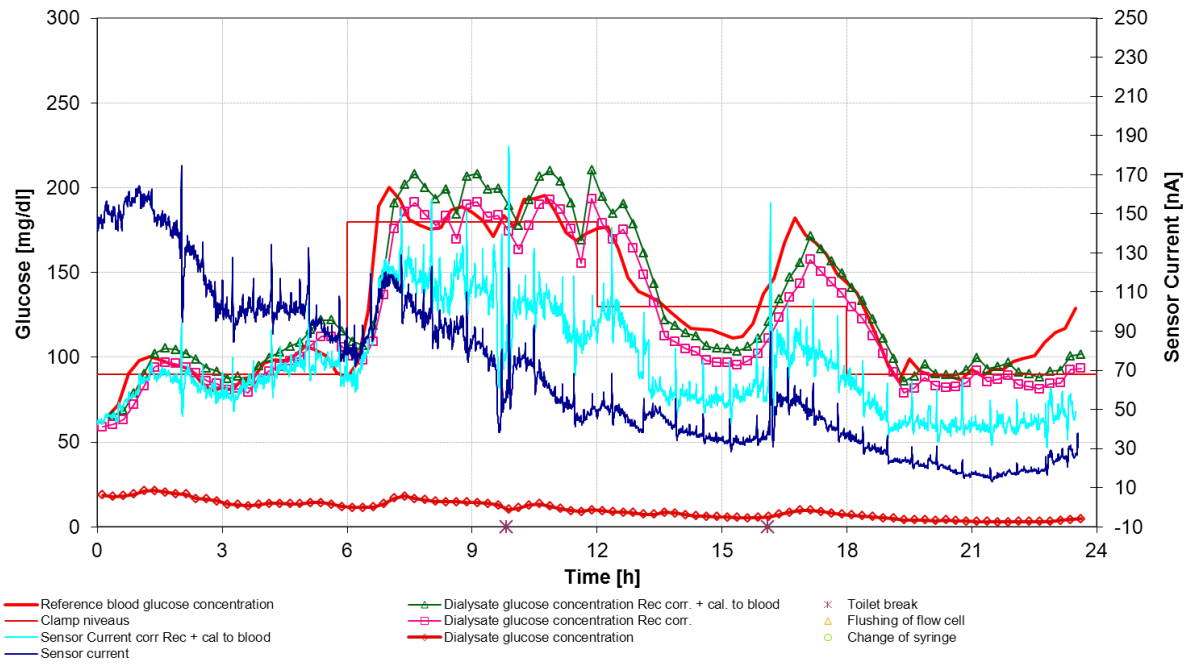

Figure 38: Reference, dialysate (uncorrected; corrected with IRT; corrected with IRT and calibrated to blood) and sensor (uncorrected; corrected with IRT + calibrated to blood) curves of subject 021.

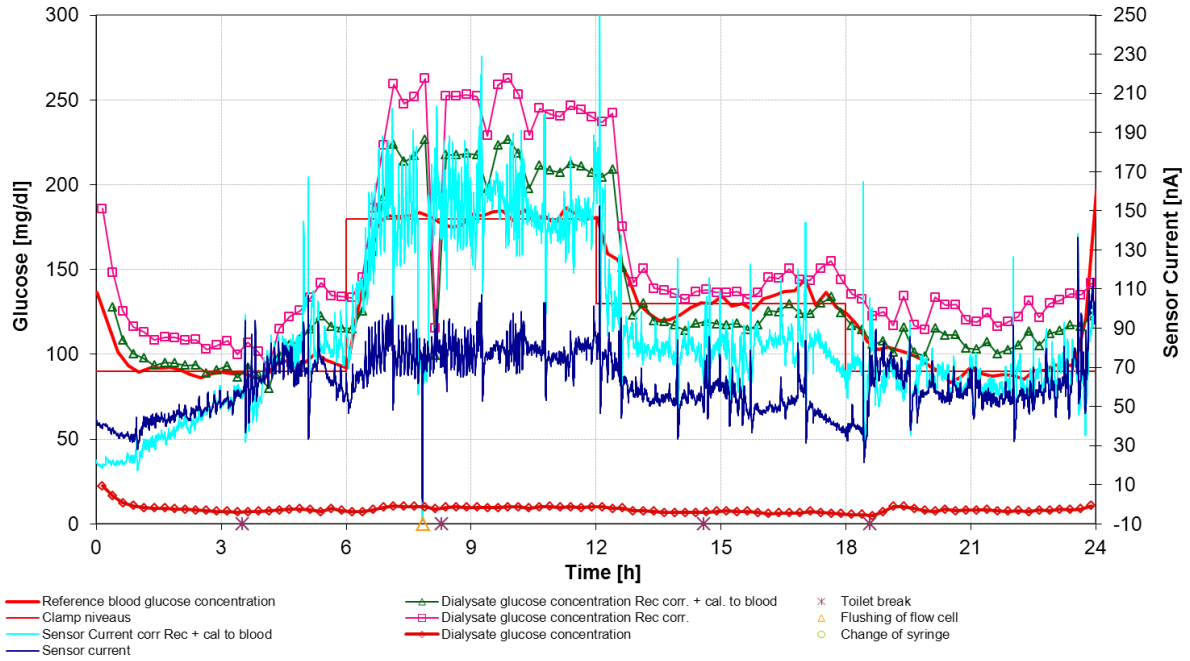

Figure 39: Reference, dialysate (uncorrected; corrected with IRT; corrected with IRT and calibrated to blood) and sensor (uncorrected; corrected with IRT + calibrated to blood) curves of subject 023.

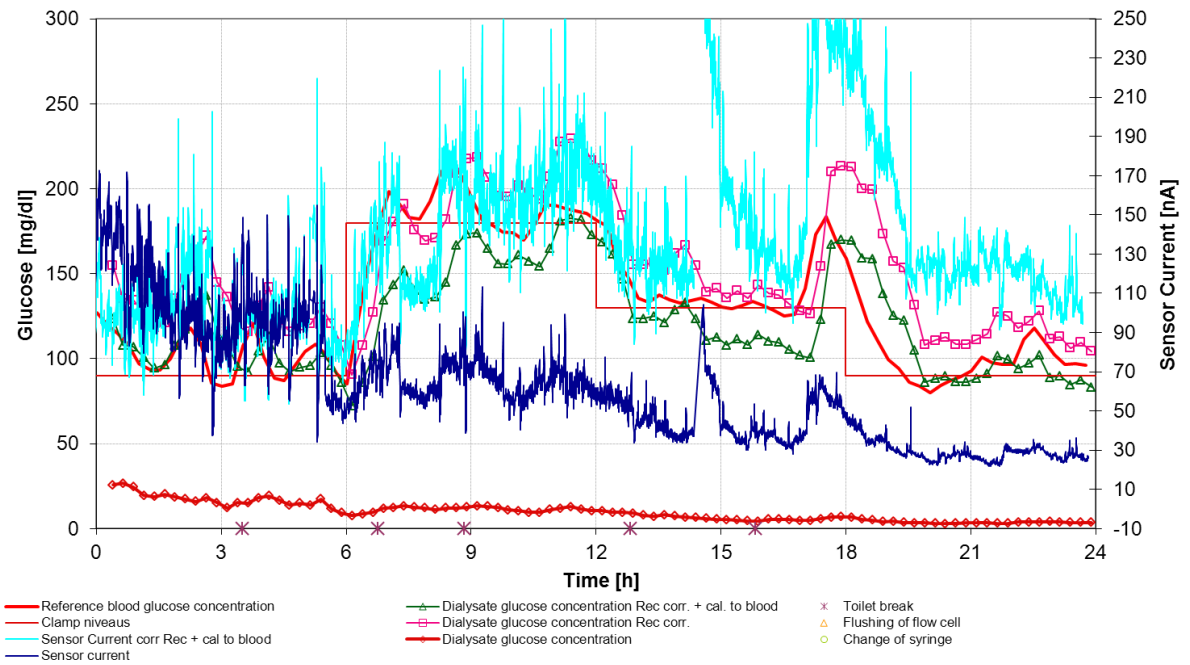

Figure 40: Reference, dialysate (uncorrected; corrected with IRT; corrected with IRT and calibrated to blood) and sensor (uncorrected; corrected with IRT + calibrated to blood) curves of subject 024.

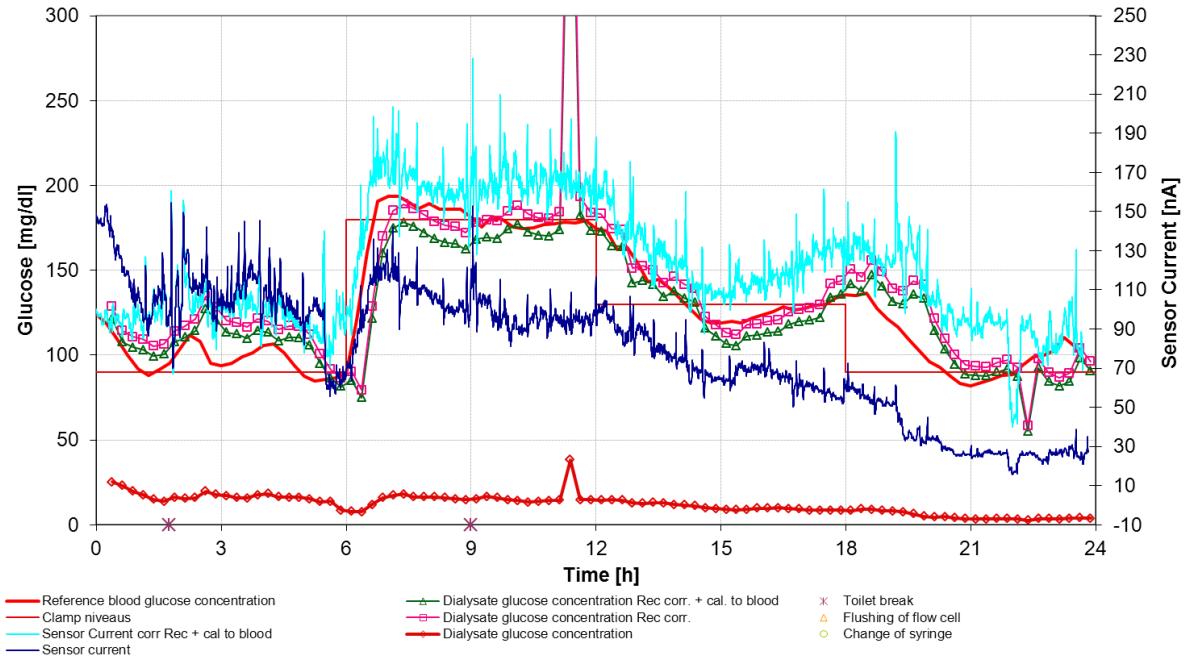

Figure 41: Reference, dialysate (uncorrected; corrected with IRT; corrected with IRT and calibrated to blood) and sensor (uncorrected; corrected with IRT + calibrated to blood) curves of subject 025.

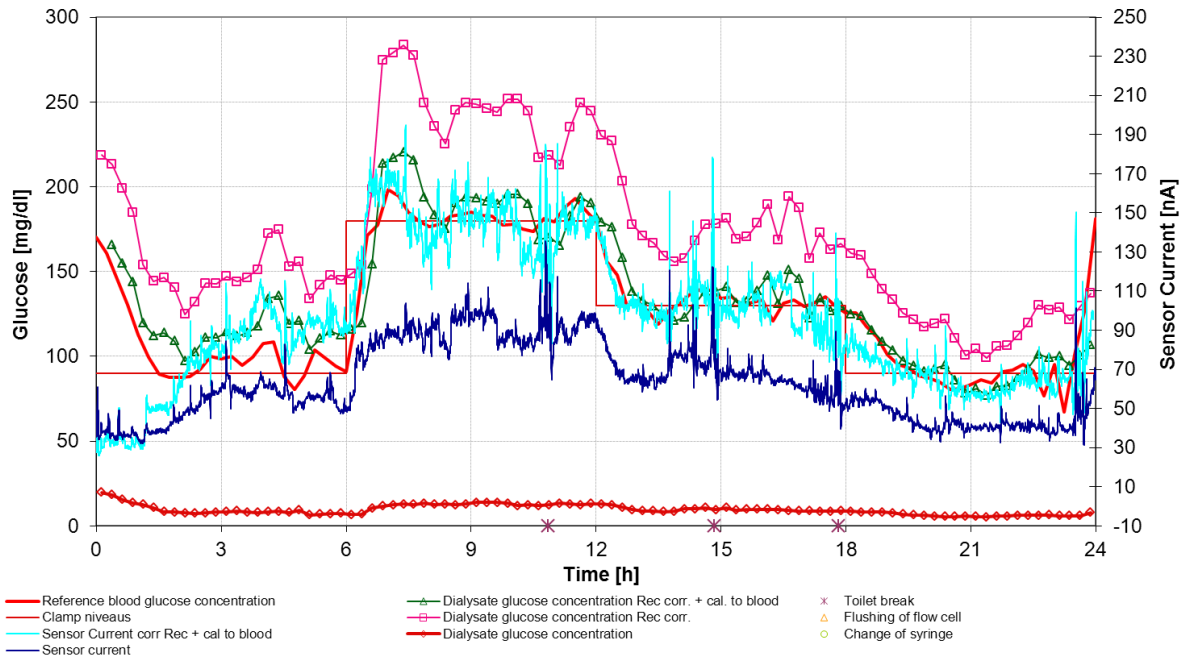

Figure 42: Reference, dialysate (uncorrected; corrected with IRT; corrected with IRT and calibrated to blood) and sensor (uncorrected; corrected with IRT + calibrated to blood) curves of subject 026.

Figure 39 and Figure 42 indicate that the sensors showed some kind of "run in behaviour" as the values within the first 4 and 3 hours, respectively, do not correlate with the dialysate concentrations as they do throughout the remainder of the experiment. As this effect occurred in subject 023 and 026, who participated on the same day, it can be speculated that this was

not a sensor specific characteristic but an external influence or handling error. It might be that the time between disconnecting the sensor from the run in pump and connecting it to the body interface, already inserted into the subject's vein, was too long. During that time, the flow cell was no longer perfused and the products of the chemical reaction accumulated within the flow channel. This could have influenced the sensor's reaction within the next few hours. As a result, the first 4 hours (subject 023) and first 3 hours (subject 026) of these experiments were excluded from any further analysis.

Moreover, sensor data during the flushing of the flow cell of subject 023 (t: 16.85h) was excluded from further analysis as well, as these data did not reflect the measurement of the dialysate but the measurement of the dialysate mixed with the flushing fluid (0.9% NaCl). The outlier in the dialysate data of subject 025 (t: 11h) was also excluded, although a re-measurement of this sample with the Super GL2 yielded the same result. As the glucose value was implausibly high, it was probably a result of glucose contamination in the sampling vial.

3.2.4 Glucose Clamp

Figure 43 shows the mean values of the blood glucose profiles (blue diamonds with a solid blue line) and the standard deviations (black bars) of subjects 021 - 026. The target glucose levels are shown as a red solid line. The individual blood glucose profiles (spot measurements) of subjects 021 – 026 are depicted in Figure 80 in the Appendix. After approximately 23 to 23.5 hours, all subjects received breakfast causing an increase of the blood glucose level.

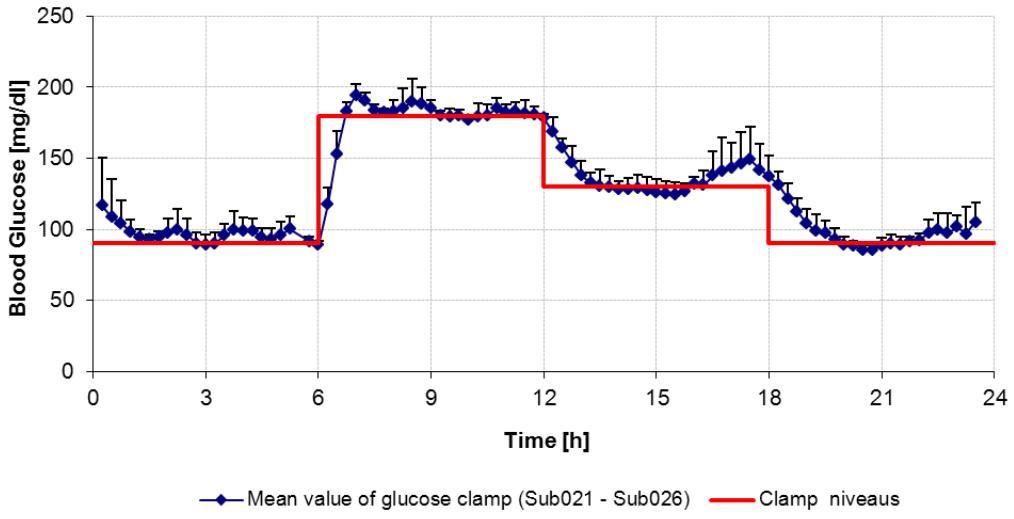

Figure 43: Mean value and standard deviation of all 5 individual glucose clamps.

3.2.5 Recovery

Figure 44A-E shows the recovery of ions and glucose for subjects 021 – 026 during the 24 hours of trial.

Starting with a flow rate of 10µl/min (subjects 021, 024 and 025) led to recoveries of 20 - 30% for glucose and ions. But recoveries at 10µl/min decreased to approximately 4% for glucose and 5% for ions in subject 021 (no systemic anticoagulation) and 9% for glucose and 7% for ions in subject 023 (systemic anticoagulation) after 23 hours.

Flow rates of 20µl/min at the beginning (subjects 023 and 026) led to recoveries of about 10% for glucose and ions and decreased to approximately 4 - 7% for glucose and 4 – 5% for ions after 23 hours (subjects 024 – 026, systemic anticoagulation).

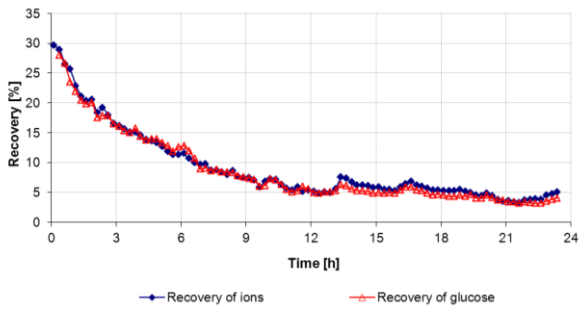

Figure 44A: Recovery of ions and glucose of subject 021 at a flow rate of 10µl/min

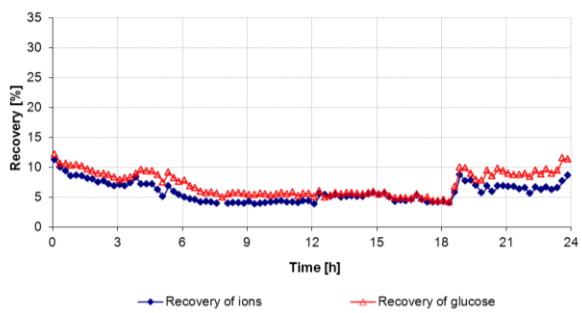

B: Recovery of ions and glucose of subject 023 at a flow rate of 20µl/min (t: 0 – 18.15h) and 10µl/min (t: 18.25 – 24h)

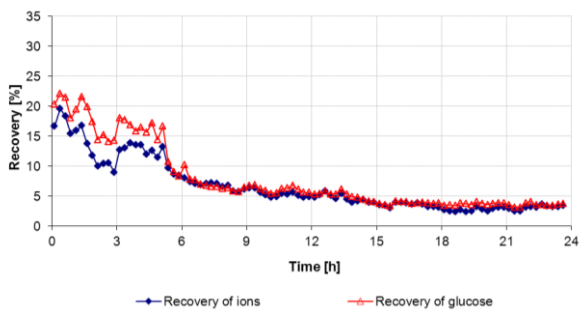

C: Recovery of ions and glucose of subject 024 at a flow rate of 10µl/min (t: 0 – 5.15h) and 20µl/min (t: 5.25 – 24h)

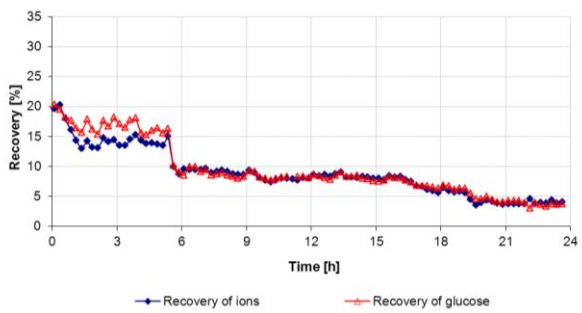

D: Recovery of ions and glucose of subject 025 at a flow rate of 10µl/min (t: 0 – 5.15h) and 20µl/min (t: 5.25 – 24h)

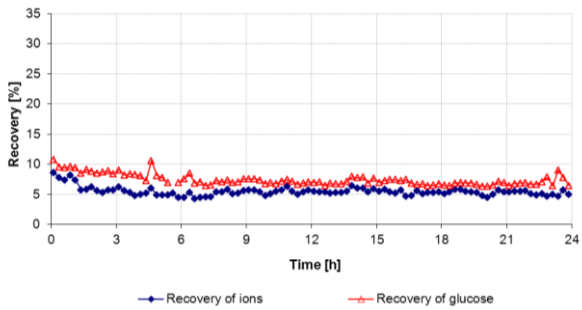

E: Recovery of ions and glucose of subject 026 at a flow rate of 20µl/min

3.2.6 Flow Rate

The individual normalized flow rates ($actual\ flow\ rate/nominal\ flow\ rate$) of the 5 systems operated in push mode are depicted in Figure 81 in the Appendix.

Figure 45 shows the mean values of these individual flow rates as blue diamonds with a blue solid line and the standard deviations as black bars. The flow rate was found to be very stable over 24 hours although the flow cell and sampling unit were attached to the MD probe's outlet.

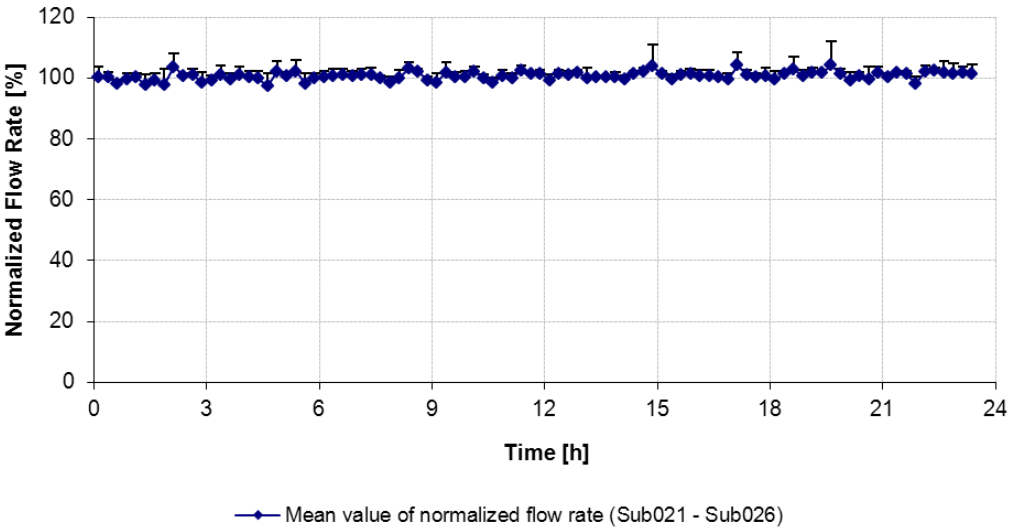

Figure 45: Mean values and standard deviations of the normalized flow rates of subjects 021 - 026.

3.2.7 Run-In Behaviour of Sensors

The individual run in data of the five system sensors and the five backup sensors during the first 10 hours are shown in Figure 82 in the Appendix.

Figure 46 shows the mean values (red solid line) and standard deviations (black bars) of these 10 sensors recorded during the first 10 hours of the run in period. The mean value of all 10 sensors was found to be 4.39 ± 1.62 nA after 10 hours and 2.23 ± 0.49 nA after 24 hours for the five backup sensors. The origin of the outliers in the sensor data of subject 023 and 024 is unknown.

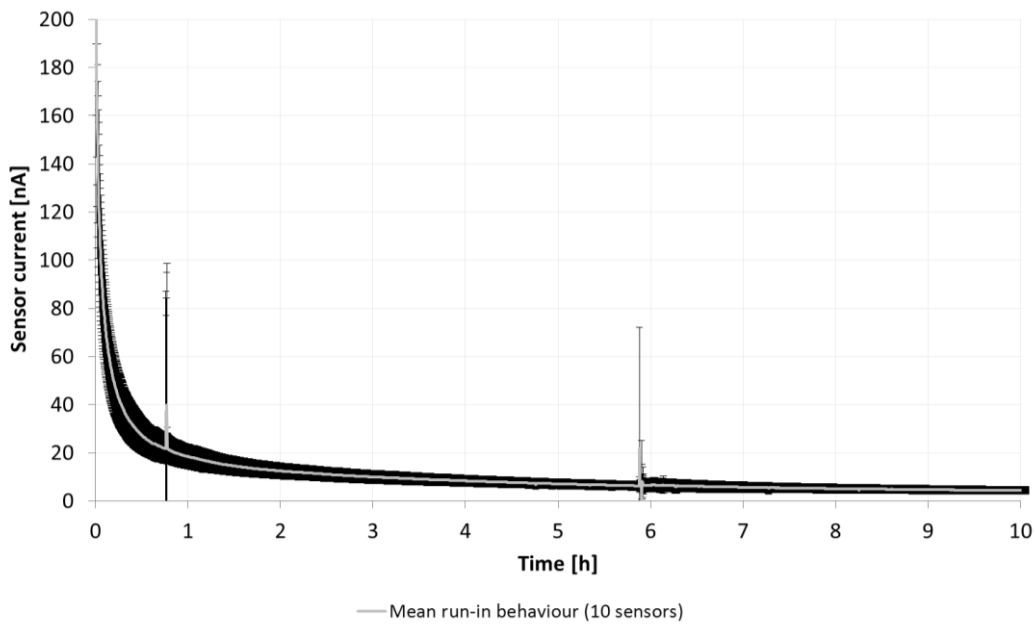

Figure 46: Mean values (red solid line) and standard deviations (black bars) of the 10 sensor currents recorded during the run in periods of subject 021 - 026 during the first 10 hours.

3.2.8 Filtering of Sensor Data

Comparing the coefficients of correlation shows that the filtering of sensor data improves the correlation with the blood reference significantly, as shown for four out of five subjects (uncalibrated and not IRT corrected) in Figure 47. Subject 021 does not show any improvement and should be excluded from evaluation as the coefficient of correlation without IRT correction is 0, due to the strongly decreasing recovery rates, and therefore can't be improved by solely applying a filter.

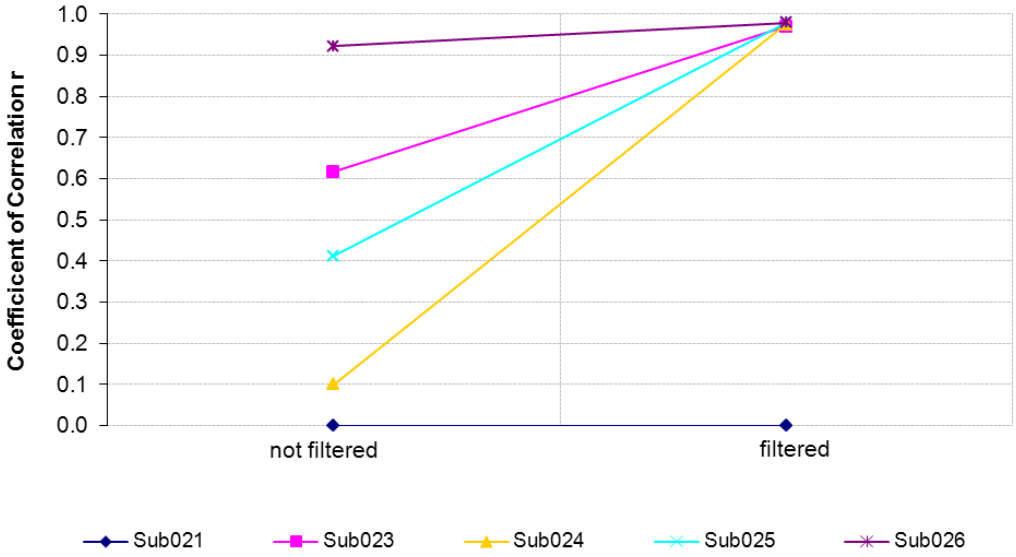

Figure 47: Improvement of the coefficient of correlation r between blood and sensor when applying a filter on the uncalibrated and not IRT corrected sensor data.

3.2.9 Correlation

Figure 48 shows the glucose profiles of subjects 021 – 026. Red curves indicate the blood glucose concentration, blue curves indicate the filtered, 1-point-calibrated and IRT corrected sensor signal and green curves indicate the dialysate glucose concentration. Calibration points are depicted as black triangles on the x-axis.

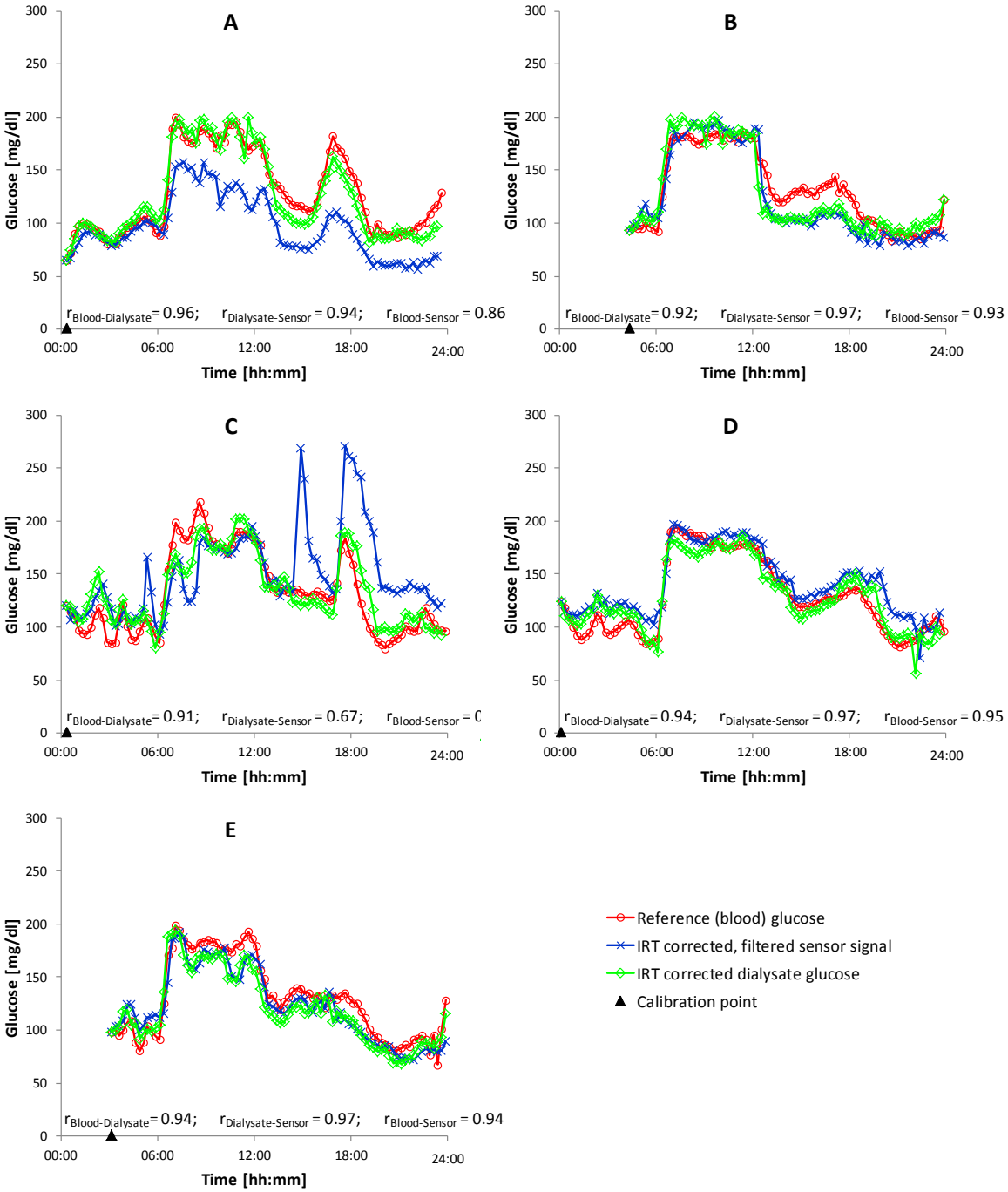

Figure 48: Glucose profiles of subjects 021 – 026. Red curves indicate the blood glucose concentration, blue curves indicate the filtered, 1-point-calibrated and IRT corrected sensor signal and green curves indicate the dialysate glucose concentration. Calibration points are depicted as black triangles.

Comparing the coefficients of correlation between blood and sensor, blood and dialysate and dialysate and sensor, revealed that dialysate and sensor data correlate better than blood and dialysate data in three out of five subjects for filtered, uncalibrated and not IRT corrected data (see Figure 49).

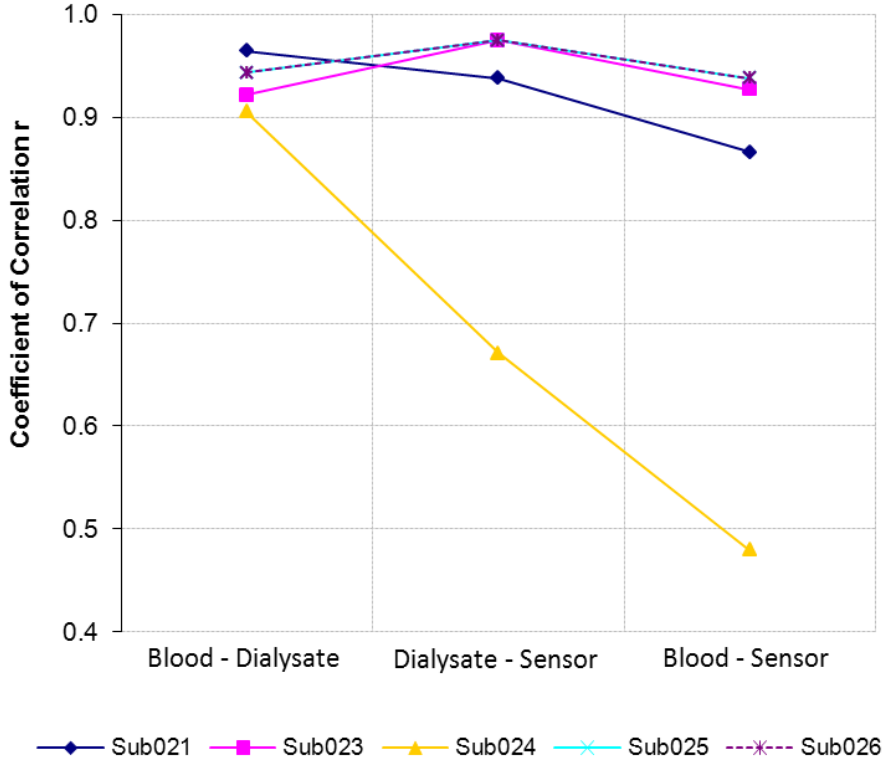

Figure 49: Coefficients of correlation r between blood and dialysate, and dialysate and sensor data indicating a worsening of the correlation between blood and sensor as a result of suboptimal MD probe conditions for filtered, 1-point-calibrated and IRT corrected data.

Figure 50 depicts the relationship between the coefficient of correlation r and mean glucose recovery of all 39 systems investigated during the first part (sampling unit) of the EU-Clamp *in vivo* trial [11]. Blue squares represent data derived from CMA64 probes whereas orange and green circles represent data derived from PME011 and PME012 probes. Unfilled symbols indicate systemic anticoagulated systems; filled symbols represent systems that were not systemic anticoagulated. The two symbols with purple circles derive from subject 014 who was not clamped. Additionally, data comparing the correlation between blood and sensor in subjects 021 - 026 during the second part of the trial are depicted as red triangles.
The yellow area represents data with a poor correlation, below 0.8, whereas the green area shows data with a good correlation, greater than 0.8.

Except for four outlying systems (CMA with $r = 0.25$ and $\overline{Rec_{Gluc}} = 8.6\%$, PME011 with $r = 0.68$ and $\overline{Rec_{Gluc}} = 23.4\%$ that can be corrected to $R = 0.90$ if two outliers are neglected, PME011 with $r = 0.41$ and $\overline{Rec_{Gluc}} = 26.6\%$ and PME011 with $r = 0.48$ and $\overline{Rec_{Gluc}} = 7.8\%$ from the noisy sensor current of subject 024) all systems are either located in the yellow or green area. All other systems show good correlation if they reached a mean recovery of more than 5%. 46.15% of all PME011 probes and 93.33% of all CM64 catheters are located in the blue area. Except for subject 024, all systems with systemic anticoagulation lie in the green area as well. As subject 024 showed a highly noisy sensor current, this outlier cannot be considered representative.

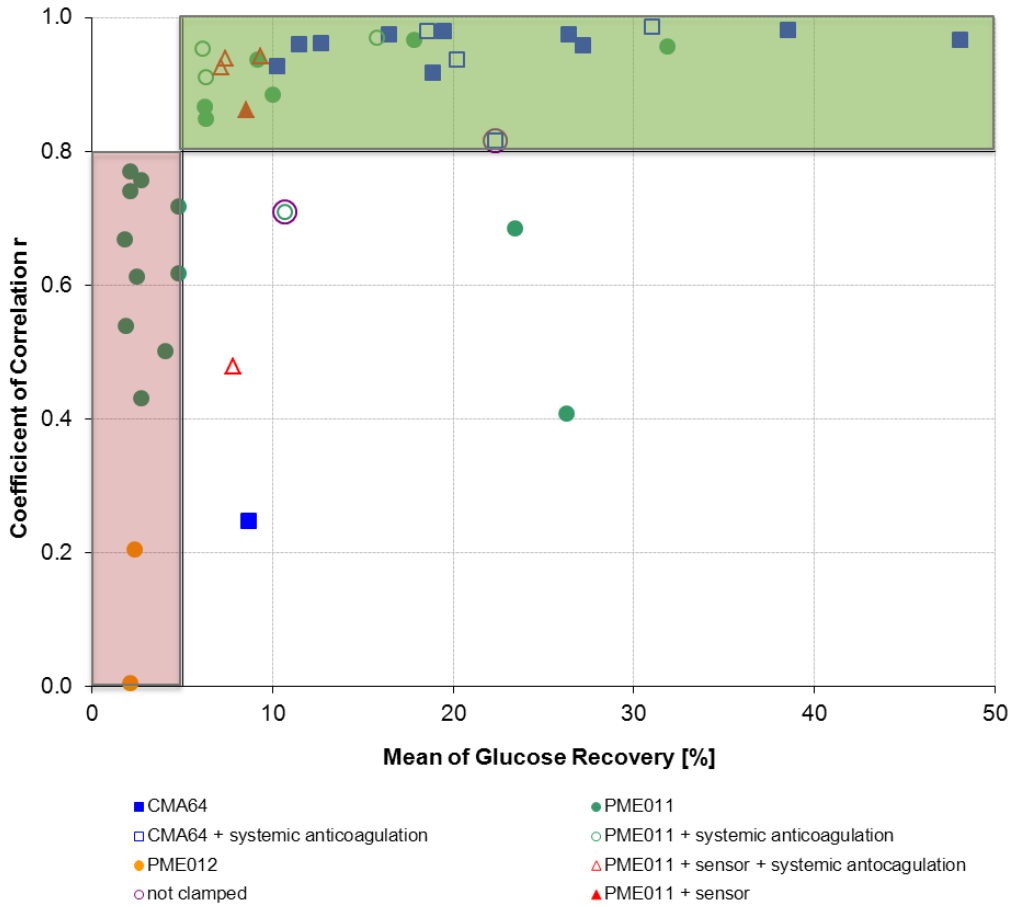

Figure 50: Relation between correlation coefficient and mean glucose recovery of subjects 001 - 0026 for IRT corrected uncalibrated and filtered data.

3.2.10 Calibrated Glucose Profiles

The filtered and shifted sensor currents that were calibrated with different calibration intervals (A: uncalibrated, not IRT corrected, B: 1-point calibrated IRT corrected, C: 30min calibration interval, not IRT corrected, D: 30min calibration interval, IRT corrected, E: 1h calibration interval, not IRT corrected, F: 1h calibration interval, IRT corrected, G: 2h calibration interval, not IRT corrected, H: 2h calibration interval, IRT corrected, I: 3h calibration interval, not IRT corrected and J: 3h calibration interval, IRT corrected) are shown as solid blue lines in Figure 51 (subject 021) and in the Appendix Figure 83 (subject 023) – Figure 86 (subject 026). The blood reference measurements are depicted as red solid lines, and green triangles indicate the time of calibration.

Subject 021:

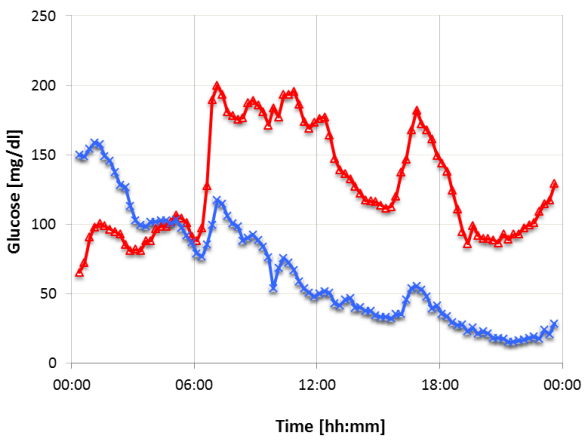

Figure 51A: uncalibrated, filtered, shifted but not IRT corrected sensor current of subject 021

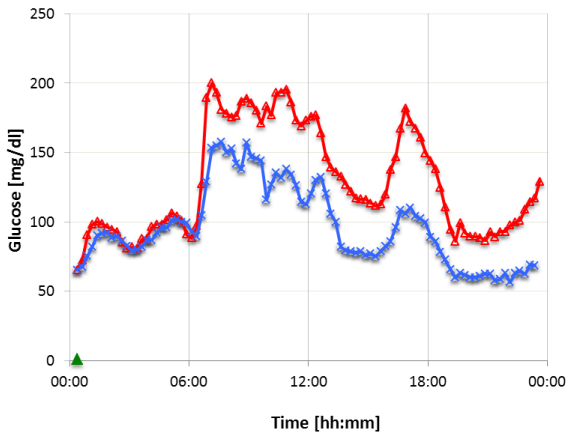

B: 1-point-calibrated, filtered, shifted and IRT corrected sensor current of subject 021

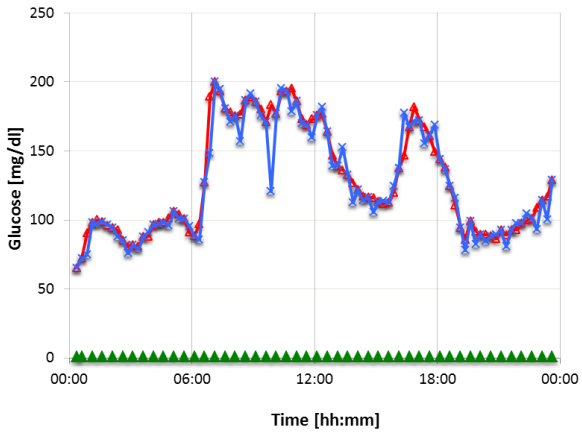

C: Filtered, shifted but not IRT corrected sensor current of subject 021 calibrated every 30 minutes.

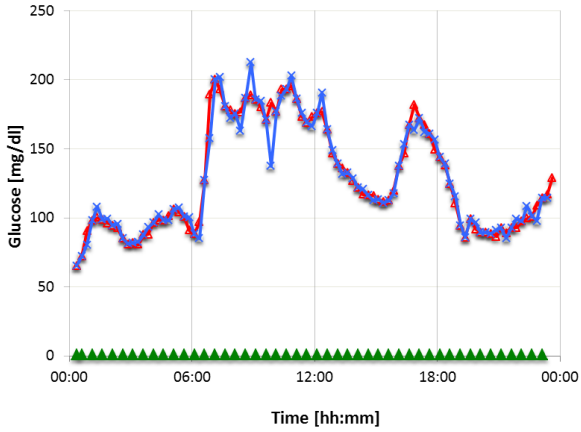

D: Filtered, shifted and IRT corrected sensor current of subject 021 calibrated every 30 minutes.

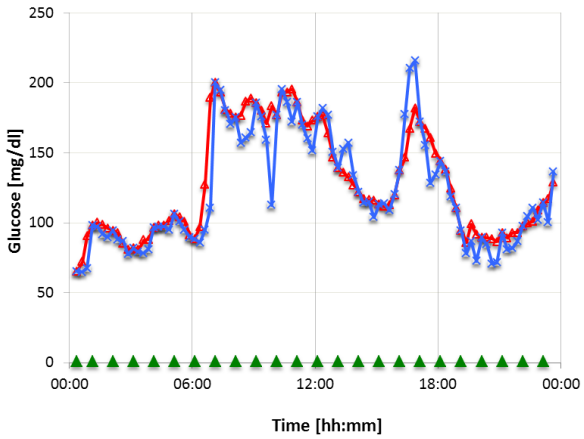

E: Filtered, shifted but not IRT corrected sensor current of subject 021 calibrated every hour.

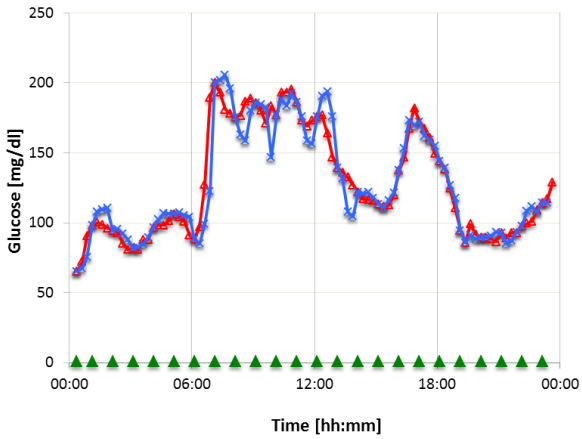

F: Filtered, shifted and IRT corrected sensor current of subject 021 calibrated every hour.

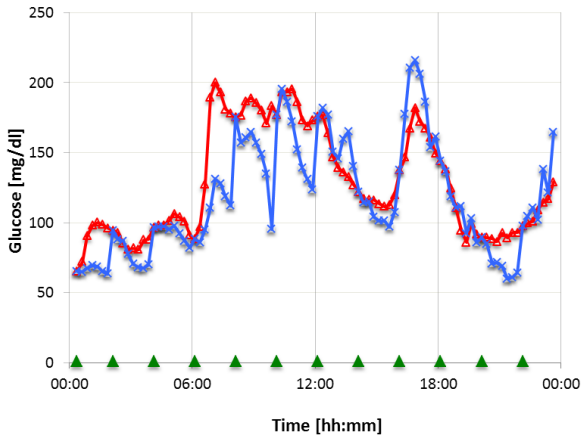

G: Filtered, shifted but not IRT corrected sensor current of subject 021 calibrated every 2 hours.

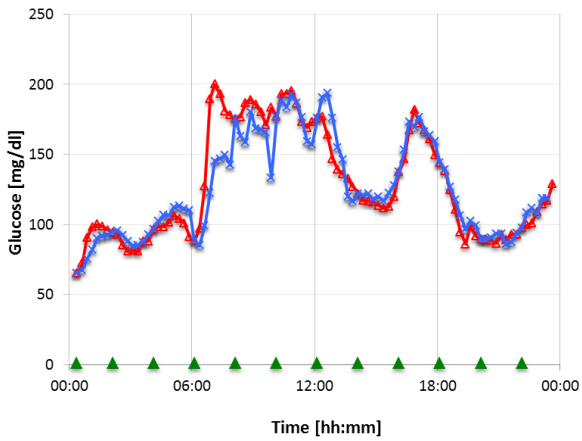

H: Filtered, shifted and IRT corrected sensor current of subject 021 calibrated every 2 hours.

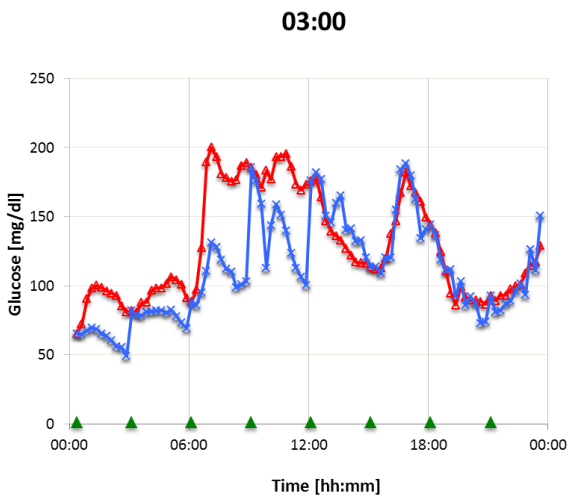

I: Filtered, shifted but not IRT corrected sensor current of subject 021 calibrated every 3 hours.

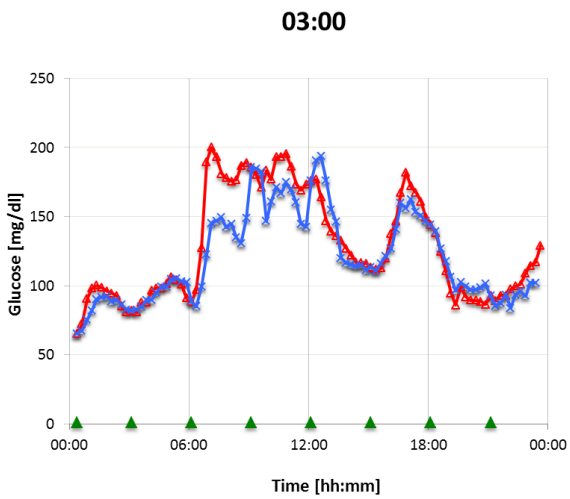

J: Filtered, shifted and IRT corrected sensor current of subject 021 calibrated every 3 hours.

3.2.11 Statistical Evaluation

Table 6 shows the mean values of system error, number of values between ±5% and ±10% SE, %PRESS, modified %PRESS, MAD; data located in the EGA zone A and B, data located in the EGA zone A, MARD and M2ARD for the filtered, shifted and IRT corrected sensor current of all five subjects compared to their blood reference. Five different calibration intervals (1-point calibrated, 30min interval, 1h interval, 2h interval and 3h interval) were evaluated. Green fields indicate the calibration interval with the best values, red fields the one with worst. The individual evaluations of subjects 021 - 026 can be found in the Appendix, Figure 87 - Figure 91.

Table 7 shows these parameters for the filtered, shifted but not IRT corrected sensor currents of all five subjects for six different calibration intervals (uncalibrated 1-point-calibrated, 30min interval, 1h interval, 2h interval, 3h interval).

	IONIC REFERENCE (LINEAR)				
	CALIBRATION INTERVAL [hh:mm]				
	1-point calibrated	00:30	01:00	02:00	03:00
	CALIBRATION POINTS in 24h				
	1	47	24	12	8
System Error (Mean Value) [%]	104.78	0.68	1.78	4.89	5.23
Values with System Error between -5% and +5% [%]	10.49	78.21	62.91	43.02	39.59
Values with System Error between -10% and +10% [%]	18.41	91.59	78.64	62.90	57.08
%PRESS	123.90	7.29	13.27	21.91	26.97
MODIFIED %PRESS	124.10	6.99	13.09	22.66	32.69
MAD [%]	296.30	0.00	0.14	0.57	0.68
r^2	0.67	0.93	0.81	0.60	0.41
EGA, A & B [%]	62.3%	99.2%	98.5%	96.8%	96.6%
EGA, A [%]	33.1%	97.7%	92.3%	81.9%	77.0%
MARD [%]	117.08	3.17	6.97	13.03	17.14
M2ARD [%]	119.51	0.02	3.47	7.25	7.96

Table 6: Statistical evaluation of the mean of all five subjects for IRT corrected sensor currents.

	IONIC REFERENCE (LINEAR)					
	CALIBRATION INTERVAL [hh:mm]					
	UNCALIBRATED	1-point-calibrated	00:30	01:00	02:00	03:00
	CALIBRATION POINTS in 24h					
	0	1	47	24	12	8
System Error (Mean Value) [%]	-45.22	-40.13	-0.32	-0.89	-0.50	-3.96
Values with System Error between -5% and +5% [%]	2.95	6.27	74.98	57.58	43.31	34.59
Values with System Error between -10% and +10% [%]	5.68	10.87	87.49	76.79	62.54	53.69
%PRESS	55.00	49.08	7.28	12.03	18.21	22.29
MODIFIED %PRESS	53.96	47.50	8.36	12.88	19.58	23.52
MAD [%]	32.97	30.60	0.00	0.14	0.55	0.93
r^2	0.28	0.28	0.93	0.83	0.65	0.51
EGA, A & B [%]	93.6%	92.7%	99.5%	99.1%	98.3%	98.0%
EGA, A [%]	9.5%	27.7%	96.4%	91.5%	83.7%	75.8%
MARD [%]	50.64	44.11	3.73	7.10	11.88	15.60
M2ARD [%]	56.65	49.98	0.01	3.41	7.05	9.15

Table 7: Statistical evaluation of the mean of all five subjects for not IRT corrected sensor currents.

3.2.12 Calibration Based on a Limit of the System Error (|SE|<10%)

Figure 52 shows the sensor currents of subjects 021 – 026 that were calibrated to stay within ±10% SE (see *1.2 Objectives*). The filtered, shifted, IRT corrected and calibrated sensor currents are depicted as a blue solid line, the blood reference measurements are shown as a red solid line and green triangles indicate the required calibration points.

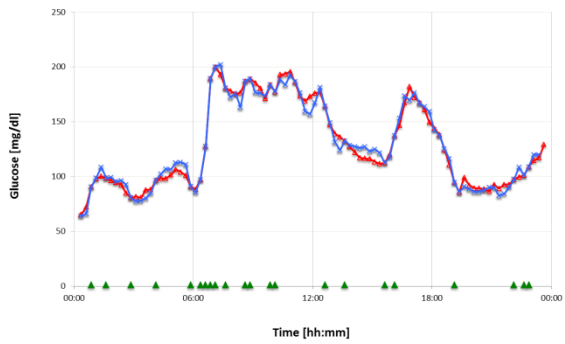

Figure 52A: Filtered, shifted and IRT corrected sensor current of subject 021 that was calibrated 22 times based on a limit of |SE|<10%.

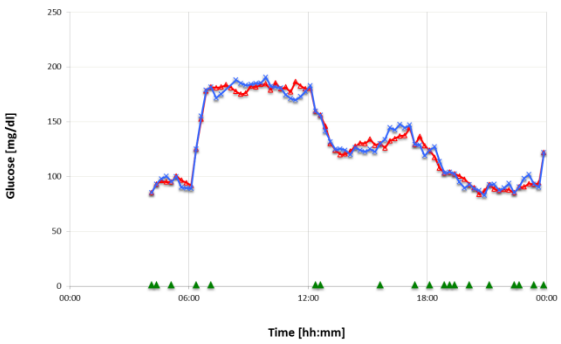

B: Filtered, shifted and IRT corrected sensor current of subject 023 that was calibrated 19 times based on a limit of |SE|<10%. The first 4 hours were excluded from analysis as described in 3.2.3 Overview Clinical Study.

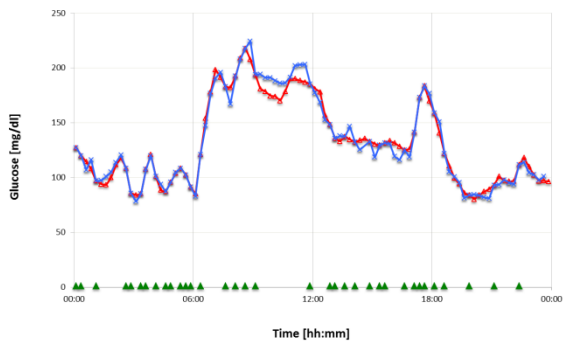

C: Filtered, shifted and IRT corrected sensor current of subject 024 that was calibrated 35 times based on a limit of |SE|<10%.

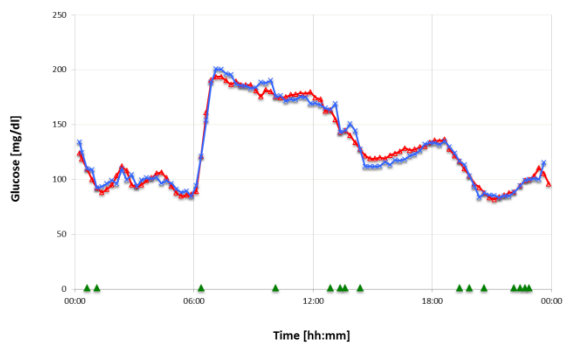

D: Filtered, shifted and IRT corrected sensor current of subject 025 that was calibrated 15 times based on a limit of |SE|<10%.

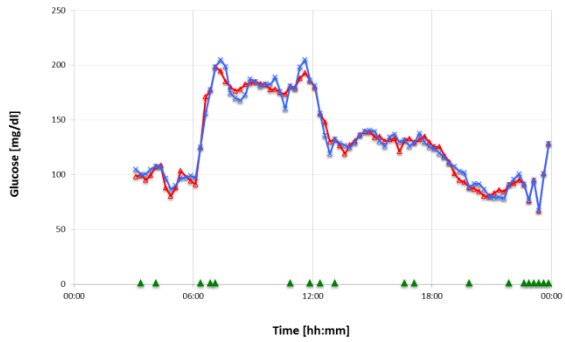

E: Filtered, shifted and IRT corrected sensor current of subject 026 that was calibrated 19 times based on a limit of |SE|<10%. The first 3 hours were excluded from analysis as described in 3.2.3 Overview Clinical Study.

Table 8 compares the minimal number of calibrations needed to stay within ±10% SE for blood and filtered and shifted sensor data that was IRT corrected and not IRT corrected for all five subjects.

number of calibration points needed to stay within |SE|<10%	subject 021	subject 023	subjects 024	subject 025	subject 026
corrected with IRT	22	19	35	15	19
not corrected with IRT	35	17	37	25	28

Table 8: Minimal number of calibrations needed to stay within |SE|<10% for IRT corrected and not IRT corrected data.

3.2.13 Regression Diagram

The accuracy of the system was evaluated according to the acceptance criteria given in ISO 15197:2003 in *2.5.4 Statistical Methods*.

Table 9 shows the percentage of data pairs which lie within the acceptable region defined by the regression analysis.
Fields marked in green indicate that more than 95% of these data pairs are within this acceptable region and therefore fulfil the acceptance criteria. To achieve this for four out of five IRT corrected data sets, a calibration every 30 minutes is required. Table 10 shows the percentage of data pairs within the acceptable region for filtered, shifted but not IRT corrected sensor currents. A calibration interval of 30 minutes would be needed to fulfil the criteria with all five subjects.

Regression Analysis [%]	1-point-calibrated	00:30	01:00	02:00	03:00
Sub021	38.7	98.9	96.8	92.5	90.3
Sub023	80.8	97.4	93.6	87.2	76.9
Sub024	5.3	94.7	78.7	66.0	59.6
Sub025	73.7	97.9	94.7	86.3	76.8
Sub026	92.8	96.4	95.2	92.8	81.9

Table 9: Regression analysis of subjects 021-026 with 5 different calibration intervals for IRT corrected sensor currents.

Regression Analysis [%]	uncalibrated	1-point-calibrated	00:30	01:00	02:00	03:00
Sub021	11.7	2.1	96.8	90.4	71.3	66.0
Sub023	0.0	35.9	97.4	94.9	85.9	73.1
Sub024	17.9	7.4	95.8	84.2	75.8	64.2
Sub025	16.7	21.9	96.9	93.8	92.7	85.4
Sub026	0.0	72.3	96.4	95.2	94.0	91.6

Table 10: Regression analysis of subjects 021-026 with 5 different calibration intervals for not IRT corrected sensor currents.

Figure 53 depicts a regression diagram for subjects 021 – 026 with a calibration interval of 30 minutes.

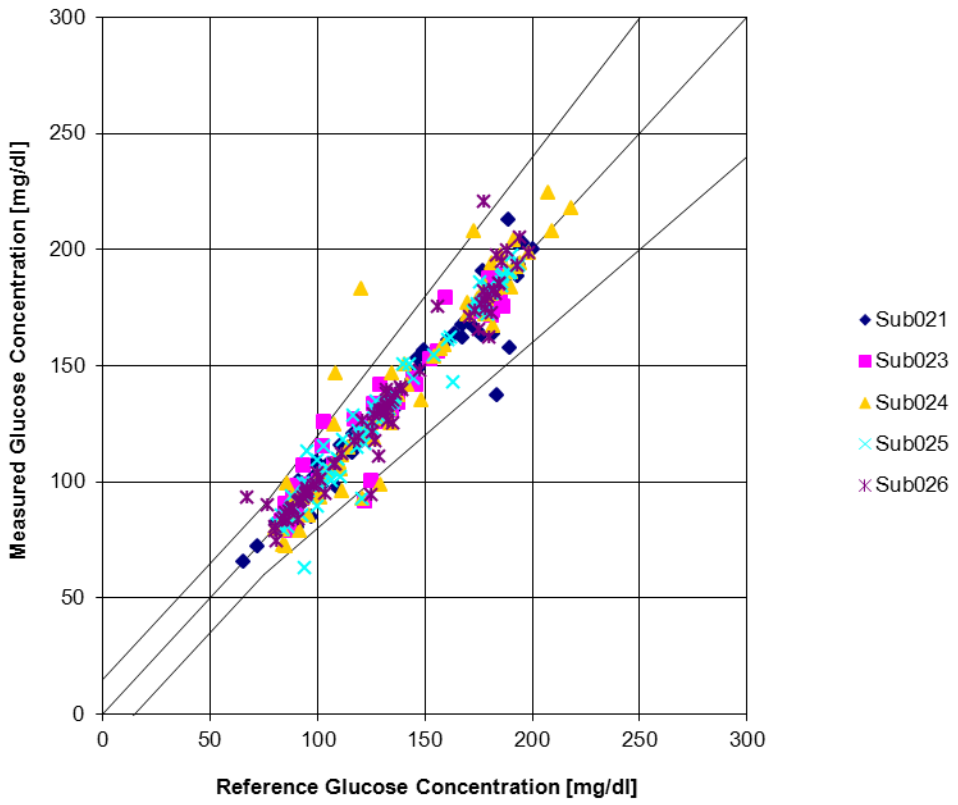

Figure 53: Regression diagram of subjects 021 - 026 with a calibration interval of 30 minutes for IRT corrected sensor currents.

3.2.14 Ultrasound Investigations

Any deposition of proteins or coagulation effect on the implanted microdialysis probes were characterized by ultrasonic scans performed after the 24 hours of trial. These ultrasound pictures can be found in the Appendix, Figure 92. In subject 021 who received no systemic anticoagulation a small clot formation on the venous catheter and the MD membrane was found. Although subjects 023 – 026 were systemically anticoagulated, subject 023 also showed a small, unexpected clot formation on the MD membrane. Pictures of the explanted MD probes can be found in the Appendix, Figure 93.

4 DISCUSSION

The aim of this thesis was to combine intravenous microdialysis technique and glucose sensors to setup a system that continuously monitors a subject's blood glucose concentration without the loss of blood. The BVT glucose sensor was successfully characterized during *in vitro* experiments and combined with the MD sampling unit that was described by Andreas Huber in [11]. The system's overall performance was investigated and optimized during further *in vitro* experiments, before additional safety parameters were implemented and the system was successfully tested in a subsequent clinical trial in 5 subjects suffering from diabetes type 1.

In the first set of experiments the BVT sensor was characterized without its flow cell by being directly immersed into cups containing test solution during *in vitro* experiments (so called "cup experiments").
This elimination of the fluidics showed that the reaction time of the sensor itself lies within a range of seconds and can therefore be neglected compared to the system's delay time caused by diffusion processes and fluidics.
Moreover, a calibration curve characterizing the sensor's behaviour in un-buffered 5% Mannitol was recorded, as prior characterizations performed by the manufacturer only comprised the sensor's behaviour in phosphate buffered solution (see Appendix, *Calibration curve of the AC1.GOD glucose sensor in phosphate buffer*) which is not allowed to be used in humans. Although the sensor currents in un-buffered solution were lower than in buffered solution, strong linear behaviour up to 10mg/dl and slightly decreasing linear behaviour up to 20mg/dl was shown.
Nevertheless, the ion content of the un-buffered test solutions has a very strong influence on the sensor signal. Un-buffered test solutions, containing no sodium chloride, led to unstable and noisy sensor currents whose calibration curve deviated most compared to those with a higher ion content. After the investigation of eight sensors, it can be concluded that lower ion contents cause higher sensor currents.
However, calibration curves for solutions with 15% and 25% ion content were almost overlapping and thus suggested some kind of saturation effect. This led to the assumption that a minimum of 15% ions is needed in the perfusate to minimize the influence of ions on the sensor current. This was also consistent with the ion dependency of the Super GL2 that requires a minimum of 15% ion content to allow reliable measurements in the lower glucose

range. As a result, 20% saline solution was added to the perfusate used during the clinical trial.

During the next *in vitro* experiments, including the system's fluidics, it was shown that the BVT flow cell is very prone to air bubble accumulation, but no solution removing these air bubbles could be found. The only sufficient alternative was the general avoidance of any air bubbles occurring within the system. Investigations strongly indicate a connection between air bubble development and outgassing effects caused by warming up of the perfusate from room temperature (perfusate within the syringe) to 36.5°C (temperature of the human body). Thus, a proper filling of the perfusate syringe, without enclosing any air, and a subsequent degassing of the perfusate, turned out to be an effective solution avoiding air bubble accumulation. Degassing within a heated ultrasound bath before applying underpressure, or using a fluid warmer with subsequent syringe filter to hold back air bubbles proved to be effective solutions. Degassing the perfusate by manually applying underpressure (detailed instructions see Appendix, *Degassing of the perfusate within a syringe applying underpressure)* turned out to be a simpler alternative yielding the same good results. Therefore, this technique was used during the clinical trial.

Mimicking *in vivo* conditions in the final *in vitro* experiments yielded promising results. This was done by combining the intravenous microdialysis with the BVT flow cell and sensor, and using degassed perfusate containing a basic conductivity of 20% NaCl, a syringe filter holding back air bubbles and heated test solutions imitating a human subject. No experiment had to be ended prematurely due to artefacts and the system, with and without syringe filter holding back air bubbles introduced to the system by improper filling of the syringe, could be operated for more than 24 hours (in some cases even 60 hours and more) without being disturbed by any air bubble accumulations.

This "final setup" then had to undergo a risk evaluation and safety check. All three major hazards – electrical, thermal and biological - could be eliminated or decreased to an acceptable limit by taking adequate measures, although BVT flow cell and sensor were neither CE-certified nor sterile. Also, the electrical safety check for type CF medical equipment was passed successfully after an isolating transformer and optocoupler had been integrated into the setup to decrease the occurring leakage currents. Altogether the risk management file was approved by the local Ethics Committee of the Medical University of

Graz and the Austrian Agency of Health and Food Safety (AGES), and no adverse events occurred during or after the clinical trial. No sensor or flow cell had to be changed during the clinical trial and no air bubbles accumulated within the flow channel.

Curves for ion and glucose recovery during the clinical trial overlapped well most of the time and, therefore, support the proportionality assumptions of the IRT in *2.2 Ionic Reference Technique*. Moreover, these curves clearly show the impact of systemic anticoagulation. Subject 021 received the anticoagulant Arixtra® within the perfusate but not systemically. The recovery curves, therefore, rapidly decreased from about 30% to approximately 5%. This is probably due to agglutination effects on the membrane that cannot be sufficiently prevented by the small dose of anticoagulant that passes by with the perfusate. All other subjects, receiving additional systemic anticoagulation, showed rather constant recoveries over 24 hours. This suggests that a systemic anticoagulation is inevitable for this setup if constant recoveries are pursued.

A constant flow rate is also important if recoveries are to be kept constant. However, as the measurement range of the BVT sensor only comprises 0 – 20mg/dl the flow rate needed to be adjusted, due to changing recoveries during the experiments, in three out of five subjects. Thereby, flow rates of either 10 or 20µl/min were chosen to stay within the sensor's measurement range and to additionally avoid dialysate concentrations falling below the LLOQ of the Super GL2. Nominal flow rates were analysed and showed hardly any deviations, implying that the system was performing very well and the use of these commercially available syringe pumps can be recommended for this application. Nevertheless, a constant flow rate that is appropriate for monitoring blood glucose values throughout the whole experiment should be chosen to avoid changing recoveries.
This also shows the need for a glucose sensor with an extended measurement range, which allows lower flow rates and, thereby, higher recoveries even during hyperglycemic phases.

The run in time of the BVT sensor could be decreased by using a 5% Mannitol solution containing ions. Otherwise the sensor shows an additional run-in behaviour when being exposed to a Mannitol solution containing glucose and ions for the first time (data not shown). But still, the sensor's run in behaviour is slow and its zero current quite high. When exposed to a 5% Mannitol-NaCl solution without any glucose, it took about 10 hours until eight out of ten sensors fell below 5nA. Five sensors, observed for up to 39 hours, even needed almost 35

hours to fall below the desired zero current limit of 2nA. As such long run in periods are not feasible for an application in humans, the sensor should be at least run in overnight (≥10 hours) to achieve a zero current of approximately 4.39 ± 1.62 nA. A run in period of 1-2 hours would be desirable.

Before *in vivo* data could be analysed it had to be processed. First, the sensor signal required at least one initial calibration, as it delivers a current value proportional to the measured glucose concentration which needs to be converted from nA values to mg/dl values.
Second, the sensor current had to be filtered as it suffered from noise artefacts. The filter used combines a sliding-average filter with a threshold filter. The advantage of this filter compared with a simplistic and commonly used sliding average filter, is the reduction of delay times, as only values caused by non-physiological behaviour are averaged (details see *2.5.1 Filter Function for Sensor* Current).
Statistical analysis proved that filtering of the sensor data significantly improves the correlation with the blood reference. The reason, therefore, is the point-to-point comparison between sensor data and reference data. Picking a sensor value during a noisy moment worsens the correlation fundamentally.
Nevertheless, this general improving effect cannot be observed for the correlation between the sensor and the dialysate as this is an interval-to-interval comparison where an additional averaging with the filter leads to an additional delay time, which declines the coefficient of correlation.

The filtered and 1-point-calibrated sensor data – not IRT corrected and IRT corrected - was then compared with the reference blood data to investigate the improvement caused by the IRT. Exemplarily, the sensor current of subject 021 in Figure 51A shows that the uncalibrated, filtered, shifted but not IRT corrected sensor current suffers from strongly decreasing recoveries and, therefore, shows a coefficient of correlation with the reference blood measurement of r = 0. Contrarily, Figure 51B shows that an IRT correction and 1-point-calibration with the first valid blood reference value would improve the correlation between sensor signal and reference blood measurements, significantly, to r = 0.86. If the current is calibrated every 30 minutes, the improvement of this correlation from the current not IRT corrected (r = 0.96) to the current IRT corrected (r = 0.98) is marginal. Still, longer calibration intervals cause bigger improvements after applying the IRT ($r_{\text{IRT corrected}} > r_{\text{not IRT corrected}}$).
This, together with the analysis of various statistical parameters in

3.2.11 Statistical Evaluation, already suggests that the IRT can improve the correlation of a monitoring device, especially if a large calibration interval is pursued and the subject is not systemically anticoagulated, leading to strongly decreasing recoveries. The mean coefficients of correlation for IRT-corrected, 1 point-calibrated and filtered data were (mean value ± standard deviation) $r_{dialysate\text{-}sensor} = 0.94 \pm 0.02$, $r_{blood\text{-}dialysate} = 0.91 \pm 0.13$ and $r_{blood\text{-}sensor} = 0.83 \pm 0.20$. The overall absolute value of the system error between blood and sensor was 13.38 ± 7.94% and the mean absolute relative difference (MARD) was 17.34 ± 7.25%

A regression analysis further showed that the IRT improves the results of four out five data sets and that the acceptance criteria, according to ISO 15197:2003, is, therefore, fulfilled by these four subjects if a calibration interval of 30 minutes is used. Subject 024, who does not fulfil the acceptance criteria, should be excluded from evaluation due to a very noisy sensor current leading to extremely low coefficients of correlation, relativizing any conclusion. Moreover, comparing the number of calibration points needed to guarantee a system error of ±10% shows that applying the IRT can decrease this number (up to ~37% in subject 021) in four out of five subjects. Only subject 023 shows a slight increase of ~12% if the IRT is applied.

Dialysate and sensor data correlate better than blood and dialysate data for all subjects for filtered, uncalibrated and not IRT corrected data. This supposes that the correlation between blood and sensor is mainly negatively influenced by the bad correlation between blood and dialysate. Yet, this is not surprising as the microdialysis probe was operated under suboptimal conditions due to the small measurement range of the BVT sensor.
This again indicates that high recoveries can improve the overall system performance, increasing the need for a glucose sensor covering a larger glucose range.

All together Figure 48 shows that the sensor signal of subjects 023, 025 and 026 correlate very well with the blood and dialysate glucose concentrations if it is IRT corrected and 1-point-calibrated. Subject 021 shows a decreasing sensor signal after 6 hours supposing that correlation could be significantly improved if a second calibration was applied at the beginning of the 180mg/dl clamp phase. Subject 024 shows a sensor signal that does neither correlate well to blood nor to dialysate glucose. But compared to the performance of the other 4 sensors this is very likely due to a malfunction of this particular sensor.

5 CONCLUSION AND OUTLOOK

The aim of the EU-CLAMP project was to develop a system based on intravenous microdialysis technique which continuously monitors the blood glucose concentration without the loss of blood. This system should then be further integrated into an automated clamp device.
The aim of this thesis was to characterize the BVT glucose sensor during *in vitro* experiments and to find optimal measurement conditions. Furthermore, the sensor was then integrated into the sampling unit and the system's overall performance was investigated and optimized during *in vitro* experiments. After implementing the required safety measures, the system was approved by the local Ethics Committee of the Medical University of Graz and the Austrian Agency of Health and Food Safety (AGES) and tested within a clinical trial in 5 subjects suffering from diabetes type 1.

As a result of certain setup requirements, for example, warming up of the perfusate within the MD in a subject's vein, or the use of flow cells that are prone to air bubble accumulation, the inevitable development of air bubbles due to outgassing effects within the system was a main issue. Degassing the perfusate by applying underpressure turned out to be an effective solution to avoid any outgassing effects. Although the method is not totally reproducible, all subsequent *in vitro* and *in vivo* experiments could be performed without being disrupted by air bubble accumulation. Hence, degassing of the perfusate should be a mandatory process when using air bubble sensitive setups.

Moreover, the specification of using the BVT glucose sensor led to severe restrictions. The BVT sensor only comprises a measurement range up to 20mg/dl in un-buffered solution although the clamp protocol could ideally yield dialysate concentrations of 180mg/dl and more. Therefore, very high flow rates had to be chosen to decrease recovery rates and, thereby, glucose concentrations in the dialysate. This strongly conflicts with the results of the first part of the EU-CLAMP project which stated that high recoveries are essential for a good correlation between dialysate and blood glucose. Andreas Huber even advised recoveries of more than 5% to obtain coefficients of correlation of more than 0.8 [11].
During the clinical trial, the sensor itself correlated well with the dialysate concentrations ($r \geq 0.98$ for all subjects for filtered and IRT corrected sensor data with a calibration interval of 30

minutes) but deviated from the blood concentrations ($r \leq 0.98$ for all subjects) as the MD probe was not operated under optimal conditions and mean recoveries were between 7 and 8%. In conclusion, recoveries should be kept as high as possible to enable the best correlation between blood and dialysate glucose. Otherwise correlation between blood and sensor glucose will never be optimized.

This thesis has shown the feasibility of a glucose monitoring device combining intravenous microdialysis and glucose sensors. Improvements, especially concerning recovery, optimal components and system integration, have to be done before this monitoring method can be further combined with an algorithm, calculating the adequate insulin dose and therefore permitting the development of an automated clamp device.

Besides improving clamp procedures for insulin characterisation in order to release new insulins to the market, a continuous glucose monitoring device could also be used in a different field of application: strict monitoring of blood glucose and an associated insulin therapy can improve the outcome in critically ill patients in intensive care (ICU) or cardiac care units (CCU) [16]. However, so far such tight control of blood glucose is associated with pain and blood loss that comes along with frequent finger sticks and blood draw. Hence, continuous glucose monitoring via microdialysis could be a suitable alternative in ICUs and CCUs. Additionally, labour costs could be reduced if an automated continuous glucose monitoring device with insulin infusion algorithm is used.
This potential will certainly lead to further research in the area of continuous glucose monitoring.

APPENDIX

Validation of the Super GL2 concerning the influence of different spike volumes

		Glucocapil #1		Glucocapil #2	
Pipette	**spiked Volume**	**Measurement 1**	**Measurement 2**	**Measurement 1**	**Measurement 2**
	[µl]	[mg/dl]	[mg/dl]	[mg/dl]	[mg/dl]
Eppendorf 100µl	20	20,80	20,90	20,50	20,90
Eppendorf 100µl	40	40,30	40,40	40,70	40,30
Eppendorf 100µl	100	95,20	95,70	96,50	96,30
Eppendorf 200µl	200	171,00	175,00	175,00	175,00
Eppendorf 1000µl	300	239,00	241,00	242,00	242,00
Eppendorf 1000µl	400	295,00	298,00	298,00	298,00
Gilson 20µl CRC INO4	20	20,40	20,70	20,80	20,70
Gilson 20µl CRC INO 1	20	20,90	21,20	21,20	21,10
Gilson 20µl CRC INO 3	20	20,70	20,60	20,90	20,60
	SD	0,26	0,23	0,23	0,20
	MV	20,51	20,68	20,73	20,69
	CV	1,28	1,13	1,13	0,98

		Glucocapil #3		Glucocapil #4	
Pipette	**spiked Volume**	**Measurement 1**	**Measurement 2**	**Measurement 1**	**Measurement 2**
	[µl]	[mg/dl]	[mg/dl]	[mg/dl]	[mg/dl]
Eppendorf 100µl	20	20,70	20,70	20,80	20,70
Eppendorf 100µl	40	40,70	40,70	40,40	40,50
Eppendorf 100µl	100	96,10	96,10	96,20	96,40
Eppendorf 200µl	200	175,00	175,00	175,00	175,00
Eppendorf 1000µl	300	241,00	240,00	242,00	241,00
Eppendorf 1000µl	400	297,00	296,00	299,00	298,00
Gilson 20µl CRC INO4	20	20,70	20,60	20,70	20,70
Gilson 20µl CRC INO 1	20	21,00	21,10	21,30	21,10
Gilson 20µl CRC INO 3	20	20,70	20,80	20,70	20,70
	SD	0,18	0,23	0,24	0,19
	MV	20,67	20,66	20,72	20,68
	CV	0,85	1,12	1,13	0,93

Figure 54: Results of the Super GL2 validation concerning the influence of different spike volumes. The different volumes were spiked into 4 different Glucocapil caps with 9 different pipettes. Standard deviation (SD), mean value (MV) and CV (coefficient of variation) are depicted as well. **[11]**

Air bubbles accumulating in the FC2.S flow cell and prohibiting any data evaluation

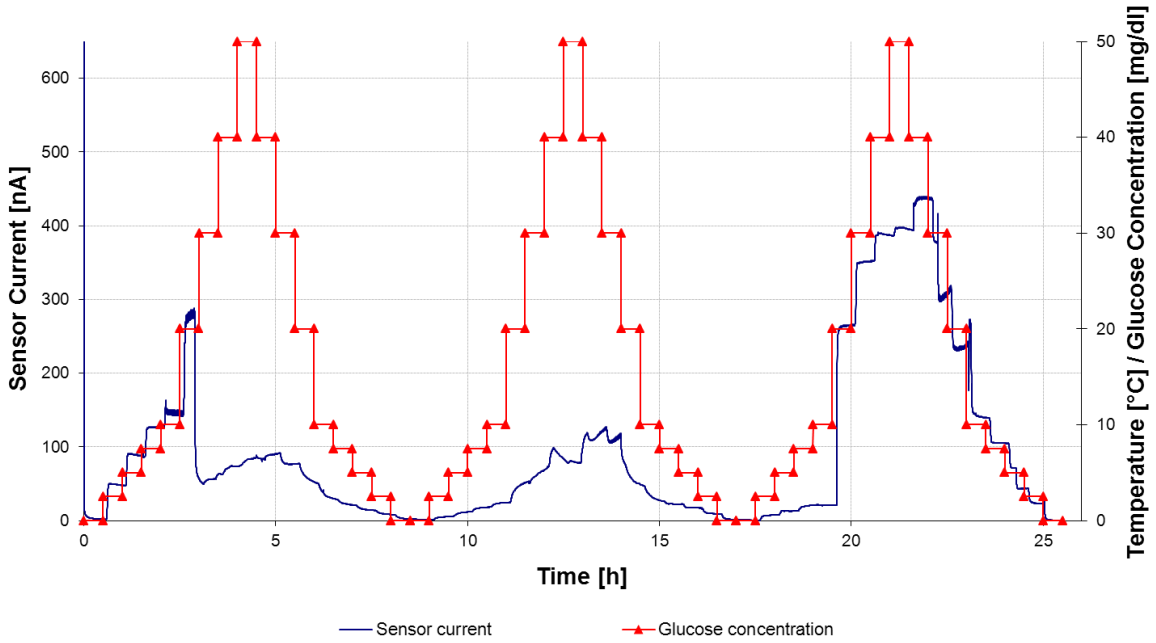

Figure 55: Air bubble artefacts disrupting the sensor signal during first *in vitro* experiments in buffered solution (50% phosphate buffer)

Calibration curve of the AC1.GOD glucose sensor in phosphate buffer

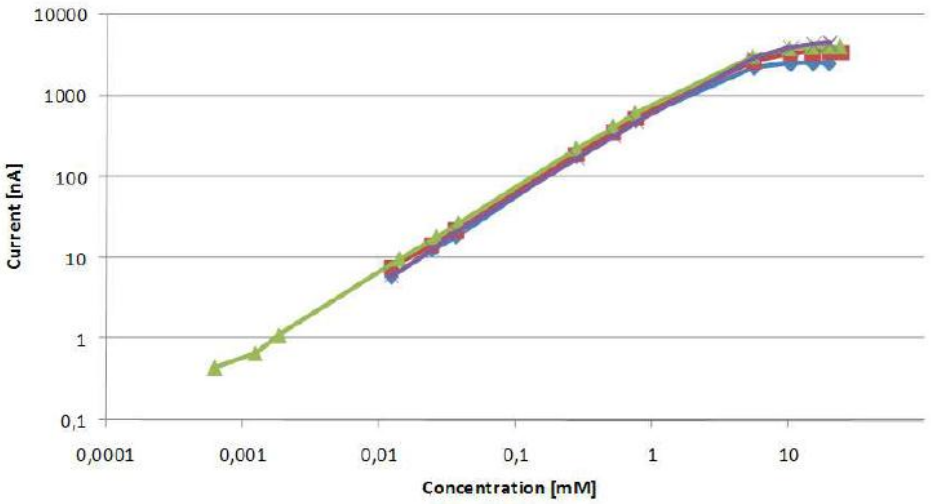

Figure 56: Calibration curve of the BVT AC1.GOD glucose sensor in phosphate buffer, performed by BVT Technologies.

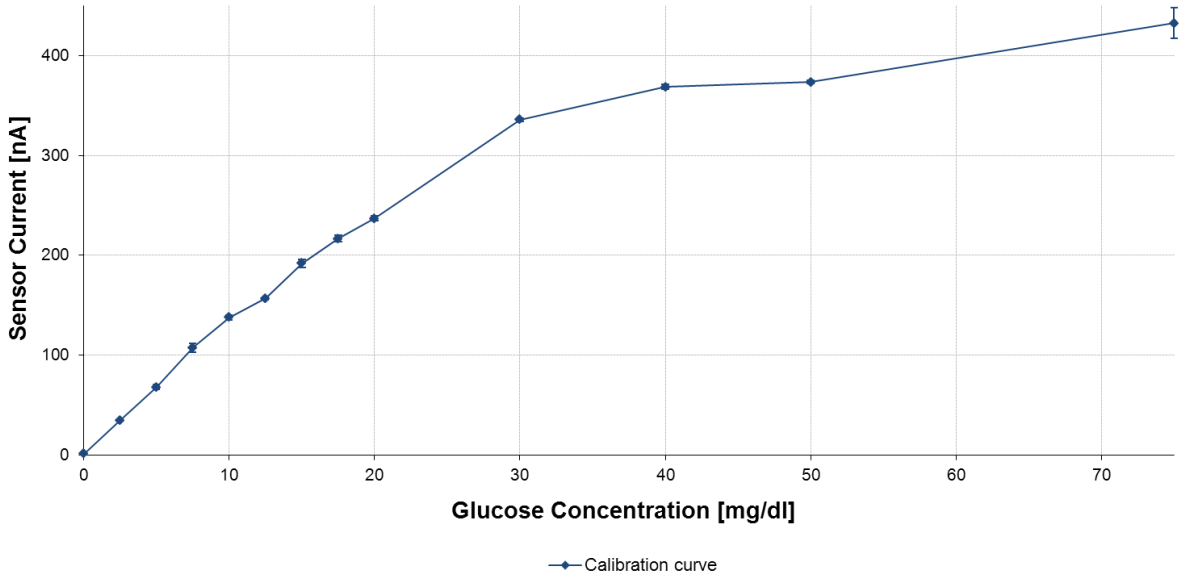

Figure 57: Calibration curve of the BVT AC1.GOD glucose sensor in phosphate buffer.

Response time investigations in the final combined system

Sys1 and Sys2 were investigated in parallel. The BBRAUN Perfusor fm was used to pump a degassed 5% Mannitol solution with Arixtra®, with a flow rate of 20µl/min, through the flow cells containing the BVT sensors. The body interfaces were immersed into three 0.9% NaCl solutions containing glucose (20, 35 and 50mg/dl) and heated to 36.5°C. The resulting sensor currents that were then used to estimate the system's response time can be seen in Figure 58 and Figure 59.

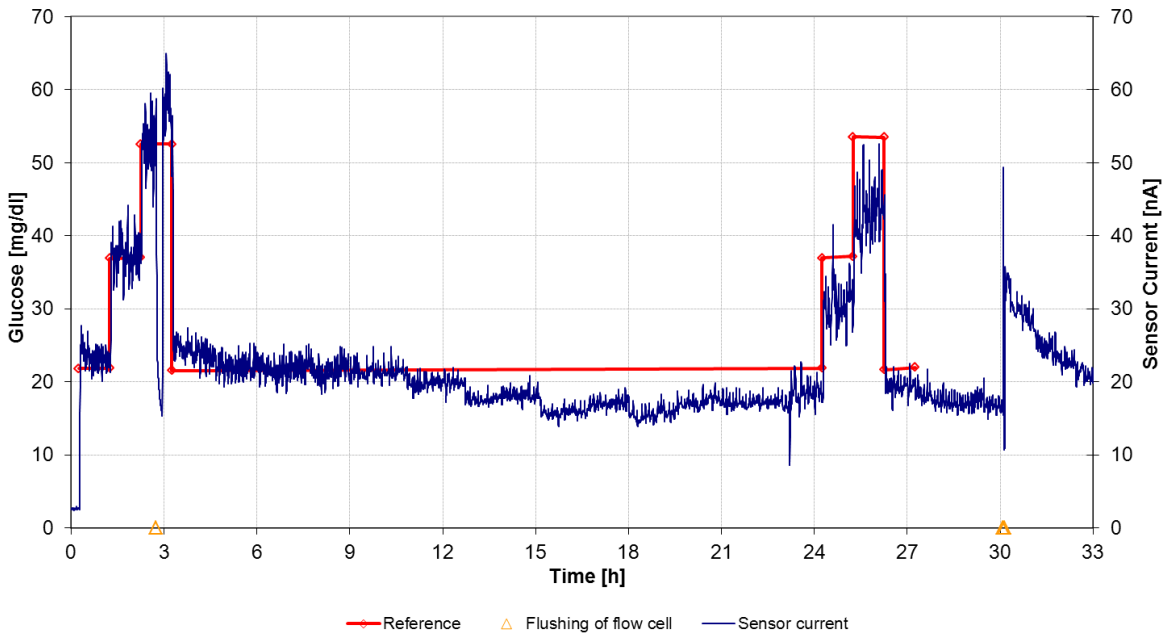

Figure 58: Sensor current of Sys1 with syringe filter used to determine the system's response time.

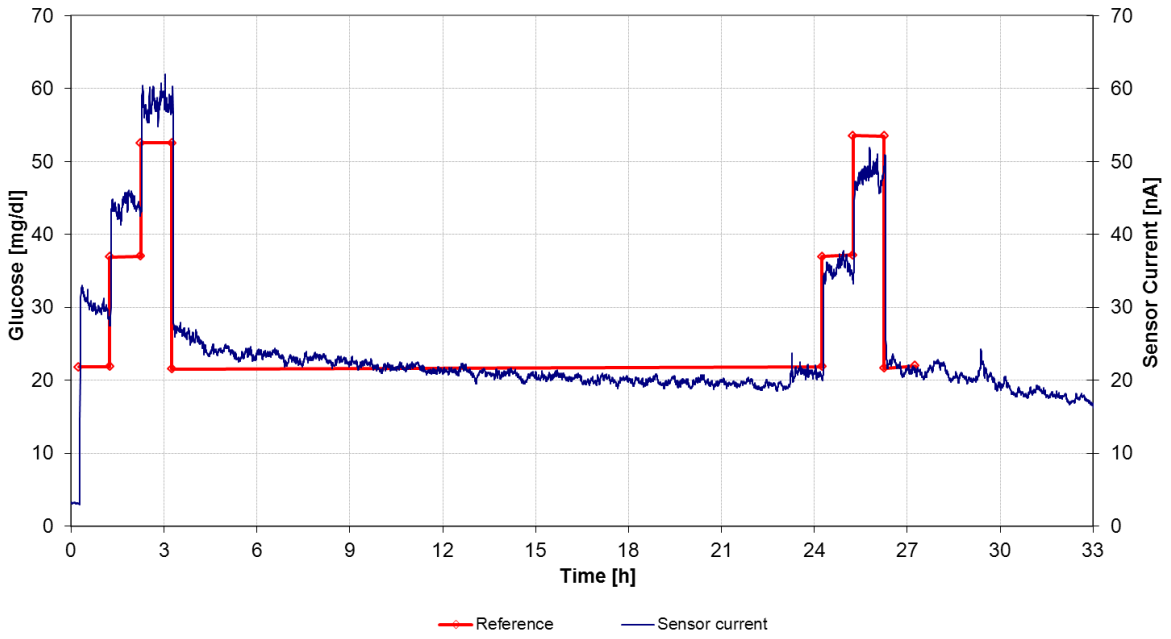

Figure 59: Sensor current of Sys2 used to determine the system's response time.

Air bubble investigations

A Belmont® Buddy fluid warmer (see Figure 15) was integrated in the combined system with one additional flow cell to investigate the outgassing effects. Figure 60 shows the setup in which the first flow cell shall detect air bubbles that outgas in the fluid warmer at 38°C and the second flow cell that shall detect air bubbles that out-gas in the body interface at 36.5°C. Three different heating conditions (a, b and c) were investigated and are depicted in Figure 60 as well. During the run in period, the sensors were perfused with a 5% Mannitol – 0.9% NaCl (9:1) solution and the probes were immersed in pure 0.9% NaCl. Afterwards, the perfusate and the NaCl solution were changed to a 5% Mannitol – 0.9% NaCl (9:1) solution with 10mg/dl glucose to visualize air bubbles.

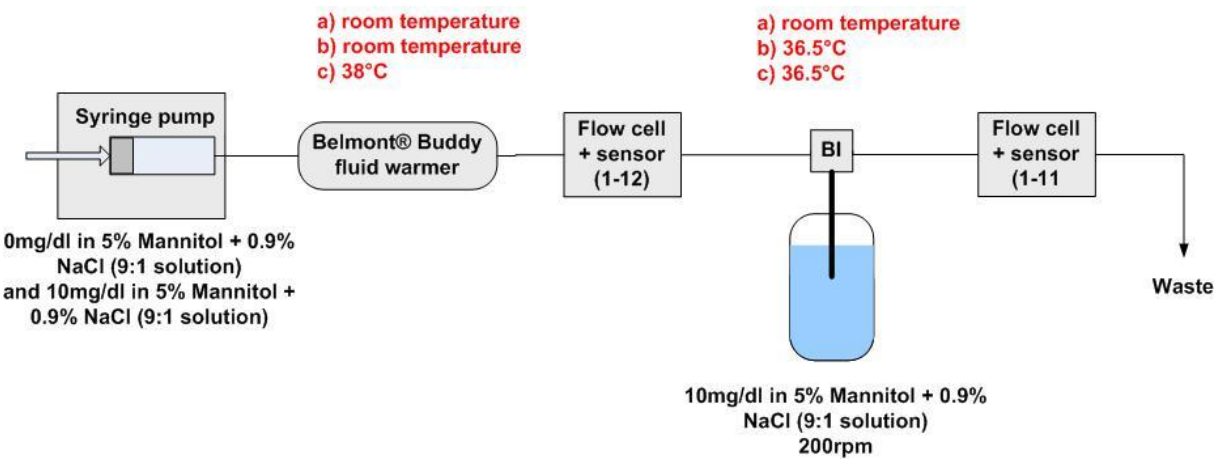

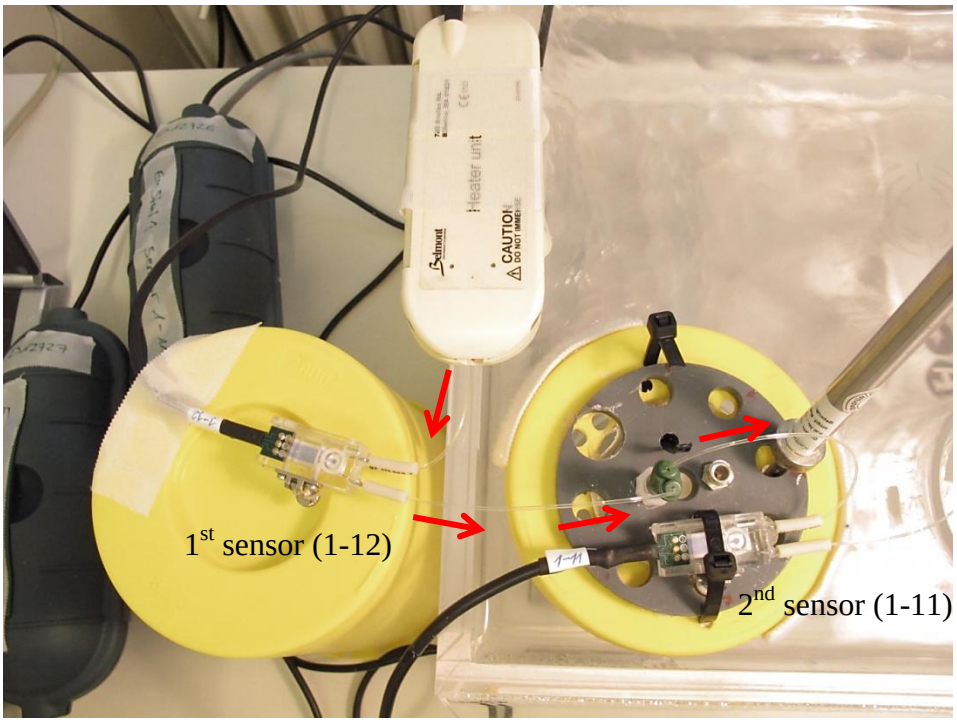

Figure 60: Setup of the in vitro air bubble investigations with a Belmont® Buddy fluid warmer.

Figure 61 shows the sensor currents received from the setup with two flow cells and a Belmont® Buddy fluid warmer. After about 23 hours the water bath was turned on. However, as both flow cells were placed on the test solution's cap in the water bath for the first 41 hours, the first sensor (1-12) suffered from an outgassing of the perfusate as well, and air bubbles accumulated within the flow channel, as a result of radiant heat. Interestingly, the second sensor (1-11) showed less air bubble artefacts during that time, supposing that the first sensor worked as kind of a "filter", holding back air bubbles. Moreover, it seemed as if the perfusate was degassed in the first flow cell leading to less outgassing effects in the second flow cell. This already indicated the use of a filter and/or degassed perfusate to overcome air bubble problems.

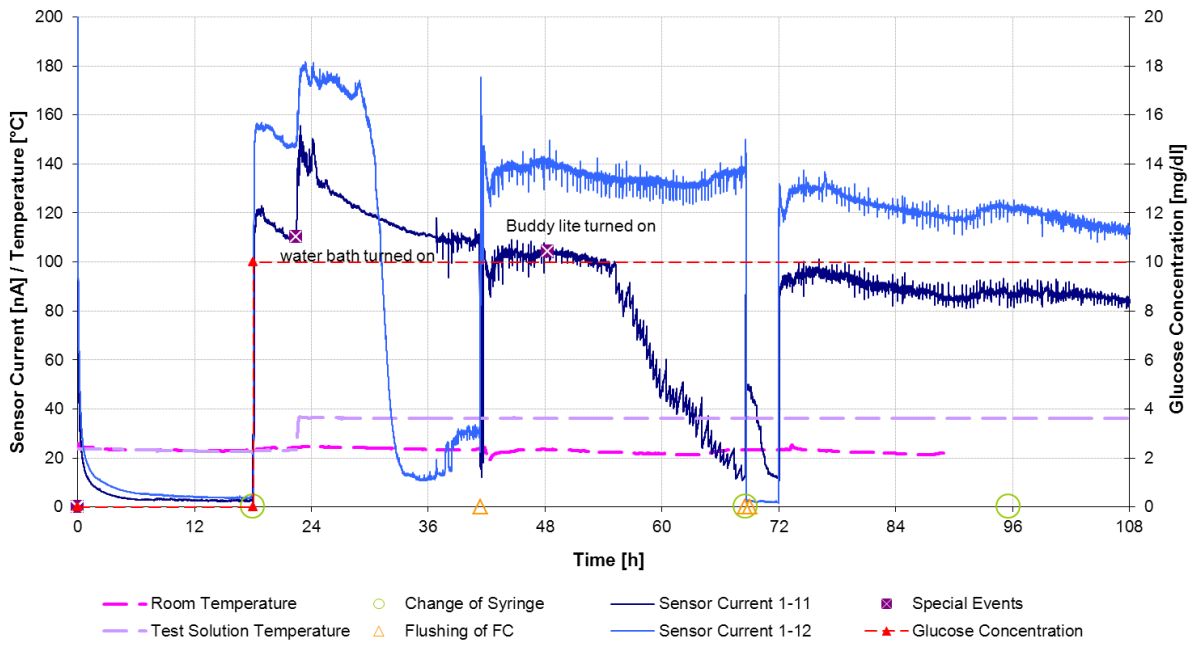

Figure 61: Sensor currents of the sensors used during air bubble investigation with a Belmont® Buddy fluid warmer.

Overview on the 9 experiments performed to find the optimal setup for in vivo investigations

Experiment	Date	Pump / Perfusate	Strategy against air bubbles	Result
1. *In vitro* setup	27.03.2012	Syringe pump / 5% Mannitol	---	✓ no air bubbles
		Syringe pump / 5% Mannitol	---	✓ no air bubbles
2. *In vitro* setup	02.04.2012	Syringe pump / 5% Mannitol + Arixtra	---	✗ air bubbles
		Syringe pump / 5% Mannitol + Arixtra	---	✗ air bubbles
3. Influence of temperature	11.04.2012	Syringe pump / 5% Mannitol + Arixtra	Water bath was turned on and off	✗ air bubbles ✓ no air bubbles
		Syringe pump / 5% Mannitol + Arixtra	Water bath was turned on and off	✗ air bubbles ✓ no air bubbles
4. Influence of temperature	15.04.2012	Syringe pump / 5% Mannitol + Arixtra	Water bath was turned on and off	✗ air bubbles ✓ no air bubbles
		Syringe pump / 5% Mannitol + Arixtra	Water bath was turned on and off	✗ air bubbles ✓ no air bubbles

5. Influence of pump	26.04.2012	Syringe pump / 5% Mannitol	---	✗ air bubbles
		Roller pump / 5% Mannitol	---	✗ air bubbles
6. Influence of heating (Buddy IV fluid warmer)	02.05.2012	Syringe pump / 5% Mannitol + 0.9% NaCl + Glucose	Perfusate was heated with Buddy IV	✓ no air bubbles
		Syringe pump / 5% Mannitol + 0.9% NaCl + Glucose	---	✗ air bubbles
7. Influence of heating (Buddy IV) + syringe filter vs. influence of degassing	07.05.2012	Syringe pump / 5% Mannitol	Perfusate was heated with Buddy IV + syringe filter	✓ no air bubbles
		Syringe pump / 5% Mannitol	Degassed perfusate (underpressure, US-bath: 30min, 40°C)	✓ no air bubbles
8. Influence of degassing + syringe filter	14.05.2012	Syringe pump / 5% Mannitol	---	✗ air bubbles
		Syringe pump / 5% Mannitol	Degassed perfusate (underpressure) + syringe filter	✓ no air bubbles
9. Final *in vitro* setup	03.07.2012	Syringe pump / 5% Mannitol	Degassed perfusate (underpressure) + syringe filter	✓ no air bubbles
		Syringe pump / 5% Mannitol	Degassed perfusate (underpressure) + syringe filter	✓ no air bubbles

Table 11: Overview on the 9 experiments performed to find the final setup for the *in vivo* investigations.

Air bubbles disrupting the sensor signal as a result of heating the perfusate

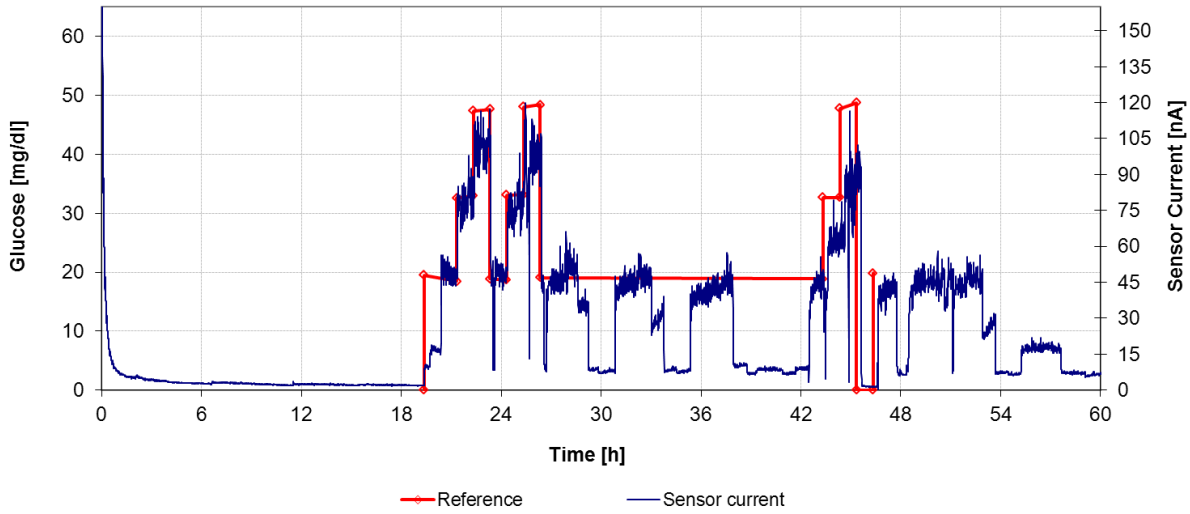

Figure 62: Air bubbles disrupting the sensor signal due to outgassing effects as a result of heating the perfusate in the combined setup during experiment 2.

Degassing of the perfusate within a syringe applying underpressure

The following steps describe how the perfusate can be simply degassed by applying under-pressure.

Filling the syringe with perfuste

- Disinfect the septum of the perfusate bottle
- Assemble a sterile needle onto the syringe, fill it with air and penetrate the sterile septum of the bottle.
- Press the air into the bottle so that the perfusate enters the syringe without under-pressure.
- Remove the syringe from the bottle.

- Remove the remaining air by holding the syringe vertically, tapping it and moving the piston forward.

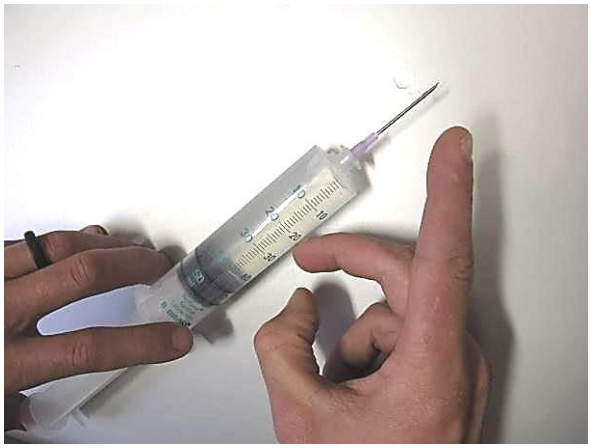

Apply under-pressure for degassing and remove air bubbles

- Close the syringe with a red sterile cap.

- Move the piston backwards when the syringe is sealed by the sterile cap and hold it in position for about 5 to 10 seconds until air bubbles occur within the syringe.

- Remove air bubbles by removing the red sterile cap, holding the syringe vertically, tapping it and moving the piston forward as described above.
- To fully degas the perfusate repeat these steps 3-4 times.

Flushing of the flow cell to remove accumulated air bubbles

The following steps describe the process for removing air bubbles by flushing the flow cell.

1. Preparing the flushing fluid

A 3ml or 5ml syringe is filled with the remaining perfusate. A rounded tip (Nordson Precision Tips, Ref: 7018314; TIP 23GA.013X.5, orange) is used to connect the syringe with the flow cell via PHARMED BPT tubing. Remaining air is removed by tapping the syringe and moving the piston forward.

2. Flushing of the flow cell

The connection between the outlet of the MD catheter and the inlet of the flow cell is disconnected. The outlet tubing of the flow cell is put into a waste container and the flushing syringe is connected to the flow cell's inlet tube. The air bubbles can then be removed by moving the syringe piston forward and flushing the fluid through the flow cell.

Do not flush the flow cell in both directions! The dialysate must not be flushed back into the MD catheter!

3. Continuing the measurement

The flushing syringe is removed, the MD catheter outlet is reconnected with the flow cell's inlet (wait until a drop of dialysate appears at the MD's outlet before connecting both to avoid air bubble introduction) and the outlet tubing of the flow cell is put into the sample vial. The sensor current will show a large peak as a result of the flushing, but the current should decrease again quickly (~ few minutes). If the sensor current does not recover or the air bubble could not be removed, one should carefully observe the continuing current and change the whole flow cell if necessary.

Risk management file

Defined Graph

inacceptable area

ALARP-Area

acceptable area

Lik					
Oft					
Occ					
Ima					
Unl					
	Mar	Min	Ser	Cri	Dis

Severity

Abbrev.	Description	Criteria	Examples
Mar	Marginal	Innconvinience or temporal afflictions or technical effect with no direct influence to subject	temporary pain; temporary constraints; bandages
Min	Minor	Temporal harm - medical intervention not necessary	heamatoma; swelling; moderate pain;
Ser	Serious	harm or handicap - medical intervention is necessary	progressive inflammation; temporary violent pain; persistent moderate pain; medication is needed
Cri	Critical	progressive handicap, a great deal of pain	Cross-contamination/infection through reuse of disposables; persistant violent pain; cardiac arrhythmias
Dis	Disastrous	permanent handicap, life-threatening disease, death	sepsis; amputation; asystole; loss of eyesight, hearing, sense; paralysis; disfigurement...

Likelihood

Abbrev.	Description	Criteria / Examples
Unl	Unlikely	failure not imaginable; very similar failures unknown yet
Ima	Imaginable	failure is slighty imaginable; scattered single cases of similar failures are known
Occ	Occasionally	failure is imaginable at clinical concept-trials or several similar failures are known
Oft	Often	failure is imaginable in one of 10 subjects or similar failures with a related frequency are already known.
Lik	Likely	failure will happen probably in one subject or permanent system fault / system design

Approval of risk analysis

Risks are evaluated by means of severity and likelihood and classified within the Risk Graph. 3 areas are possible:

Green =Aacceptable area : Risk is acceptable

Yellow = ALARP area (As Low As Reasonably Possible) = Risk is acceptable, measures should be taken to achive further risk decrease, if possible

RED = inacceptable area: Risks within this area have to be shifted at least into the ALARP-area. If this is not possible with appropriate measures, risk-benefit-analysis have to be done. In exceptuional cases, the residual risk can be accepted, if expected benefit exceeds the risks.

Figure 63: Detailed risk management matrix.

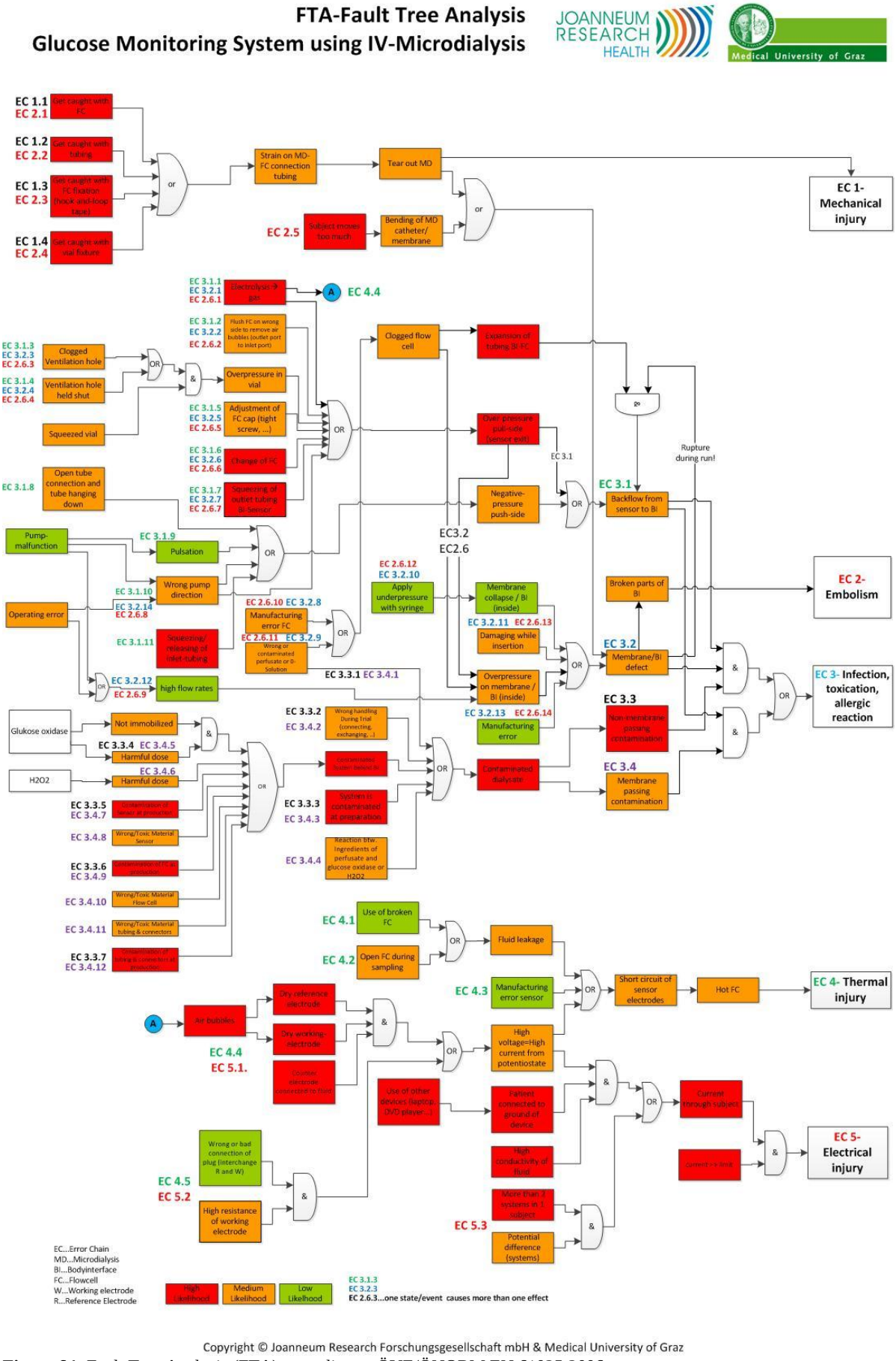

Figure 64: Fault Tree Analysis (FTA) according to ÖVE/ÖNORM EN 61025:2006.

Identified risks												Estimation after meaures							
Nr.	FTA Ref.	Component Function Process	Failure Mode	Cause	Effect	Likelihood		Severity		Risk Area	Remarks	Measures	Responisible	Likelihood		Severity		Risk Area	Additional Risk out of measure
	EC 1	**Mechanical Injury**																	
1	EC1.1	FC	Strain on MD-FC connection tubing	get caught with FC	Tear out MD-catheter-mechanical injury	ima	2	min	2			SOP: safe fixing of system (tubing, flowcell, connectors…) at subject	JR/MUG	ima	2	min	2		no
2	EC1.2	tubing		get caught with tubing		occ	3	min	2					ima	2	min	2		
3	EC1.3	FC-Fixation		get caught with FC-fixing tape		ima	2	min	2					ima	2	min	2		
4	EC1.4	Vial		get caught withvial fixture		ima	2	min	2					ima	2	min	2		
	EC 2	**Embolism**																	
5	EC2.1	FC	Strain on MD-FC connection tubing	get caught with FC	Tear out of MD-cathteter - defct/broken membrane/BI - embolism	ima	2	ser	3		certified BI	SOP: safe fixing of system (tubing, flowcell, connectors…) at subject SOP: Check bodyinterfaces after explantation - in case of defect instantaneous medical action/observation	JR/MUG	ima	2	ser	3		no
6	EC2.2	tubing		get caught with tubing		ima	2	ser	3					ima	2	ser	3		
7	EC2.3	FC fixation		get caught with FC-fixing tape		ima	2	ser	3					ima	2	ser	3		
8	EC2.4	vial fixation		get caught withvial fixture		ima	2	ser	3					ima	2	ser	3		
9	EC2.5	subject	folding of MD-catheter/membrane	subject moves too much	membrane defect - embolism	unl	2	ser	3		certified BI	SOP: Check bodyinterfaces after explantation - in case of defect instantaneous medical action/observation	JR / MUG	ima	1	ser	3		no
10	EC2.6.1	Sensor	Electrolysis/gas	Permanent state	over-pressure on membrane - membrane defect - embolism	unl	1	ser	3		rigid vials placed in holder are used--> squeezing only possible while changing Change of volume is very small is relatively unlikely, that small particles can be detached, even if membrane breakes (CE-marked BI)	none	--	unl	1	ser	3		no
11	EC2.6.2	FC	FC flushed on wrong side	Handling error		occ	3	ser	3			SOP: observation of blood in dialysate in (SOP) --> explantation	JR / MUG	ima	2	ser	3		no
12	EC2.6.3	Vial	Clogged ventilation hole + squeezed vial	Ventilation hole too small Soft material of vial		ima	2	ser	3			SOP: do not squeeze vial, do not hold ventilation hole shut; Design: sufficient diameter of ventilation hole; Design: Use of rigid vials	JR / MUG	unl	1	ser	3		no
13	EC2.6.4	Vial	Ventilation hole held shut + squeezed vial	Handling error Soft material of vial		unl	1	ser	3				JR / MUG	unl	1	ser	3		no
14	EC2.6.5	FC	Adjustment of FC	Handling due to leakage		unl	1	ser	3		Change of volume and pressure due to this action is very small	none	--	unl	1	ser	3		--
15	EC2.6.6	FC	Exchange of FC	Clogged FC, sensor defect, leakage, air bubbles		ima	2	ser	3			SOP: continuous pumping while changing FC (avoid air bubbles)	JR / MUG	unl	1	ser	3		no
16	EC2.6.7	Outlet tubing	Squeezing of outlet tubing btw. BI and sensor	Handling, soft tubing, movement of subject & equipment		ima	2	ser	3			Design: Use of ~~short,~~ rigid tubing --> contradicts with measure "decrease distance between BI-Sensor" --> increase distance is much more important than the small change of Volume generated by squeezing --> only use of rigid tubing as measure	JR / MUG	unl	1	ser	3		no

17	EC2.6.8	JR-Pump	wrong pump direction	JR-pump: wrong insertion of tubing (Push-Pull mode)	Positive pressure pull side - membrane defect - embolism	occ	3	ser	3		Pressure from push and pull side to BI	SOP: training of operators and staff (for pump-handling) SOP: Check bodyinterfaces after explantation - in case of defect instantaneous medical action/observation	JR / MUG	ima	2	ser	3		no
18	EC2.6.9	BBraun-Pump	High flow rates	Pump malfunction, technical defect, operating error	High flow rates - overpressure on membrane - membrane/BI defect - embolism	ima	2	ser	3		BBraun pump has internal pressure sensor	SOP: training of operators and staff (for pumps), use of CE-marked pumps SOP: Check bodyinterfaces after explantation - in case of defect instantaneous medical action/observation	JR / MUG	unl	1	ser	3		no
19	EC2.6.10	FC	Clogged flow cell	Manufacturing error	Overpressure membrane, expansion / rupture - backflow - embolism	ima	2	ser	3		is controlled in run-in period; Reaction in perfusate has never been seen in previous experiments	SOP: visual control of FC before trial (particles, open channels) SOP: Check bodyinterfaces after explantation - in case of defect instantaneous medical action/observation	JR/MUG	unl	1	ser	3		no
20	EC2.6.11	FC	Clogged flow cell	wrong or contaminated perfusate or 0-solution (coagulation of substances)		unl	1	ser	3					unl	1	ser	3		
21	EC2.6.12	BI	Membrane collapse	Apply underpressure with syringe (to remove air bubbles)	Defect membrane - embolism	unl	1	ser	3		Membranes are relatively stable against underpressure evaluted in EC 3 in combination with other points CE-marked BI, trained physicians and staff	Evaluate available Data of Probe Scientific (resistance against underpressure)	Probe / JR / MUG	unl	1	ser	3		no
22	EC2.6.13	BI	Membrane/BI defect	Damaged during insertion, damaged during trial		ima	2	ser	3					ima	2	ser	3		
23	EC2.6.14	BI	Membrane/BI defect	manufacturing error,		unl	1	ser	3					unl	1	ser	3		
	EC 3.1	**Backflow Sensor --> Bodyinterface**																	
24	EC3.1.1	Sensor	Electrolysis/gas	Permanent state	Overpressure pull side - backflow from sensor to BI;	ima	2	mar	1		**all points of EC 3.1 are evaluted in EC 3 in combination with other points**	none	--	ima	2	mar	1		--
25	EC3.1.2	FC	FC flushed on wrong side	Handling error		occ	3	mar	1			SOP: observation of blood in dialysate in (SOP) --> explantation	JR / MUG	ima	2	mar	1		no
26	EC3.1.3	Vial	Clogged ventilation hole + squeezed vial	Ventilation hole too small Soft material of vial		ima	2	mar	1		no problem, if mebrane of BI is ok Use of rigid vials placed in holder --> squeezing only possible while changing	SOP: do not squeeze vial, do not hold ventilation hole shut; Design: sufficient diameter of ventilation hole; Design: Use of rigid vials	JR / MUG	unl	1	mar	1		no
27	EC3.1.4	Vial	Ventilation hole held shut + squeezed vial	Handling error Soft material of vial		unl	1	mar	1					unl	1	mar	1		no
28	EC3.1.5	FC	Adjustment of FC	Handling due to leakage		ima	2	mar	1		Change of volume and pressure due to this action is very small	none	--	ima	2	mar	1		--
29	EC3.1.6	FC	Exchange of FC	Clogged FC, sensor defect, leakage, air bubbles		ima	2	mar	1			SOP: continuous pumping while changing FC (avoid air bubbles)	JR / MUG	ima	2	mar	1		no
30	EC3.1.7	Outlet tubing	Squeezing of outlet tubing btw. BI and sensor	Handling, soft tubing, movement of subject & equipment		ima	2	mar	1			Design: Use of short, rigid tubing --> contradicts with measure "decrease distance between BI-Sensor" --> increase distance is much more important than the small change of Volume generated by squeezing --> only use of rigid tubing as measure	JR / MUG	unl	1	mar	1		no

31	EC3.1.8	Inlet tubing	Open tube connection, tube hanging down	Change of pump or inlet tubing	Negative pressure push side - backflow from sensor to BI	occ	3	mar	1			SOP: stop pump, disconnect tubing, connect new tubing	JR / MUG	ima	2	mar	1		no
32	EC3.1.9	Pump	pulsation at peristaltic pump	permanent state		occ	3	mar	1			Design: increase distance BI-Sensor (calculation of save distance)	JR / MUG	unl	1	mar	1		no
33	EC3.1.10	BBraun Pump	wrong pump direction	technical defect, handling		unl	1	mar	1		CE-marked infusion pump	none	--	unl	1	mar	1		--
34	EC3.1.10	Pump	wrong pump direction	JR-pump: wrong insertion of tubing (Push-Pull mode)		occ	3	mar	1			Warning: Insertion of tubing with right direction	JR / MUG	ima	2	mar	1		no
35	EC3.1.11	Inlet tubing	Squeezing/releasing of inlet tubing (BI)	Handling, soft tubing, movement of subject and equipment		occ	3	mar	1		long tubing is used	Design: increase distance BI-Sensor (calculation of safety distance) Design: rigid tubing	JR / MUG	ima	2	mar	1		no
	EC 3.2	**Membrane / Bodyinterface defect / broken**																	
36	EC3.2.1	Sensor	Electrolysis/gas	Permanent state	over-pressure on membrane - membrane defect	unl	1	mar	1		**all points of EC 3.2 are evaluted in EC 3 in combination with other points**	none	--	unl	1	mar	1		--
37	EC3.2.2	FC	FC flushed on wrong side	Handling error		occ	3	mar	1		high pressure possible	SOP: observation of blood in dialysate in (SOP) --> explantation	JR / MUG	ima	2	mar	1		no
38	EC3.2.3	Vial	Clogged ventilation hole + squeezed vial	Ventilation hole too small Soft material of vial		ima	2	mar	1			SOP: do not squeeze vial, do not hold ventilation hole shut; Design: sufficient diameter of ventilation hole; Design: Use of rigid vials	JR / MUG	ima	2	mar	1		no
39	EC3.2.4	Vial	Ventilation hole held shut + squeezed vial	Handling error Soft material of vial		unl	1	mar	1					unl	1	mar	1		
40	EC3.2.5	FC	Adjustment of FC	Handling due to leakage		unl	1	mar	1		Change of volume and pressure due to this action is very small	none	--	unl	1	mar	1		--
41	EC3.2.6	FC	Exchange of FC	Clogged FC, sensor defect, leakage, air bubbles		unl	1	mar	1			SOP: continuous pumping while changing FC (avoid air bubbles)	JR / MUG	unl	1	mar	1		no
42	EC3.2.7	Outlet tubing	Squeezing of outlet tubing btw. BI and sensor	Handling, soft tubing, movement of subject & equipment		ima	2	mar	1			Design: Use of short, rigid tubing --> contradicts with measure "decrease distance between BI-Sensor" --> increase distance is much more important than the small change of Volume generated by squeezing --> only use of rigid tubing as measure	JR / MUG	unl	1	mar	1		no
43	EC3.2.8	FC	Clogged flow cell	Manufacturing error	Overpressure membrane, expansion / rupture - backflow	ima	2	mar	1			SOP: Check of FC before Trial	JR/MUG	ima	2	mar	1		no
44	EC3.2.9	FC	Clogged flow cell	wrong or contaminated perfusate or 0-solution (coagulation of substances)		unl	1	mar	1		not seen yet at clinical trials	none	--	unl	1	mar	1		--

45	EC3.2.10	BI	Membrane collapse	Apply underpressure with syringe (to remove air bubbles)	Defect membrane	ima	**2**	mar	**1**		Membranes are relatively stable against underpressure	SOP: training of operators and staff SOP: Check bodyinterfaces after explantation - in case of defect instantaneous medical action/observation	JR/MUG	unl	**1**	mar	**1**		no
46	EC3.2.11	BI	Membrane/BI defect	Damaged during insertion, manufacturing error, damaged during trial	Defect membrane	ima	**2**	mar	**1**		CE-marked BI, trained physicians ans staff	SOP: Check bodyinterfaces after explantation - in case of defect instantaneous medical action/observation	JR/MUG	ima	**2**	mar	**1**		no
47	EC3.2.12	BBraun-Pump	High flow rates	Pump malfunction, technical defect, operating error	High flow rates - overpressure on membrane - membrane/BI defect	occ	**3**	mar	**1**		internal pressure sensor of BBraun-pump	SOP: training of operators and staff (max. flow rate 50 µl/min, CMA 10µl/min (for pumps), use of CE-marked pumps Evaluation: Data from Probe (pressure-resistance) SOP: Check bodyinterfaces after explantation - in case of defect instantaneous medical	JR / MUG / Probe	ima	**2**	mar	**1**		no
48	EC3.2.14	JR-Pump	wrong pump direction	JR-pump: wrong insertion of tubing (Push-Pull mode)	Positive pressure pull side - membrane defect	occ	**3**	mar	**1**			SOP: training of operators and staff (for pumps) SOP: Check bodyinterfaces after explantation - in case of defect instantaneous medical action/observation	JR/MUG	ima	**2**	mar	**1**		no
	EC 3.3	**Non-Membrane-passing contamination**																	
49	EC3.3.2	System - during trial	microbiological contamination	wrong handling (connecting, exchanging…)	non-membrane passing contamination of dialysate	oft	**4**	mar	**1**		**all points of EC 3.3 are evaluted in EC 3 in combination with other points**	SOP: training of staff for hygienic manipulation of equipment during preparation and trial	JR/MUG	occ	**3**	mar	**1**		no
50	EC3.3.3	System - at preparation	microbiological contamination	wrong handling	non-membrane passing contamination of dialysate	oft	**4**	mar	**1**				JR/MUG	occ	**3**	mar	**1**		no
51	EC3.3.4	Sensor	Extractable toxic substances from sensor	Not immobilized GOD exceeding harmful dose	non-membrane passing contamination of dialysate & System behind BI	occ	**3**	mar	**1**			Evaluation: Data from BVT Evaluation: GOD which could penetrate membrane	JR / MUG / BVT	unl	**1**	mar	**1**		no
52	EC3.3.5	Sensor	microbiological contamination	contamination in production	non-membrane passing contamination of dialysate & System behind BI	lik	**5**	mar	**1**		no cleanroom production of sensors and flow cells available	none	--	lik	**5**	mar	**1**		--
53	EC3.3.6	FC				lik	**5**	mar	**1**				--	lik	**5**	mar	**1**		--
54	EC3.3.7	Tubing BI-FC				occ	**3**	mar	**1**		injection moulding-high temperatures			occ	**3**	mar	**1**		

	EC3.4	**Membrane-passing contamination**																	
55	EC3.4.2	System - during trial	contamination with toxic substances	contamination during trial - wrong handling (connecting, exchanging…)	membrane passing contamination of dialysate	ima	**2**	mar	**1**		**all points of EC 3.4 are evaluted in EC 3 in combination with other points** amount of harmful toxic substances is relatively low in clinical environment	none	--	ima	**2**	mar	**1**		--
56	EC3.4.3	System - at preparation	contamination with toxic substances	wrong handling		ima	**2**	mar	**1**					ima	**2**	mar	**1**		
57	EC3.4.4	Dialysate	contamination with toxic substances	Reaction between Arixtra and glucose oxidase & H2O2		unl	**1**	mar	**1**			none	--	unl	**1**	mar	**1**		--
58	EC3.4.5	Sensor	Extractable toxic substances from sensor	Not immobilized GOD exceeding harmful dose	membrane passing contamination of dialysate & System behind BI	occ	**3**	mar	**1**			Evaluation: Data from BVT Evaluation: GOD which could penetrate membrane	JR/MUG JR/MUG	unl	**1**	mar	**1**		no
59	EC3.4.6	Sensor		H2O2 exceeding harmful dose		occ	**3**	mar	**1**			Calculation and evaluation of possible dose Data from BVT	JR / MUG / BVT	unl	**1**	mar	**1**		no
60	EC3.4.7	Sensor		contamination in production		occ	**3**	mar	**1**		no cleanroom production of sensors and flow cells available	none	--	occ	**3**	mar	**1**		--
61	EC3.4.8	Sensor		toxic material of sensor		occ	**3**	mar	**1**		not known yet	none	--	occ	**3**	mar	**1**		--
62	EC3.4.9	FC	Extractable substances from FC	contamination in production		occ	**3**	mar	**1**		no cleanroom production of sensors and flow cells available	none	--	occ	**3**	mar	**1**		--
63	EC3.4.10	FC		toxic material	membrane passing contamination of dialysate & System behind BI	occ	**3**	mar	**1**		not known yet	none	--	occ	**3**	mar	**1**		--
64	EC3.4.11	Tubing BI-FC	Extractable toxic substances from tubing	toxic material	membrane passing contamination of dialysate & System behind BI	occ	**3**	mar	**1**			Design: Use of biocompatible tubing	JR/MUG	unl	**1**	mar	**1**		no
	EC 3	**Infection, Toxication (Result of combined error chains 3.1; 3.2; 3.3; 3.4)**																	
65	EC3.1 +EC3.4	System	Backflow + membrane passing contamination of dialysate	all of EC 3.1 + all of EC 3.4	Infection, toxication, allergic reaction	occ	**3**	min	**2**		amount of membrane-passing substances is too low to cause an acute intoxication	Use of CE certified BI, pumps SOP: training of physicians and staff (insertion of BI, pumps, handling, preparation),	JR/MUG	ima	**2**	min	**2**		no
66	EC3.1 + EC3.2 + EC3.3	System	Backflow + non-membrane passing contamination of dialysate + Membrane defect	all of EC 3.1 + all of EC 3.2 + all of EC 3.4	Infection, toxication, allergic reaction	occ	**3**	ser	**3**		Backflow would be dedected at least every 15 minutes, when no dialysate samples available	Design: Prevent Backflow by Design or increasing Distance between BI and Sensor + all measures out of EC 3.1, 3.2; 3.3; 3.4		ima	**2**	ser	**3**		

	EC 4	**Thermal Injury**																	
67	EC4.1	Sensor/FC	Short circuit of sensor electrodes	Fluid leakage by use of broken FC	Thermal injury due to hot FC	ima	**2**	min	**2**		Leakage as a result of a broken FC would be obersevd during run-in period; Leakage has never been seen in previous experiments	Calculate/measure: maximum power which can by converted to termal energy SOP: Do not place flow cell directly on skin Calculate / measure: temperature	JR/MUG	unl	**1**	mar	**1**		no
68	EC4.2	Sensor/FC	Short circuit of sensor electrodes	Fluid leakage by opening during sampling		occ	**3**	min	**2**			SOP: do not open FC during trial SOP: connection of electrodes, Training of staff; SOP: Check electrode connections before trial		ima	**2**	mar	**1**		
69	EC4.3	Sensor/FC	short circuit of sensor electrodes	Manufacturig error		ima	**2**	min	**2**					ima	**2**	mar	**1**		
70	EC4.4	Sensor/FC	high output voltage of potentiostat	Dry reference electrode + dry working electrode + counter electrode connected to fluid		ima	**2**	min	**2**		constellation of dry electrodes seems unlikely			unl	**1**	mar	**1**		
71	EC4.5	Sensor/FC	high output voltage of potentiostat	Wrong connection of plug (interchange of reference electrode and working electrode)		occ	**3**	min	**2**					unl	**1**	mar	**1**		
	EC 5	**Electrical Injury**																	
72	EC5.1	Potentiostate +Sensor	Dry reference electrode + dry working electrode + counter electrode connected to fluid --> High output voltage of potentiostate + patient connected to ground of device + high conductivity of fluid	Air bubbles, bad connection of electrodes + use of other devices by the patient (laptop, DVD-player) + short tubing, big diameter of tubing, conductivity of fluid itself	high current trough patient - in worst case dead	occ	**3**	des	**5**		see also figure 1	classification of applied part (B, BF, CF) and definition of limits for allowed leakage currents of system Evaluation of maximum output current of used potentionstate Calculation / measurement of conductivity with used perfusate Decrease conductivity by increasing distance BI-sensor Use of adequate potentiostate (maximium current below physiological threshold) No use of line-powered-devices by subjects (laptop...) Use of insulating transformers	JR/MUG	ima	**2**	mar	**1**		no

73	EC5.2	Potentiostate +Sensor	Wrong (interchange reference electrode and working electrode) or bad connection of plug --> High output voltage of potentiostate + patient connected to ground of device + high conductivity of fluid	Manufacturing error, handling error + use of other devices by the patient (laptop, DVD-player) + short tubing, big diameter of tubing, conductivity of fluid itself	high current trough patient - in worst case dead	ima	2	des	5		further evaluation of this point together with other points	classification of applied part (B, BF, CF) and definition of limits for alowed leakage currents of system SOP: Check electrode connection before trial Evaluation: maximum output current of used potentionstate Calculation / measurement: conductivity with used perfusate Design: Decrease conductivity by increasing distance BI-sensor Design: Use of adequate potentiostate -maximium current below defined limit (physiological threshold) SOP / Design: no use of line-powered devices by subjects (laptop...)	JR/MUG	uni	1	mar	1	no
74	EC5.3	Systems	2 or more systems with different potential + high conductivity of fluid	study design, use of commen insulated transformator or common laptop etc.	Current through subject	oft	4	des	5			Calculation / measurement: maximum current through subject Calculation / measurement: conductivity with used perfusate Design: decrease conductivity by increasing distance BI-sensor Design: Use of insulating transformer for each system and potentiostate, laptop ...	JR/MUG	ima	2	mar	1	no

Figure 65: Failure Mode and Effects Analysis (FMEA) according to ÖVE/ÖNORM EN31010:2009.

Conclusion and Evaluation of Residual Risk

Risk analysis for Introduction of a non CE-marked sensor into an online monitoring system by using microdialysis was done and documented according following Norms:
EN ISO 14971 - Medical devices - Application of risk management to medical devices
ÖVE/ÖNORM ÖVE/ÖNORM EN 31010 – Risk Assessment techniques
ÖVE/ÖNORM EN 61025 - Fault Tree Analysis

Procedure

Following procedure were used to perform risk analysis for project EU-CLAMP and the aim to implement a glucose sensor into an existing setup for in vivo sampling of glucose using Microdialysis (MD):

1. Identification of relevant harms out of EN ISO 14971
2. Fault Tree Analysis to identify relevant causes for these harms (according ÖVE/ÖNORM EN 61025 FTA-Fault Tree Analysis)
3. Evaluation of causes about their likelihood in the fault tree (high-medium-low = red-orange-green) according ÖVE/ÖNORM EN 31010 Risk management – Risk assessment techniques (Points 1-3 see attachment Fault Tree and figures 1-3)
4. FMEA: Creation of risk management plan (definition of severity and likelihood)
5. FMEA: Transfer of error chains (FTA) into FMEA
6. Evaluation of risks
7. Definition of measures and new risks out of measures
8. Conclusion and evaluation of residual risk

Results

In risk analysis, 74 specific risks were identified. No one of these Risks lies within the inacceptable area after defined measures. An additional Evaluation for 11 Risks (summarized to 6 risks) within the ALARP-area can be found on next page.

Main risks:

Mechanical Injuries:
there are slightly increased risks due to additional fixture and tubing of flow cell which all can be reduced by adequate measures.

Infection and Toxication:
Because of the size of the devices (sensor, flow cell), it is very unrealistic that the amount of toxic substances can cause serious injuries. But the components sensor and flow cell are not manufactured at cleanroom conditions and sterilised yet, so that microbiological contamination cannot be excluded.
Microbiological contamination of subject can only occur within this system, if a backflow from sensor/Flow cell takes place and the membrane of the body interface is disrupted. Therefore, the most critical point is a clogged flow cell which can cause defect membrane (overpressure) and Backflow (when disrupting) at the same time. This is also critical to embolism. Existing design of flow cell and check of patency before trial are sufficient to avoid this.

Embolism:
Embolism by parts of a broken Body Interface is only possible, when high pressure is applied. The most critical point is a clogged flow cell or wrong pump mode with JR-Pump (2x push instead of push -pull at Body interface - off level use, this would be no risk in skin at microperfusion !). This can be preveted by trained staff and checks before clinical trial.
Electrical Insuries:
Current through patients can be generated by air bubbles (high voltage-high current from potentiostate due dry electrodes), wrong connection of sensor electrodes and connection of subject to ground of device. This theoretical currents can be limited to harmless amounts by increasing distance BI--> sensor, use of potentiostate with low output current. Further, isolating transformators have to be used and subject are forbitten to use additional devices with high-voltage power supply (laptop, DVD-player...)

Thermal injuries is impossible due to the low energy which is converted at the flow cell (will be calculated ad evaluated)

Conclusion: ***the residual risk is accepted, the overall risk is for the planed clinical trial is under control when all defined measures are executed successfully.***

	After measures, following residual risks are remaining in the ALARP-area and were evaluated specific:
1.	**Strain on MD-FC connection tubing when get caught by parts of the equipment (tubing, flowcell…) --> Rip out of MD-cathteter - defct/broken membrane/BI - embolism:** Rip out of BI can never be avoided completely, because people are moving and connection tubings are necessary. The risk of embolism can be seen as controlled, since a CE-marked Bodyinterface is used. This residual risk is accepted
2.	**Folding of MD-catheter/membrane --> membrane defect --> embolism:** Folding of catheter within the vein by moving of extremities cannot be avoided completely, CE-marked Bodyinterface is designed for this purpose. This residual risk is accepted.
3.	**Flow Cell flushed on wrong side --> over-pressure on membrane - membrane defect - embolism:** handling errors cannot be avoided completely but will be decreased by Training (SOP). Even if membrane breakes, it is relatively unlikely, that small particles can be detached (CE-marked Body Interface).
4.	**Wrong pump direction --> positive pressure pull side - membrane defect - embolism: extisting risk at JR-pump.** Cannot be avoided completely since JR-pump is designed to operate in push/pull-mode. Even if membrane breakes, it is relatively unlikely, that small particles can be detached (CE-marked Body Interface). Intensive Training (SOP) will additionally decrease this risk to be acceptable.
5.	**Damaged BI during insertion, damaged during trial --> Membrane/BI defect --> embolism:** Even if membrane breakes, it is relatively unlikely, that small particles can be detached (CE-marked Body Interface). This risk is evident at every application of the bodyinterface. Resiudal risk is accepted.
6.	**Microbiological contamination by flow cell or sensor when membrane is defect and backflow from sensor to Bodyinterface occur:** Microbiologigal contamination cannot be avoided yet by lack of sterile production of flow cell and sensor. It is very unlikely, that all defects occur together, additionally powerfull measures are estimeted to prevent backflow. Therefore the overall risk of Infection is powerful decreased.

Figure 66: Conclusion, evaluation and implemented measures within the complete risk management file.

Classification of applied parts according to IEC 60601-1

8.3 Classification of APPLIED PARTS

a) *An APPLIED PART that is specified in the ACCOMPANYING DOCUMENTS as suitable for DIRECT CARDIAC APPLICATION shall be a TYPE CF APPLIED PART.

NOTE Other restrictions may apply for cardiac applications.

Compliance is checked by inspection.

b) *An APPLIED PART that includes a PATIENT CONNECTION that is intended to deliver electrical energy or an electrophysiological signal to or from the PATIENT shall be a TYPE BF APPLIED PART or TYPE CF APPLIED PART.

Compliance is checked by inspection.

c) An APPLIED PART not covered by *a)* or *b)* shall be a TYPE B APPLIED PART, TYPE BF APPLIED PART or TYPE CF APPLIED PART.

Compliance is checked by inspection.

d) *For a part that is identified according to 4.4 as needing to be subject to the requirements for an APPLIED PART (except for marking), the requirements for a TYPE B APPLIED PART shall apply unless the RISK MANAGEMENT PROCESS identifies a need for the requirements for a TYPE BF APPLIED PART or TYPE CF APPLIED PART to apply.

Figure 67: Classification of applied parts according to IEC 60601-1.

Classification of medical electrical systems according to IEC 60601-1

Table J1 – Some examples of MEDICAL ELECTRICAL SYSTEMS for illustration

	Situation No.	Medically used room: Inside the PATIENT ENVIRONMENT	Medically used room: Outside the PATIENT ENVIRONMENT	Non-medically used room	Examples of possible causes for exceeding LEAKAGE CURRENT limits	Practical means of compliance Apply 16.5 in all situations
1	1a Items A and B are ME EQUIPMENT				No causes of exceeding LEAKAGE CURRENT	– No further measures are necessary
1	1b Items A and B are ME EQUIPMENT powered via a MULTIPLE SOCKET-OUTLET	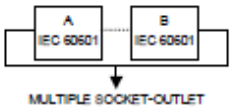			Earth conductor of the MULTIPLE SOCKET-OUTLET is broken	– Additional PROTECTIVE EARTH CONNECTION (for A or B) or, – Separating transformer
1	1c Item A is ME EQUIPMENT and B is Non-ME EQUIPMENT				Due to high TOUCH CURRENT of B	– Additional PROTECTIVE EARTH CONNECTION (for B) or, – Separating transformer (for B)
1	1d Item A is ME EQUIPMENT and B is non-ME EQUIPMENT powered via a MULTIPLE SOCKET-OUTLET	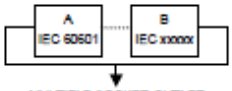			The earth conductor of the MULTIPLE SOCKET-OUTLET is broken or, Due to high TOUCH CURRENT of B	– Additional PROTECTIVE EARTH CONNECTION (for A or B) or, – Separating transformer
1	1e Item A is ME EQUIPMENT powered from specified power supply in item B	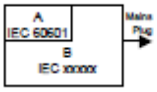			Due to high TOUCH CURRENT of B	– Additional PROTECTIVE EARTH CONNECTION (for B) or, – Separating transformer (for B)
1	1f Item A is ME EQUIPMENT powered from NON-ME EQUIPMENT power supply in B	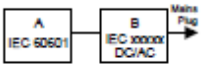				
2	2a Items A and B are ME EQUIPMENT	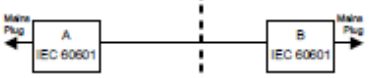			No causes of exceeding LEAKAGE CURRENT	– No further measures are necessary
2	2b Items A and item B are ME EQUIPMENT powered via a MULTIPLE SOCKET-OUTLET	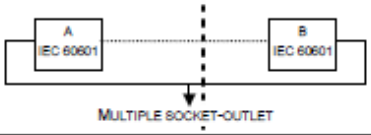			Earth conductor of the MULTIPLE SOCKET-OUTLET is broken	– Additional PROTECTIVE EARTH CONNECTION (for A or B) or, – Separating transformer

Situation No.		Medically used room: Inside the PATIENT ENVIRONMENT	Medically used room: Outside the PATIENT ENVIRONMENT	Non-medically used room	Examples of possible causes for exceeding LEAKAGE CURRENT limits	Practical means of compliance Apply 16.5 in all situations
2	2c Item A is ME EQUIPMENT and item B is non-ME EQUIPMENT				Due to high TOUCH CURRENT of B See rationale of 16.5	– Do not use metal connector housing or, – SEPARATION DEVICE
	2d Item A is ME EQUIPMENT and item B is non-ME EQUIPMENT powered via a MULTIPLE SOCKET-OUTLET	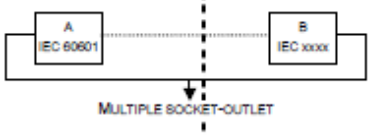			The earth conductor of the MULTIPLE SOCKET-OUTLET is broken	– Additional PROTECTIVE EARTH CONNECTION (for A or B) or, – Separating transformer
3	3a Items A and B are ME EQUIPMENT	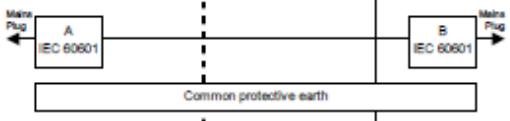			No causes of exceeding LEAKAGE CURRENT	– No further measures are necessary
	3b Item A is ME EQUIPMENT and item B is non-ME EQUIPMENT	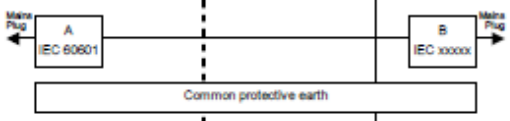			Due to high TOUCH CURRENT of B See rationale of 16.5	– Do not use metal connector housing for SIGNAL INPUT/OUTPUT PART or, – SEPARATION DEVICE
	3c Item A is ME EQUIPMENT and item B in is ME EQUIPMENT or non-ME EQUIPMENT	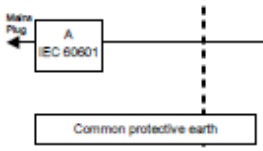		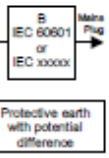	*a)* Potential difference between PROTECTIVE EARTH CONNECTION's of A and B *b)* Due to high TOUCH CURRENT of B. See rationale of 16.5	– Additional PROTECTIVE EARTH CONNECTION for (A), – SEPARATION DEVICE. – Do not use metal connector housing

NOTE 1 IEC 60601: MEDICAL ELECTRICAL EQUIPMENT in compliance with IEC 60601

NOTE 2 IEC xxxxx: Non-medical equipment in compliance with relevant IEC safety standards.

NOTE 3 Separating transformer: see 16.9.2.1

NOTE 4 If equipment "B" is outside the PATIENT ENVIRONMENT and if equipment "A" is a CLASS II equipment and has accessible conductive parts connected to the PROTECTIVE EARTH CONNECTION of equipment "B" than additional SAFETY measures may be necessary for example: Additional protective earth for "B" or separating transformer or SEPARATION DEVCIE.

Figure 68: Classification of medical electrical (ME) systems according to IEC 60601-1, Annex J.

Classification of ME Systems and ME Equipment based upon the protection against electrical shock according to IEC 60601-1

CLASS I
Adjective referring to electrical equipment in which protection against electric shock does not rely on BASIC INSULATION only, but which includes an additional safety precaution in that means are provided for ACCESSIBLE PARTS of metal or internal parts of metal to be PROTECTIVELY EARTHED.

CLASS II
Adjective referring to electrical equipment in which protection against electric shock does not rely on BASIC INSULATION only, but in which additional safety precautions such as DOUBLE INSULATION or REINFORCED INSULATION are provided, there being no provision for protective earthing or reliance upon installation conditions.

INTERNAL ELECTRICAL POWER SOURCE
Electrical power source for operating equipment that is a part of the equipment and which produces electrical current from some other form of energy (such as chemical, mechanical, solar, or nuclear).

NOTE: An INTERNAL ELECTRICAL POWER SOURCE may be inside the principal part of equipment, attached to the outside, or contained in a separate ENCLOSURE.

Setups failing the safety check according to the criteria given in IEC 60601-1.

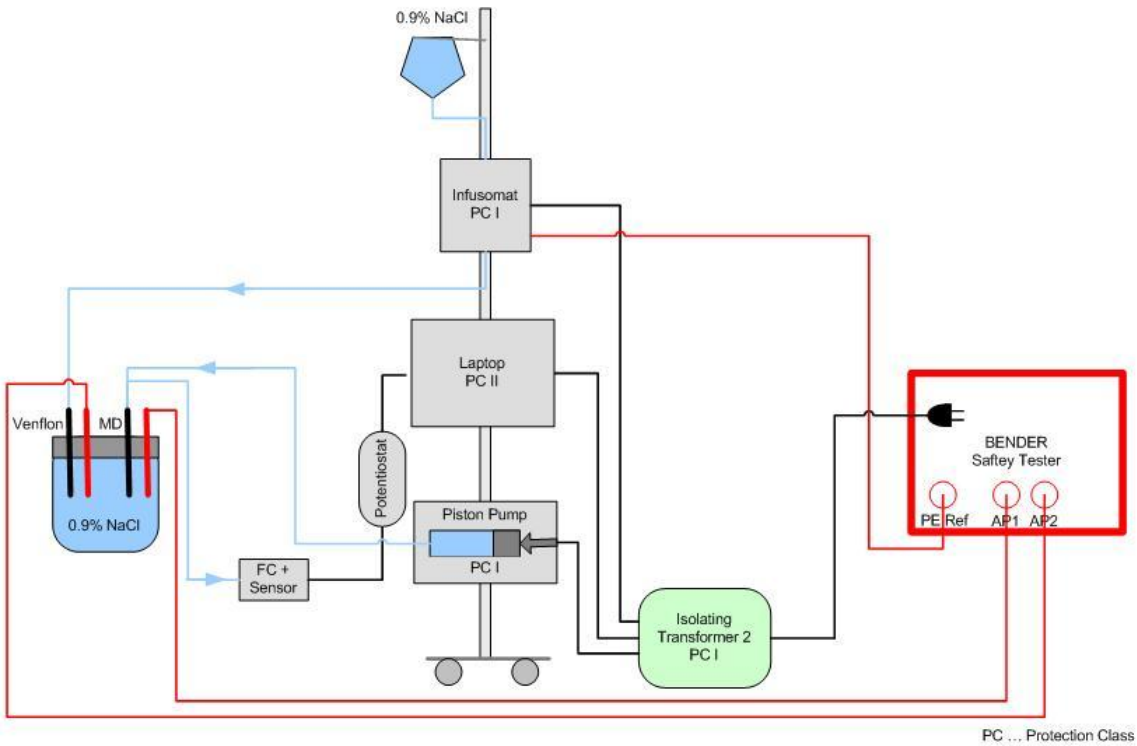

Figure 69: Safety check setup with one isolating transformer.

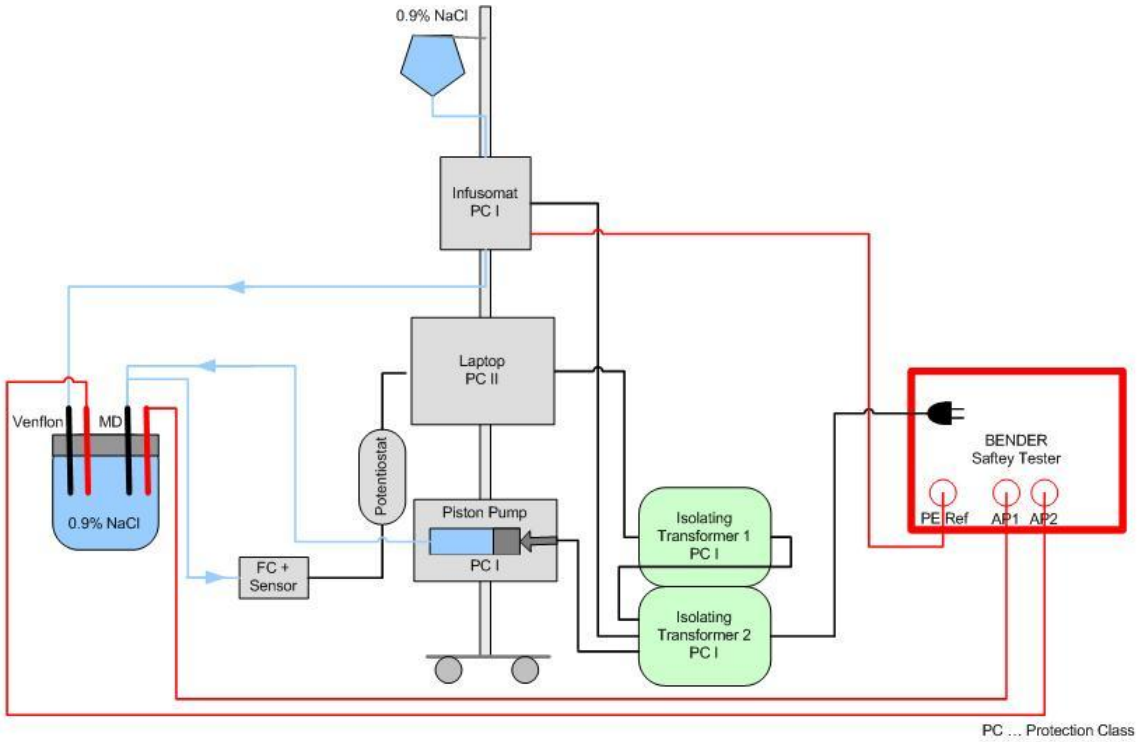

Figure 70: Safety check setup with two isolating transformers.

Electrical Safety Check

The following information was extracted from ISO/ EN 60601-1 [34]. Pictures were extracted from the Unimet 1000ST technical manual:

<u>Tested safety parameters:</u>

- PE Resistance
- PE measuring current
- Load current
- Operating voltage
- Power consumption
- Earth leakage current
- Patient leakage current
- Patient auxiliary current
- Enclosure leakage current (equivalent to Touch current)

EARTH LEAKAGE CURRENT:

Current flowing from the main part through or across the insulation into the protective earth conductor.

The allowable values of the earth leakage current for CF devices are 500µA in normal condition (NC) and 500µA in single fault condition (SFC), respectively.

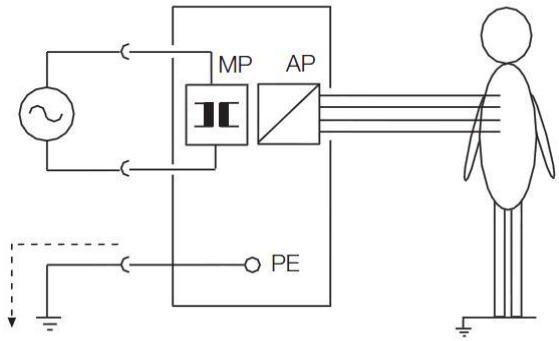

Figure 71: Measuring earth leakage current.

TOUCH CURRENT (prior to the 3rd Edition called ENCLOSURE LEAKAGE CURRENT):

Current flowing from the enclosure or from parts thereof, excluding patient connections, accessible to the operator or patient in normal use, through an external path other than the protective earth conductor, to earth or to another part of the enclosure.

Note: the meaning of this term is the same as that of "enclosure leakage current" in the 1st and 2nd editions of this standard. The term has been changed to align with IEC 60990-1 and to reflect the fact that the measurement now applies also to parts that are normally protectively earthed.

The allowable values of the touch current for CF devices are 100µA in normal condition and 500µA in single fault condition.

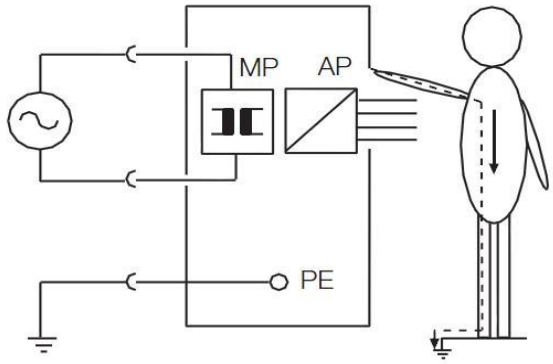

Figure 72: Measuring touch current.

PATIENT LEAKAGE CURRENT:

Current flowing from the patient connections via the patient to earth or originating from the unintended appearance of a voltage from an external source on the patient and flowing from the patient via the patient connections of an F-type applied part to earth.

The allowable values of the patient leakage current for CF devices are 10µA in normal condition and 50µA in single fault condition.

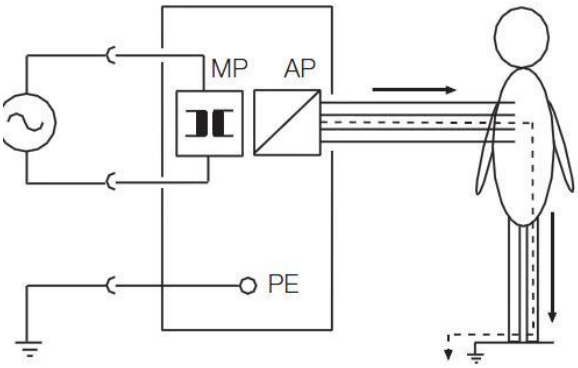

Figure 73: Measuring patient leakage current.

PATIENTEN AUXILLARY CURRENT:

Current flowing in the patient in normal use between any patient connection and all other patient connections and not intended to produce a physiological effect.

The allowable values of the patient auxiliary current for CF devices are 10µA in normal condition and 50µA in single fault condition.

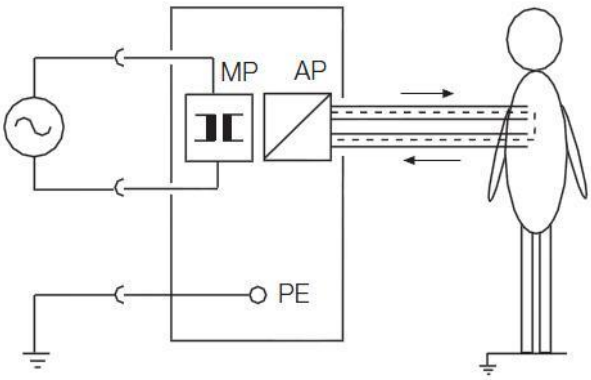

Figure 74: Measuring patient auxiliary current.

PROTECTIVE EARTH (PE):

For ME EQUIPMENT with a non-detachable power supply cord, the impedance between the protective earth pin in the MAINS PLUG and any part that is protectively earthed shall not exceed 200mΩ.

Compliance is checked by the following test:

A current of 25A or 1.5 times the highest rated current of the relevant circuit(s), whichever is greater (± 10 %), from a current source with a frequency of 50Hz or 60Hz and with a no-load voltage not exceeding 6V, is passed for 5s to 10s through the protective earth terminal or the protective earth contact in the appliance inlet or the protective earth pin in the mains plug and each protectively earthed part.

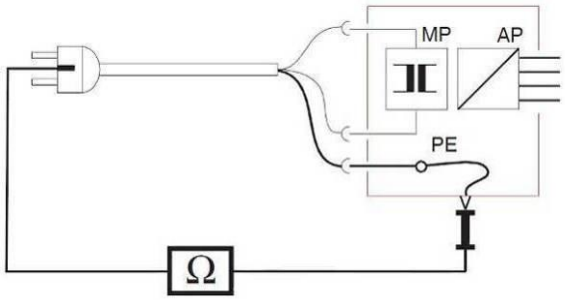

Figure 75: Measuring protective earth (PE).

Disposables and components of system1 and system2 tested within the safety check

DISPOSABLES					
Device/Solution	**Manufacturer**	**Ref. Nr.**	**Lot Nr.**	**Exp. Date**	**Comment**
0.9% NaCl	FRESENIUS-KABI	1-16417	14EL1004	2016-10	0.9% NaCl was also used as perfusate to illustrate the worst case concerning conductivity in fluids
15% Mannitol	FRESENIUS-KABI	1-20984	16EL0252	2014-10	1/3 Mannit 15% + 2/3 ddH_2O
Venflon	BD; BBRAUN	391453; 4269136S-01	10J1341E; 2D24258346	2015-08; 2017-04	1.2 x 45mm, 18GA; 1.3 x 45mm, 18G
Infusomat Space Line	BBRAUN	8700036SP	1k14218STA	2013-10	n.a.
Valve Operated Y-Connector	IMPROMEDIFORM GmbH	MF1532	MU001	2017-03	n.a.
Extension Set E87-P	CODAN	71.4310	F76635-1	2014-02	150cm, d=0.9/2.0mm, vol=1.15ml
Perfusor Syringe OPS	BBRAUN	8728810F	11L0982028, 12A2682021 and 11G0582026	2016-11 2017-01 and 2016-07	50ml
Syringe Filter	NALGENE	190-2520	524882	n.a.	0.2µm
PHARMED BPT Tubing	COLE PARMER	96880-00	536923	n.a.	ID: 0.02IN, OD: 0.145IN, WALL: 0.0625IN
Glucose Sensor	BVT Technologies	AC1.GOD	1-19, 1-24, 2-1 and 3-9	n.a.	n.a.
Flow Cell	BVT Technologies	FC2.S	n.a.	n.a.	n.a.
MicroEye	Probe Scientific	PME011	11008004	2012-03	n.a.

Table 12: Disposable equipment used for the safety check measurements.

SYSTEM 1 (yellow)					
Device/Solution	**Manufacturer**	**Ref. Nr.**	**Lot Nr.**	**Exp. Date**	**Comment**
Space Tower	BBRAUN	8713145	18566	n.a.	n.a.
Infusomat Space	BBRAUN	8713050	83073	n.a.	For glucose infusion
Perfusor Space	BBRAUN	8713030	96033	n.a.	For insulin infusion
Perfusor fm	BBRAUN	8713820	57917	n.a.	N49309
Isolating Transformer 2	DeMeTec	IPS-1400R3-8K	54116322	n.a.	G-0012
Potentiostat	Palm Sens	EmStat	ES12726	n.a.	G-0099
USB to USB Isolator	BAASKE MEDICAL	USB 1.1 Isolator MED	0146120010	n.a.	G-0094. UL 60601-1 certified, Direct Current
Lifebook	Fujitsu Siemens	E8020 WB1	YBDV018910	n.a.	Inventory no.: 37999
ULF-Infusion Stand	Böhm Medical	INFUSIO U-51806	n.a.	n.a.	n.a.
ULF-Tabletop	Böhm Medical	U-54550	n.a.	n.a.	40 x 32cm, 30°
ULF-Sterile Material Basket	Böhm Medical	U-51463	n.a.	n.a.	30 x 20 x 10cm
ULF-Stainless Steel Bowl	Böhm Medical	U-51403	n.a.	n.a	n.a.
ULF-Handhold	Böhm Medical	Vario U-51000	n.a.	n.a.	n.a.
Safety Tester BENDER	BENTRON	Unimet 1100ST	0401001206	n.a.	G-0035

Table 13: Equipment used for the safety check measurement of Sys1.

SYSTEM 2 (green)					
Device/Solution	**Manufacturer**	**Ref. Nr.**	**Lot Nr.**	**Exp. Date**	**Comment**
Space Tower	BBRAUN	8713145	17558	n.a.	n.a.
Infusion Space	BBRAUN	8713050	90914	n.a.	For glucose infusion
Perfusor Space	BBRAUN	8713030	92207	n.a.	For insulin infusion
Perfusor fm	BBRAUN	8713820	43178	n.a.	N45089
Isolating Transformer 1	DeMeTec	IPS-1400R3-8K	54116320	n.a.	G-0054
Potentiostat	Palm Sens	EmStat	ES12727	n.a.	G-0100
USB to USB Isolator	BAASKE MEDICAL	USB 1.1 Isolator MED	0146119001	n.a.	G-0095. UL 60601-1 certified, Direct Current
Lifebook	Fujitsu Siemens	E8210 WB2	YB2C002104	n.a.	Inventory no.: 38872
ULF-Tabletop	Böhm Medical	U-54550	n.a.	n.a.	40 x 32cm, 30°
ULF-Sterile Material Basket	Böhm Medical	U-51463	n.a.	n.a.	30 x 20 x 10cm
ULF-Stainless Steel Bowl	Böhm Medical	U-51403	n.a.	n.a	n.a.
ULF-Handhold	Böhm Medical	Vario U-51000	n.a.	n.a.	n.a.
Safety Tester BENDER	BENTRON	Unimet 1100ST	0401001206	n.a.	G-0035

Table 14: Equipment used for the safety check measurement of Sys2.

BENDER results of the electrical safety check (PC I)

BENDER

Test protocol

Bender GmbH&Co.KG
Postfach 1161
35301 Grünberg
Tel: +49(0)6401-807 730

Device data

Device ID:	EU-CLAMP_SYS1	**Cable length [m]**	-
Type/Model	60601/I /CF/2/UamAWT	**Nominal power [kW]**	-
Manufacturer	-	**Test sequence**	Automatic
Serial No.	-	**Applied part**	Type CF
Device designation	-	**Patient connections**	2
Test standard	UL 2601-1	**Building**	-
Kind of equipment	Standard device	**Department**	-
Protection Class	Class I	**Room**	-
Nominal voltage [V]	230	**Comment**	-

Test no.	Measurement	Threshold	Result	Unit	Passed
3	PE resistance, permanently attached cord	0.200	0.128	Ohm	Yes
83	PE measuring current		25.5	A	-
80	Load current		0.553	A	-
81	Operating voltage		231	V	-
82	Power consumption		0.126	kVA	-
7	Earth leakage current NC	0.500	0.017	mA	Yes
11	Earth leakage current SFC AP earthed	0.500	0.016	mA	Yes
12	Earth leakage current NC FE earthed	0.500	0.016	mA	Yes
31	Patient leakage current SFC U-AP	0.050	0.019	mA	Yes
33	Patient leakage current SFC ph. rev. U-AP	0.050	0.020	mA	Yes
34	Patient leakage current SFC U-AP FE earthed	0.050	0.019	mA	Yes
223	Patient leakage current NC DC	0.010	0.001	mA	Yes
225	Patient leakage current SFC DC PE open	0.050	0.001	mA	Yes
229	Patient leakage current NC DC FE earthed	0.010	0.001	mA	Yes
230	Patient leakage current SFC DC FE earthed PE open	0.050	0.001	mA	Yes
235	Patient auxiliary current NC DC	0.010	0.001	mA	Yes
237	Patient auxiliary current SFC DC PE open	0.050	0.001	mA	Yes
241	Patient auxiliary current NC DC FE earthed	0.010	< 0.001	mA	Yes
242	Patient auxiliary current SFC DC PE open FE earthed	0.050	0.001	mA	Yes
323	Patient leakage current NC AC	0.010	0.002	mA	Yes
325	Patient leakage current SFC AC PE open	0.050	0.003	mA	Yes
329	Patient leakage current NC AC FE earthed	0.010	0.002	mA	Yes
330	Patient leakage current SFC AC FE earthed PE open	0.050	0.003	mA	Yes
335	Patient auxiliary current NC AC	0.010	< 0.001	mA	Yes
337	Patient auxiliary current SFC AC PE open	0.050	< 0.001	mA	Yes
341	Patient auxiliary current NC AC FE earthed	0.010	< 0.001	mA	Yes
342	Patient auxiliary current SFC AC PE open FE earthed	0.050	< 0.001	mA	Yes
8	Earth leakage current NC ph. rev.	0.500	0.064	mA	Yes
32	Patient leakage current SFC U-AP ph. rev.	0.050	0.016	mA	Yes
224	Patient leakage current NC DC PE open	0.010	0.001	mA	Yes
226	Patient leakage current SFC DC PE open ph. rev.	0.050	0.001	mA	Yes
236	Patient auxiliary current NC DC ph. rev.	0.010	0.001	mA	Yes
238	Patient auxiliary current SFC DC PE open ph. rev.	0.050	0.005	mA	Yes
324	Patient leakage current NC AC ph. rev.	0.010	0.003	mA	Yes
326	Patient leakage current SFC PE open ph. rev.	0.050	0.009	mA	Yes
336	Patient auxiliary current NC AC ph. rev.	0.010	< 0.001	mA	Yes
338	Patient auxiliary current SFC AC PE open ph. rev.	0.050	< 0.001	mA	Yes
9	Earth leakage current SFC conductor open	1.000	0.079	mA	Yes
13	Earth leakage current SFC AP+FE earthed conductor open	1.000	0.077	mA	Yes
227	Patient leakage current SFC DC conductor open	0.050	0.001	mA	Yes

Device ID: : EU-CLAMP_SYS1 **Type/Model** : 60601/I /CF/2/UamAWT

Page 1/2 | SN: 0401001206 | UNIMET®1000/1100ST V7.70 | Print date: 13.08.2012

Test no.	Measurement	Threshold	Result	Unit	Passed
239	Patient auxiliary current SFC DC conductor open	0.050	0.001	mA	Yes
327	Patient leakage current SFC AC conductor open	0.050	0.003	mA	Yes
339	Patient auxiliary current SFC AC conductor open	0.050	< 0.001	mA	Yes
373	Patient leakage current SFC AC conductor open 3ph	0.050	< 0.001	mA	Yes
10	Earth leakage current SFC conductor open ph. rev.	1.000	0.079	mA	Yes
228	Patient leakage current SFC DC conductor open ph. rev.	0.050	0.001	mA	Yes
240	Patient auxiliary current SFC DC conductor open ph. rev.	0.050	0.001	mA	Yes
328	Patient leakage current SFC AC conductor open ph. rev.	0.050	0.003	mA	Yes
340	Patient auxiliary current SFC AC conductor open ph. rev.	0.050	< 0.001	mA	Yes

Test result: **>> Passed <<**

Test date : 13.08.2012

Test engineer : Hernach

p.p.

Signature

Device ID: : EU-CLAMP_SYS1 **Type/Model** : 60601/I /CF/2/UamAWT

Page 2/2 SN: 0401001206 UNIMET®1000/1100ST V7.70 Print date: 13.08.2012

Figure 76: BENDER protocol for Sys1 with isolating transformer, UBS to USB isolator and BBRAUN Space Tower.

BENDER

Test protocol

Bender GmbH&Co.KG
Postfach 1161
35301 Grünberg
Tel: +49(0)6401-807 730

Device data

Device ID:	EU-CLAMP_SYS2	**Cable length [m]**	-
Type/Model	60601/I /CF/2/UamAWT	**Nominal power [kW]**	-
Manufacturer	-	**Test sequence**	Automatic
Serial No.	-	**Applied part**	Type CF
Device designation	-	**Patient connections**	2
Test standard	UL 2601-1	**Building**	-
Kind of equipment	Standard device	**Department**	-
Protection Class	Class I	**Room**	-
Nominal voltage [V]	230	**Comment**	-

Test no.	Measurement	Threshold	Result	Unit	Passed
3	PE resistance, permanently attached cord	0.200	0.126	Ohm	Yes
83	PE measuring current		25.4	A	-
80	Load current		0.545	A	-
81	Operating voltage		230	V	-
82	Power consumption		0.124	kVA	-
7	Earth leakage current NC	0.500	0.061	mA	Yes
11	Earth leakage current SFC AP earthed	0.500	0.059	mA	Yes
12	Earth leakage current NC FE earthed	0.500	0.061	mA	Yes
31	Patient leakage current SFC U-AP	0.050	0.016	mA	Yes
33	Patient leakage current SFC ph. rev. U-AP	0.050	0.020	mA	Yes
34	Patient leakage current SFC U-AP FE earthed	0.050	0.016	mA	Yes
223	Patient leakage current NC DC	0.010	0.001	mA	Yes
225	Patient leakage current SFC DC PE open	0.050	0.001	mA	Yes
229	Patient leakage current NC DC FE earthed	0.010	0.001	mA	Yes
230	Patient leakage current SFC DC FE earthed PE open	0.050	0.001	mA	Yes
235	Patient auxiliary current NC DC	0.010	0.001	mA	Yes
237	Patient auxiliary current SFC DC PE open	0.050	0.005	mA	Yes
241	Patient auxiliary current NC DC FE earthed	0.010	0.001	mA	Yes
242	Patient auxiliary current SFC DC PE open FE earthed	0.050	0.005	mA	Yes
323	Patient leakage current NC AC	0.010	0.002	mA	Yes
325	Patient leakage current SFC AC PE open	0.050	0.008	mA	Yes
329	Patient leakage current NC AC FE earthed	0.010	0.002	mA	Yes
330	Patient leakage current SFC AC FE earthed PE open	0.050	0.008	mA	Yes
335	Patient auxiliary current NC AC	0.010	< 0.001	mA	Yes
337	Patient auxiliary current SFC AC PE open	0.050	< 0.001	mA	Yes
341	Patient auxiliary current NC AC FE earthed	0.010	< 0.001	mA	Yes
342	Patient auxiliary current SFC AC PE open FE earthed	0.050	< 0.001	mA	Yes
8	Earth leakage current NC ph. rev.	0.500	0.017	mA	Yes
32	Patient leakage current SFC U-AP ph. rev.	0.050	0.018	mA	Yes
224	Patient leakage current NC DC PE open	0.010	0.001	mA	Yes
226	Patient leakage current SFC DC PE open ph. rev.	0.050	0.001	mA	Yes
236	Patient auxiliary current NC DC ph. rev.	0.010	< 0.001	mA	Yes
238	Patient auxiliary current SFC DC PE open ph. rev.	0.050	0.001	mA	Yes
324	Patient leakage current NC AC ph. rev.	0.010	0.001	mA	Yes
326	Patient leakage current SFC PE open ph. rev.	0.050	0.002	mA	Yes
336	Patient auxiliary current NC AC ph. rev.	0.010	< 0.001	mA	Yes
338	Patient auxiliary current SFC AC PE open ph. rev.	0.050	< 0.001	mA	Yes
9	Earth leakage current SFC conductor open	1.000	0.077	mA	Yes
13	Earth leakage current SFC AP+FE earthed conductor open	1.000	0.076	mA	Yes
227	Patient leakage current SFC DC conductor open	0.050	0.001	mA	Yes

Device ID:	: EU-CLAMP_SYS2	**Type/Model**	: 60601/I /CF/2/UamAWT

Page 1/2	SN: 0401001206	UNIMET®1000/1100ST V7.70	Print date:	13.08.2012

Test no.	Measurement	Threshold	Result	Unit	Passed
239	Patient auxiliary current SFC DC conductor open	0.050	0.001	mA	Yes
327	Patient leakage current SFC AC conductor open	0.050	0.002	mA	Yes
339	Patient auxiliary current SFC AC conductor open	0.050	< 0.001	mA	Yes
373	Patient leakage current SFC AC conductor open 3ph	0.050	< 0.001	mA	Yes
10	Earth leakage current SFC conductor open ph. rev.	1.000	0.077	mA	Yes
228	Patient leakage current SFC DC conductor open ph. rev.	0.050	0.001	mA	Yes
240	Patient auxiliary current SFC DC conductor open ph. rev.	0.050	0.001	mA	Yes
328	Patient leakage current SFC AC conductor open ph. rev.	0.050	0.002	mA	Yes
340	Patient auxiliary current SFC AC conductor open ph. rev.	0.050	< 0.001	mA	Yes

Test result: **>> Passed <<**

Test date : 13.08.2012

Test engineer : Hernach

p.p.

Signature

Device ID:	: EU-CLAMP_SYS2	**Type/Model**	: 60601/I /CF/2/UamAWT

Page 2/2	SN: 0401001206	UNIMET®1000/1100ST V7.70	Print date:	13.08.2012

Figure 77: BENDER protocol for Sys2 with isolating transformer, UBS to USB isolator and BBRAUN Space Tower.

BENDER results for the safety check of the laptop (PC II)

BENDER

Test protocol

Bender GmbH&Co.KG
Postfach 1161
35301 Grünberg
Tel: +49(0)6401-807 730

Device data

Device ID:	EU-CLAMP_LAP_SYS2	**Cable length [m]**	-
Type/Model	60601/II /CF/1/UamAWT	**Nominal power [kW]**	-
Manufacturer	-	**Test sequence**	Automatic
Serial No.	-	**Applied part**	Type CF
Device designation	-	**Patient connections**	1
Test standard	UL 2601-1	**Building**	-
Kind of equipment	Standard device	**Department**	-
Protection Class	Class II	**Room**	-
Nominal voltage [V]	230	**Comment**	-

Test no.	Measurement	Threshold	Result	Unit	Passed
80	Load current		0.477	A	-
81	Operating voltage		226	V	-
82	Power consumption		0.108	kVA	-
14	Enclosure leakage current NC	0.100	0.004	mA	Yes
20	Enclosure leakage current NC AP earthed	0.100	0.004	mA	Yes
21	Enclosure leakage current NC FE earthed	0.100	0.004	mA	Yes
31	Patient leakage current SFC U-AP	0.050	0.008	mA	Yes
33	Patient leakage current SFC ph. rev. U-AP	0.050	0.008	mA	Yes
34	Patient leakage current SFC U-AP FE earthed	0.050	0.007	mA	Yes
223	Patient leakage current NC DC	0.010	0.001	mA	Yes
229	Patient leakage current NC DC FE earthed	0.010	0.001	mA	Yes
323	Patient leakage current NC AC	0.010	< 0.001	mA	Yes
329	Patient leakage current NC AC FE earthed	0.010	< 0.001	mA	Yes
15	Enclosure leakage current NC ph. rev.	0.100	0.001	mA	Yes
32	Patient leakage current SFC U-AP ph. rev.	0.050	0.008	mA	Yes
224	Patient leakage current NC DC PE open	0.010	0.001	mA	Yes
324	Patient leakage current NC AC ph. rev.	0.010	< 0.001	mA	Yes
18	Enclosure leakage current SFC conductor open	0.500	0.004	mA	Yes
227	Patient leakage current SFC DC conductor open	0.050	0.001	mA	Yes
327	Patient leakage current SFC AC conductor open	0.050	< 0.001	mA	Yes
373	Patient leakage current SFC AC conductor open 3ph	0.050	< 0.001	mA	Yes
19	Enclosure leakage current SFC conductor open ph. rev.	0.500	0.004	mA	Yes
228	Patient leakage current SFC DC conductor open ph. rev.	0.050	0.001	mA	Yes
328	Patient leakage current SFC AC conductor open ph. rev.	0.050	< 0.001	mA	Yes

Test result: **>> Passed <<**

Test date : 11.06.2012
Test engineer : Greiner

p.p.
Signature

Device ID:	: EU-CLAMP_LAP_SYS2	**Type/Model**	: 60601/II /CF/1/UamAWT

Page 1/1	SN: 0401001206	UNIMET®1000/1100ST V7.70	Print date:	11.06.2012

Figure 78: BENDER protocol of Sys1 with the laptop tested as PC II device.

BENDER

Test protocol

Bender GmbH&Co.KG
Postfach 1161
35301 Grünberg
Tel: +49(0)6401-807 730

Device data

Device ID:	EU-CLAMP_LAP_SYS1	**Cable length [m]**	-
Type/Model	60601/II /CF/1/UamAWT	**Nominal power [kW]**	-
Manufacturer	-	**Test sequence**	Automatic
Serial No.	-	**Applied part**	Type CF
Device designation	-	**Patient connections**	1
Test standard	UL 2601-1	**Building**	-
Kind of equipment	Standard device	**Department**	-
Protection Class	Class II	**Room**	-
Nominal voltage [V]	230	**Comment**	-

Test no.	Measurement	Threshold	Result	Unit	Passed
80	Load current		0.442	A	-
81	Operating voltage		226	V	-
82	Power consumption		0.099	kVA	-
14	Enclosure leakage current NC	0.100	< 0.001	mA	Yes
20	Enclosure leakage current NC AP earthed	0.100	< 0.001	mA	Yes
21	Enclosure leakage current NC FE earthed	0.100	< 0.001	mA	Yes
31	Patient leakage current SFC U-AP	0.050	0.013	mA	Yes
33	Patient leakage current SFC ph. rev. U-AP	0.050	0.014	mA	Yes
34	Patient leakage current SFC U-AP FE earthed	0.050	0.014	mA	Yes
223	Patient leakage current NC DC	0.010	0.001	mA	Yes
229	Patient leakage current NC DC FE earthed	0.010	< 0.001	mA	Yes
323	Patient leakage current NC AC	0.010	0.001	mA	Yes
329	Patient leakage current NC AC FE earthed	0.010	0.001	mA	Yes
15	Enclosure leakage current NC ph. rev.	0.100	0.003	mA	Yes
32	Patient leakage current SFC U-AP ph. rev.	0.050	0.012	mA	Yes
224	Patient leakage current NC DC PE open	0.010	0.001	mA	Yes
324	Patient leakage current NC AC ph. rev.	0.010	0.002	mA	Yes
18	Enclosure leakage current SFC conductor open	0.500	0.003	mA	Yes
227	Patient leakage current SFC DC conductor open	0.050	0.001	mA	Yes
327	Patient leakage current SFC AC conductor open	0.050	0.002	mA	Yes
373	Patient leakage current SFC AC conductor open 3ph	0.050	< 0.001	mA	Yes
19	Enclosure leakage current SFC conductor open ph. rev.	0.500	0.003	mA	Yes
228	Patient leakage current SFC DC conductor open ph. rev.	0.050	0.001	mA	Yes
328	Patient leakage current SFC AC conductor open ph. rev.	0.050	0.002	mA	Yes

Test result: **>> Passed <<**

Test date : 11.06.2012
Test engineer : Greiner

Signature

Device ID:	: EU-CLAMP_LAP_SYS1	**Type/Model**	: 60601/II /CF/1/UamAWT

Page 1/1	SN: 0401001206	UNIMET®1000/1100ST V7.70	Print date:	11.06.2012

Figure 79: BENDER protocol of Sys2 with the laptop tested as PC II device.

Individual glucose clamp curves of subject 021 - 026

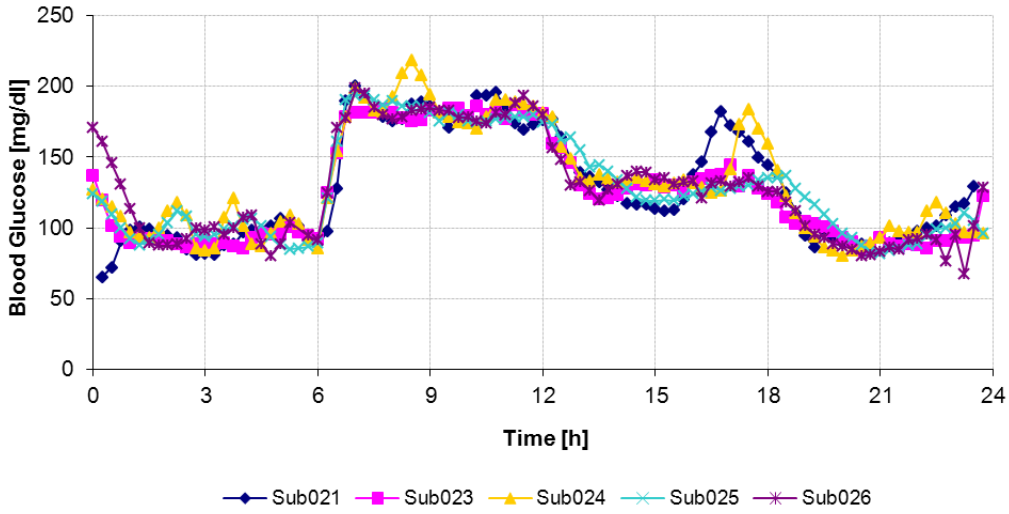

Figure 80: Individual blood glucose profiles of subject 021 - 026.

Individual flow rates of subject 021 - 026

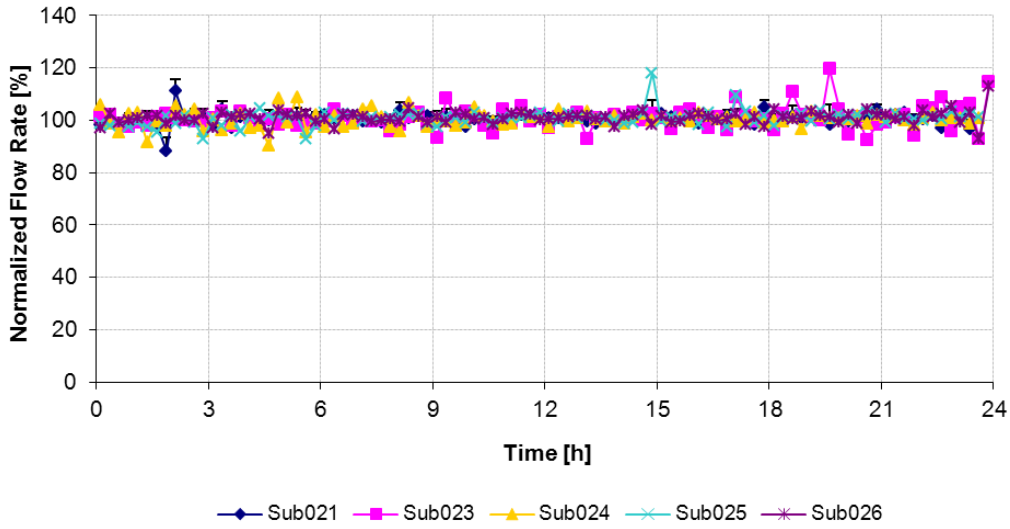

Figure 81: Individual flow rates of subject 021 - 026.

Run in behaviour of the 10 sensors used during the clinical trial

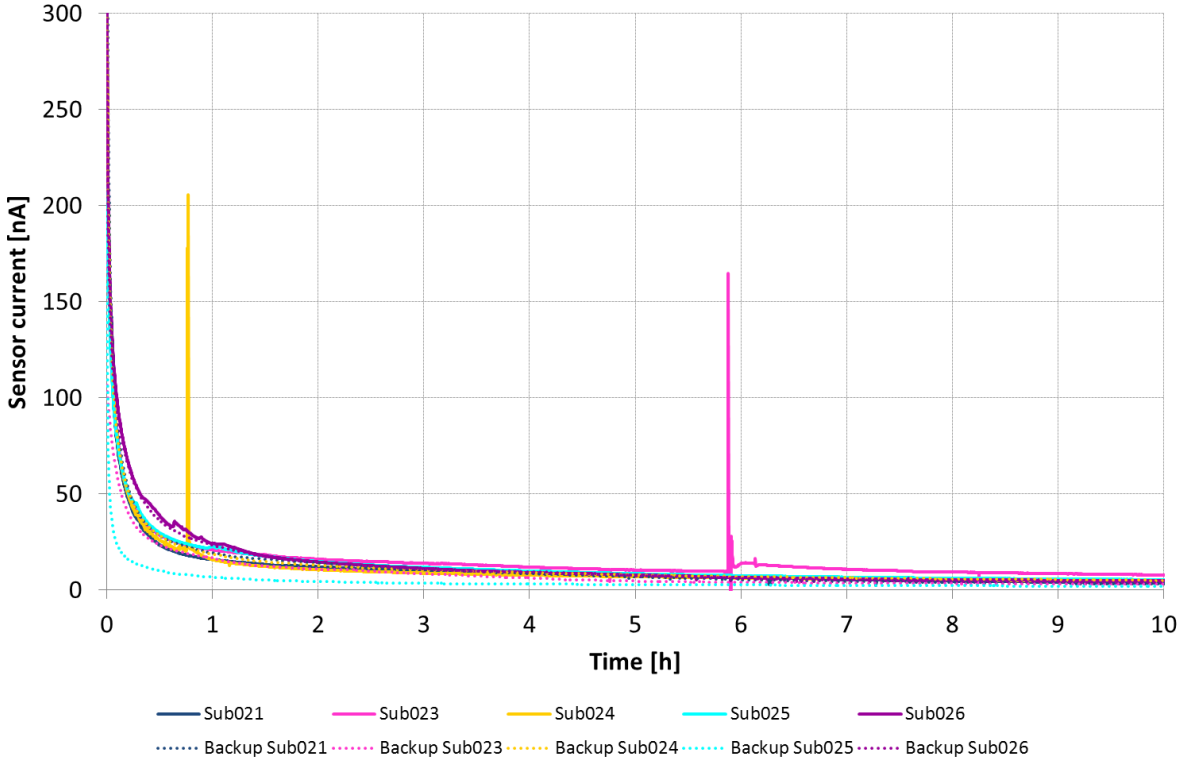

Figure 82: Individual run in currents of the subjects 021 - 026 during the first 10 hours.

Calibrated Glucose Profiles of Subject 023 – 026

Subject 023:

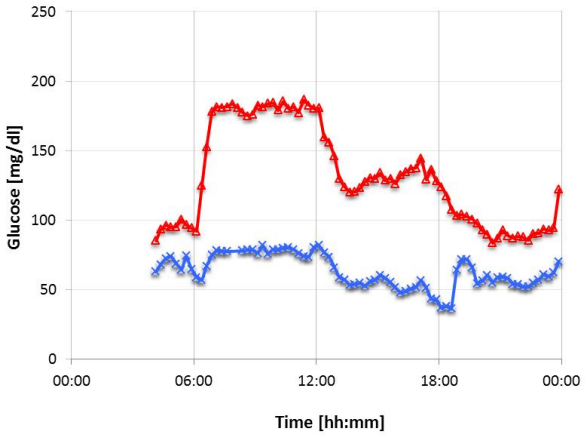

Figure 83A: Uncalibrated, filtered, shifted but not IRT corrected sensor current of subject 023.

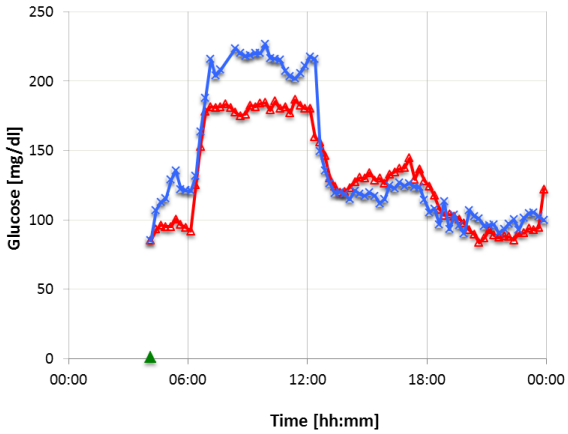

B: 1-point-calibrated, filtered, shifted and IRT corrected sensor current of subject 023.

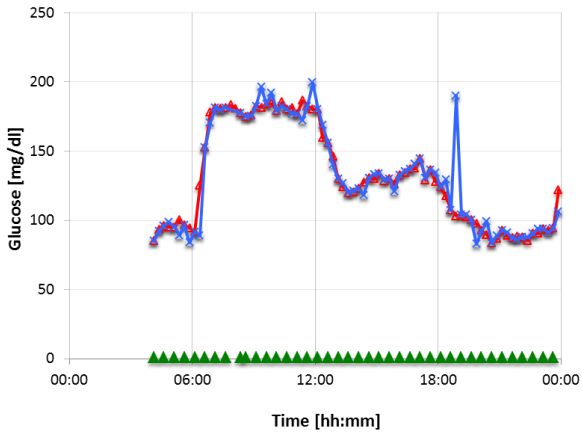

C: Filtered, shifted but not IRT corrected sensor current of subject 023 calibrated every 30 minutes.

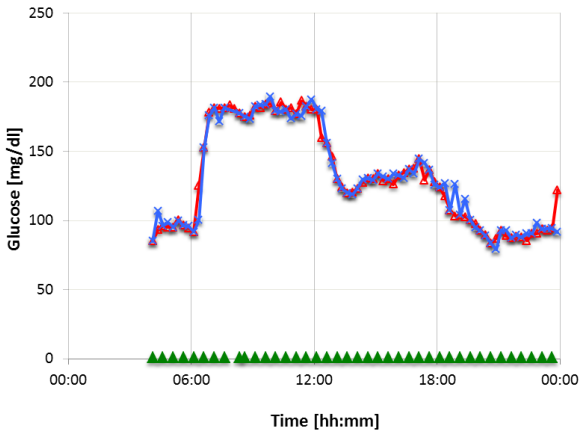

D: Filtered, shifted and IRT corrected sensor current of subject 023 calibrated every 30 minutes.

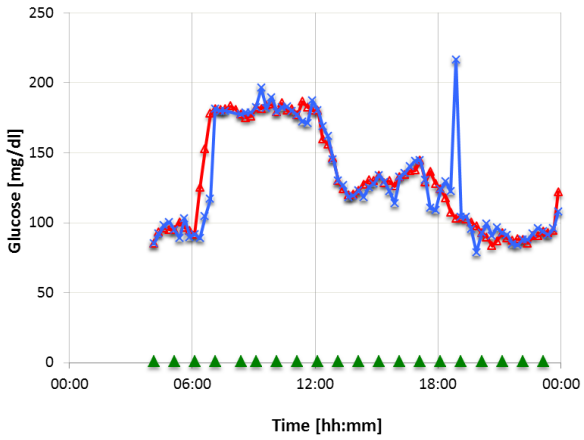

E: Filtered, shifted but not IRT corrected sensor current of subject 023 calibrated every hour.

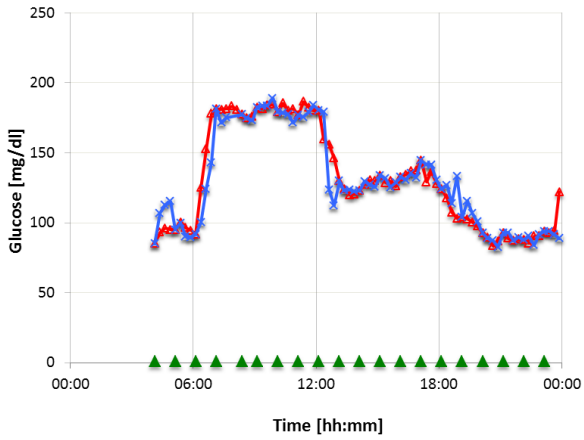

F: Filtered, shifted and IRT corrected sensor current of subject 023 calibrated every hour.

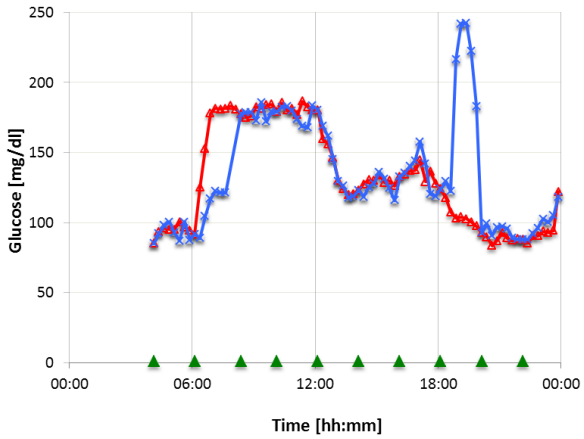

G: Filtered, shifted but not IRT corrected sensor current of subject 023 calibrated every 2 hours.

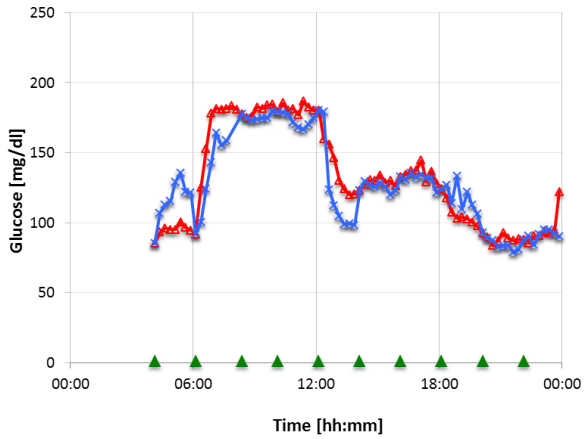

H: Filtered, shifted and IRT corrected sensor current of subject 023 calibrated every 2 hours.

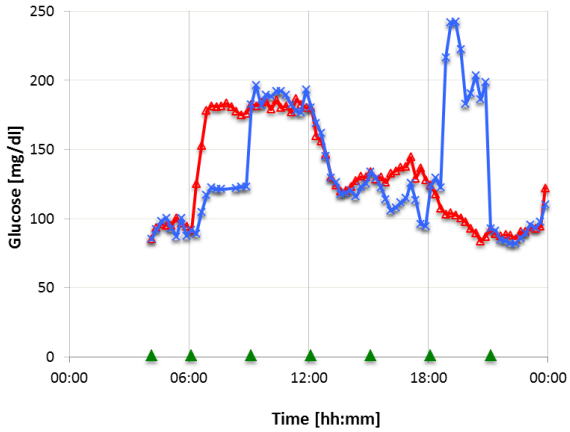

I: Filtered, shifted but not IRT corrected sensor current of subject 023 calibrated every 3 hours.

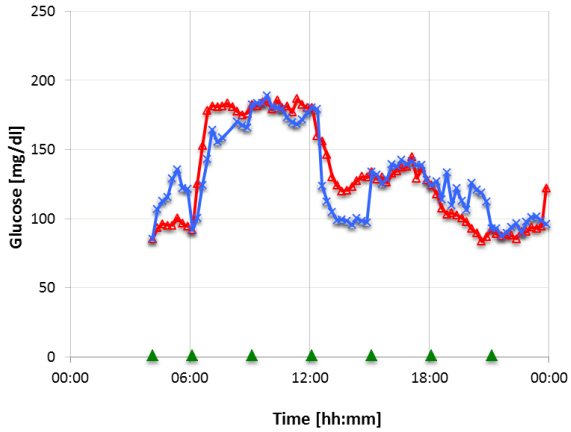

J: Filtered, shifted and IRT corrected sensor current of subject 023 calibrated every 3 hours.

Subject 024:

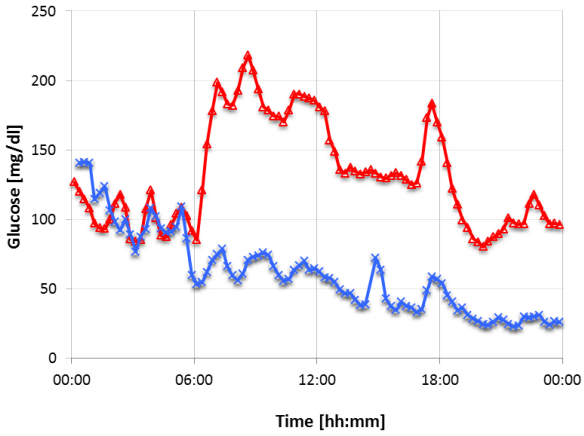

Figure 84A: Uncalibrated, filtered, shifted but not IRT corrected sensor current of subject 024.

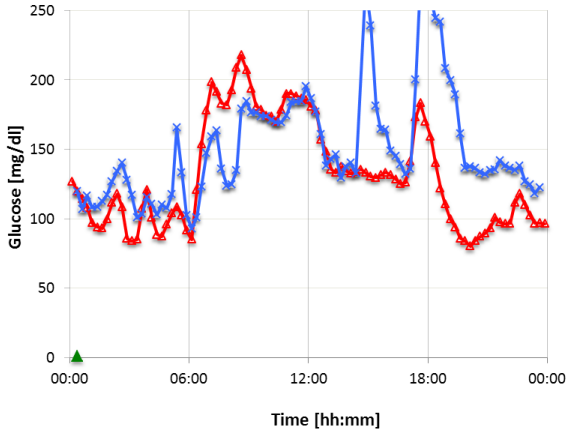

B: 1-point-calibrated, filtered, shifted and IRT corrected sensor current of subject 024.

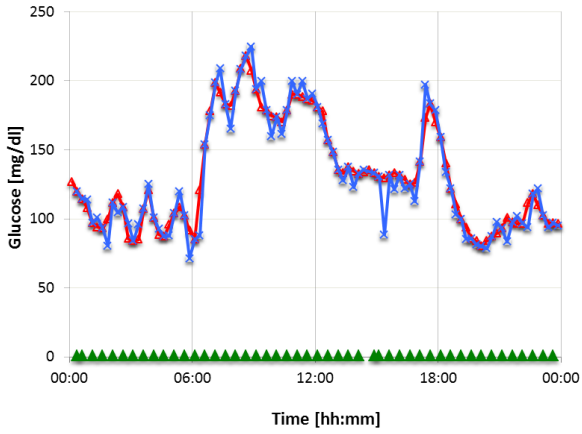

C: Filtered, shifted but not IRT corrected sensor current of subject 024 calibrated every 30 minutes.

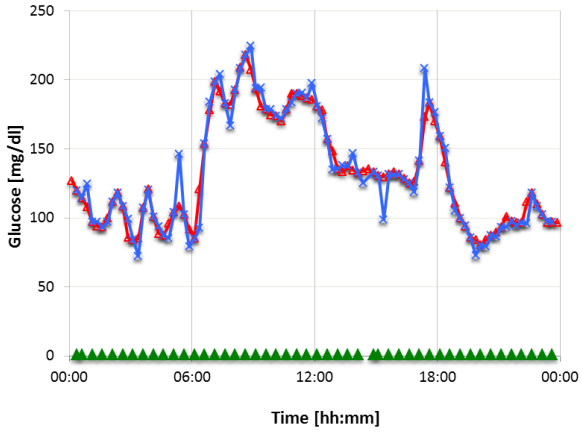

D: Filtered, shifted and IRT corrected sensor current of subject 024 calibrated every 30 minutes.

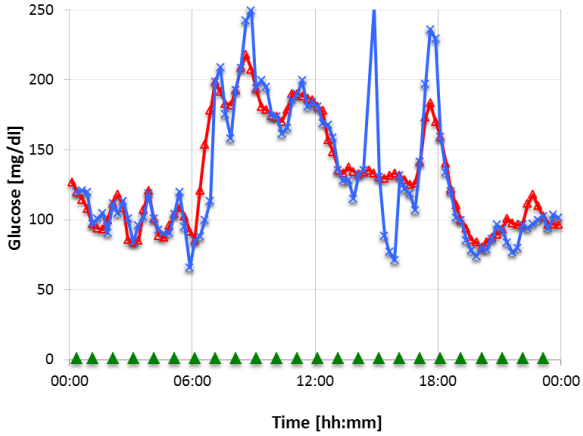

E: Filtered, shifted but not IRT corrected sensor current of subject 024 calibrated every hour.

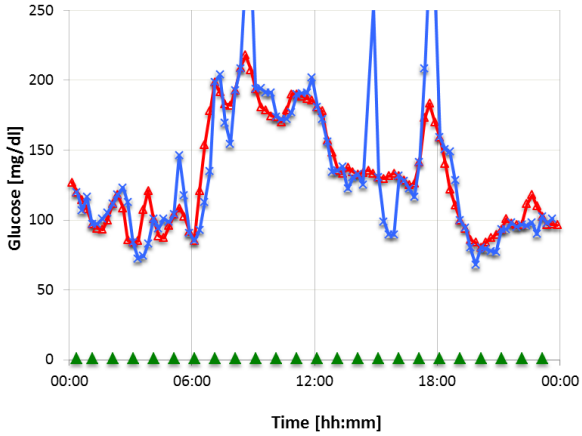

F: Filtered, shifted and IRT corrected sensor current of subject 024 calibrated every hour.

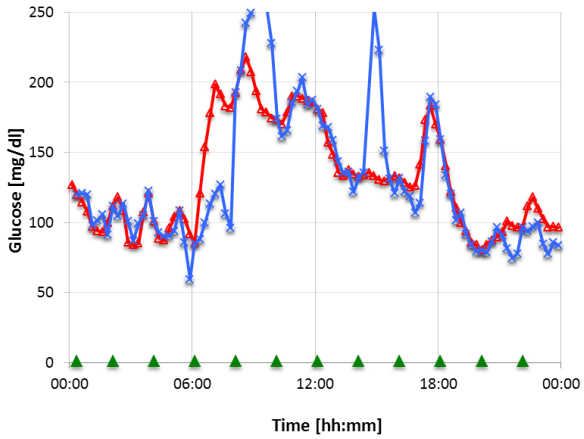

G: Filtered, shifted but not IRT corrected sensor current of subject 024 calibrated every 2 hours.

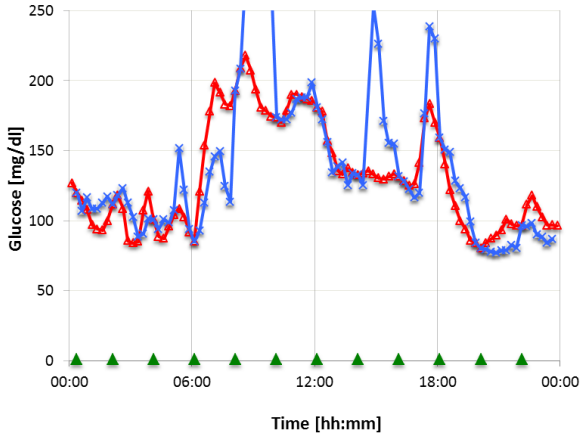

H: Filtered, shifted and IRT corrected sensor current of subject 024 calibrated every 2 hours.

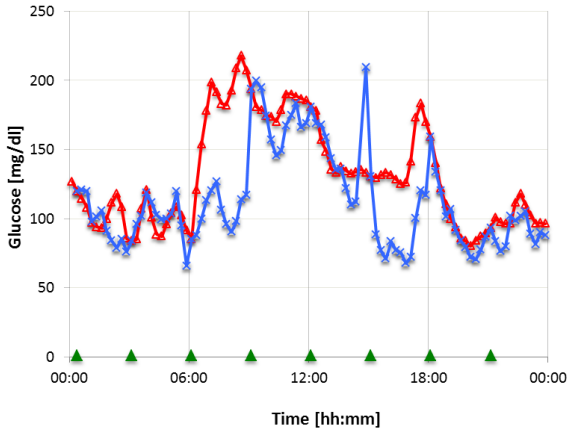

I: Filtered, shifted but not IRT corrected sensor current of subject 024 calibrated every 3 hours.

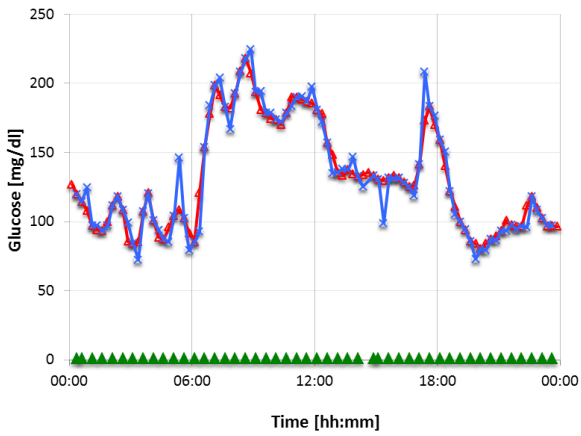

J: Filtered, shifted and IRT corrected sensor current of subject 024 calibrated every 3 hours.

Subject 025:

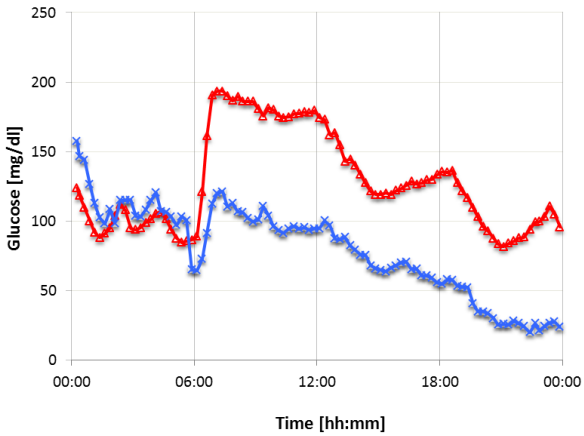

Figure 85A: Uncalibrated, filtered, shifted but not IRT corrected sensor current of subject 025

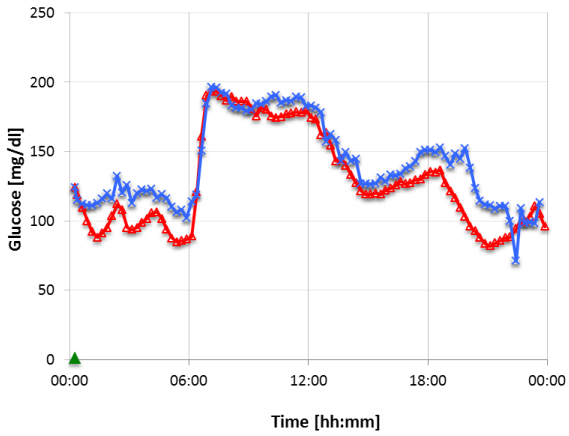

B: 1-point-calibrated, filtered, shifted and IRT corrected sensor current of subject 025

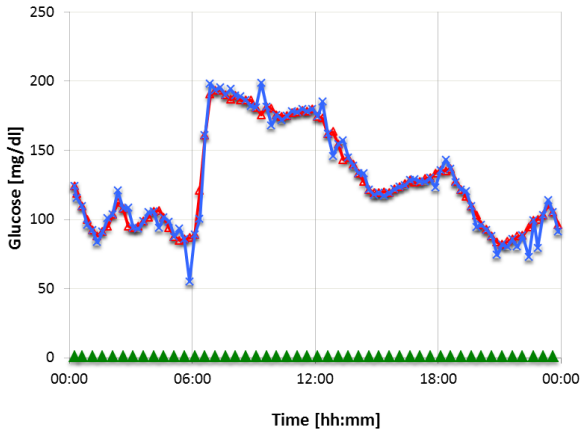

C: Filtered, shifted but not IRT corrected sensor current of subject 025 calibrated every 30 minutes.

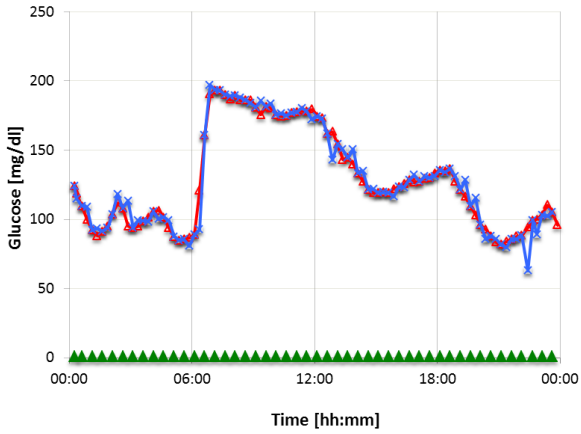

D: Filtered, shifted and IRT corrected sensor current of subject 025 calibrated every 30 minutes.

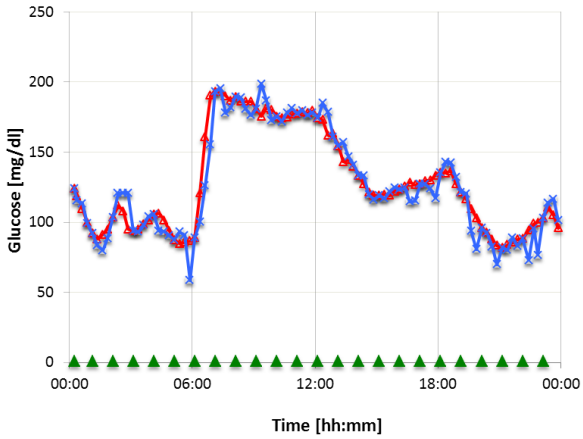

E: Filtered, shifted but not IRT corrected sensor current of subject 025 calibrated every hour.

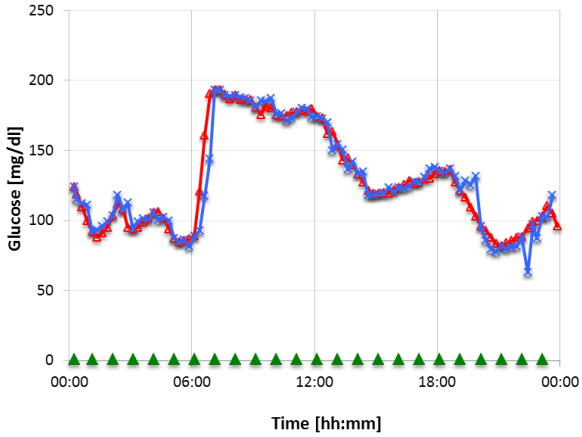

F: Filtered, shifted and IRT corrected sensor current of subject 025 calibrated every hour.

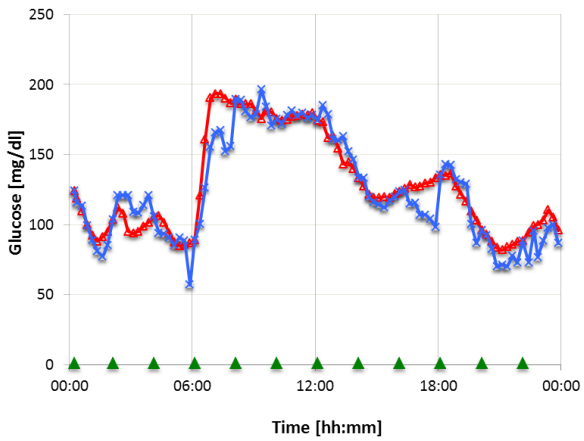

G: Filtered, shifted but not IRT corrected sensor current of subject 025 calibrated every 2 hours.

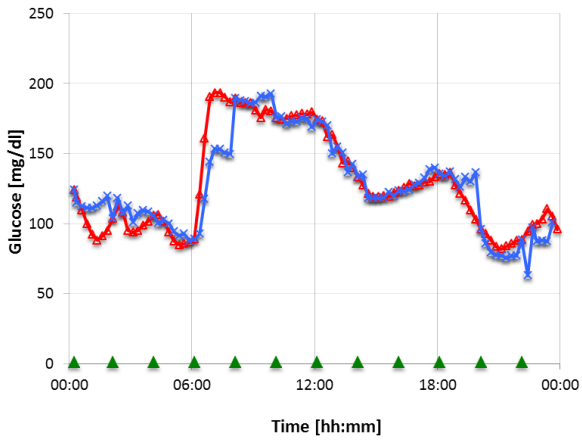

H: Filtered, shifted and IRT corrected sensor current of subject 025 calibrated every 2 hours.

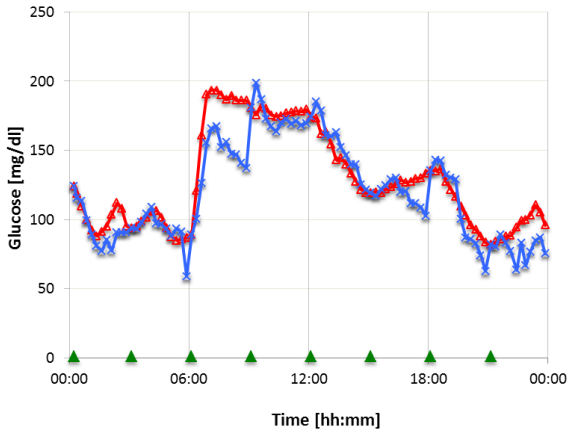

I: Filtered, shifted but not IRT corrected sensor current of subject 025 calibrated every 3 hours.

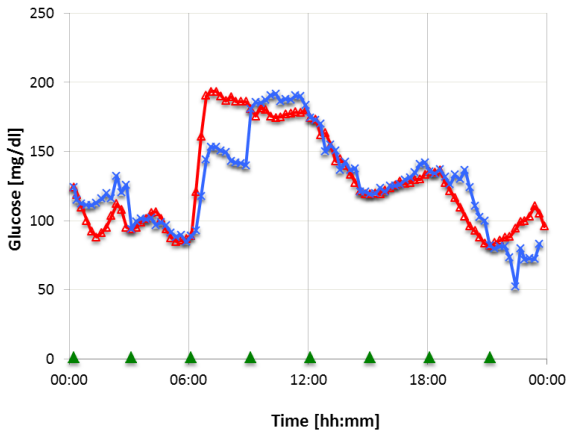

J: Filtered, shifted and IRT corrected sensor current of subject 025 calibrated every 3 hours.

Subject 026:

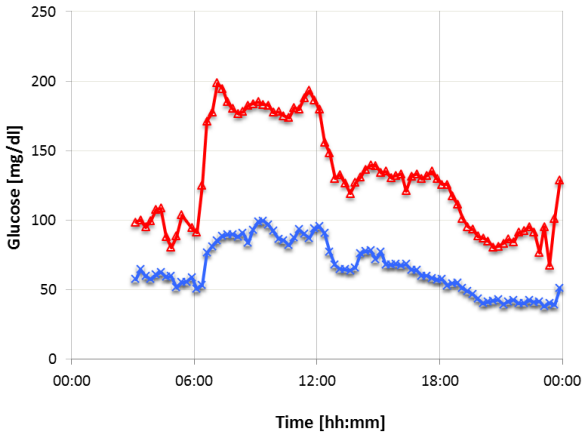

Figure 86A: Uncalibrated, not filtered, not shifted and not IRT corrected sensor current of subject 026.

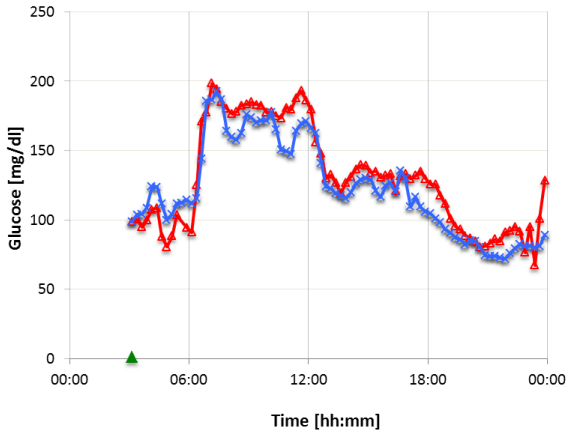

B: 1-point-calibrated, filtered, shifted and IRT corrected sensor current of subject 026.

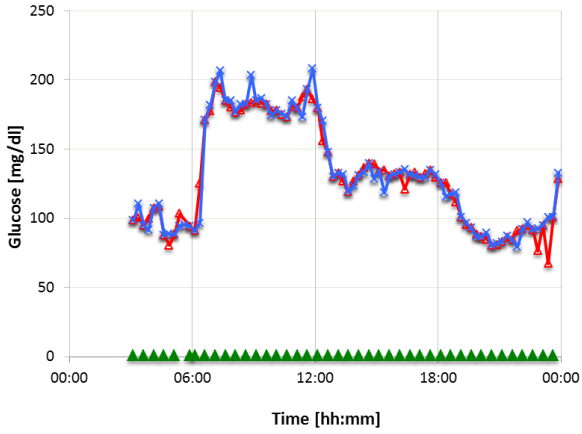

C: Filtered, shifted but not IRT corrected sensor current of subject 026 calibrated every 30 minutes.

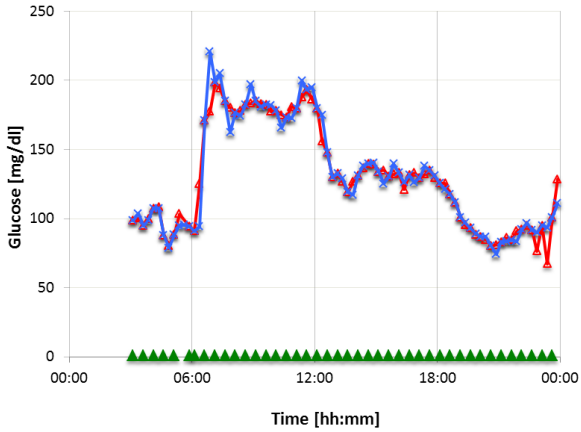

D: Filtered, shifted and IRT corrected sensor current of subject 026 calibrated every 30 minutes.

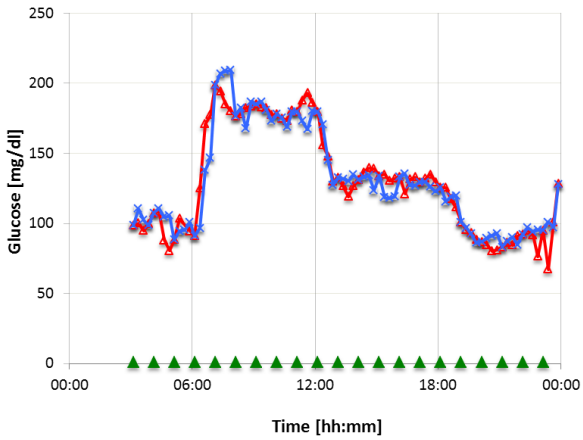

E: Filtered, shifted but not IRT corrected sensor current of subject 026 calibrated every hour.

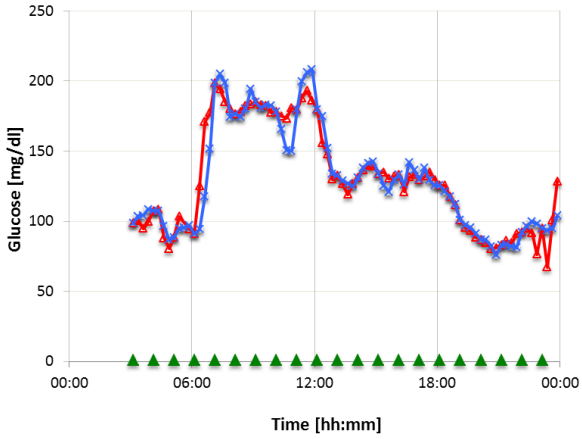

F: Filtered, shifted and IRT corrected sensor current of subject 026 calibrated every hour.

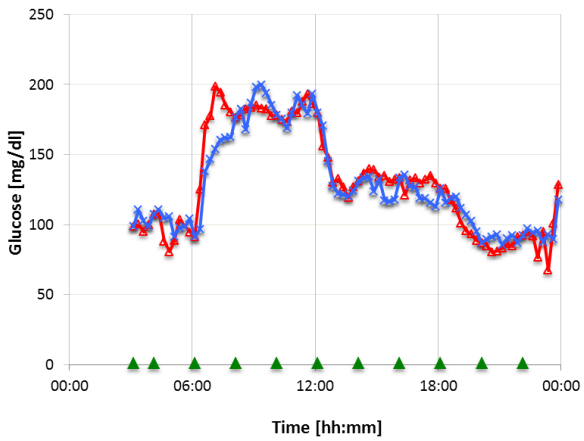

G: Filtered, shifted but not IRT corrected sensor current of subject 026 calibrated every 2 hours.

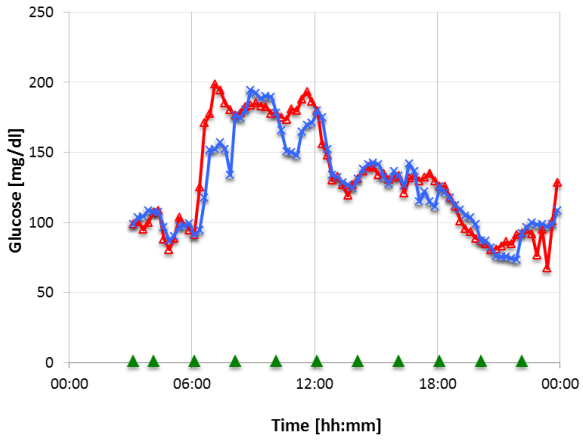

H: Filtered, shifted and IRT corrected sensor current of subject 026 calibrated every 2 hours.

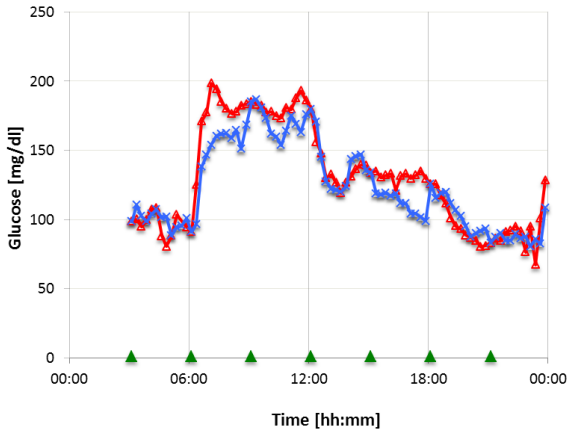

I: Filtered, shifted but not IRT corrected sensor current of subject 026 calibrated every3 hours.

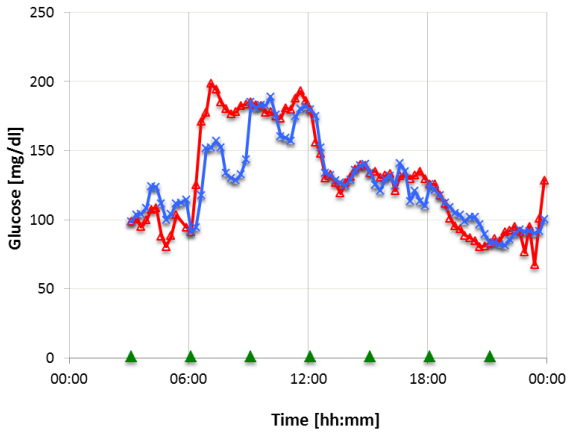

J: Filtered, shifted and IRT corrected sensor current of subject 026 calibrated every 3 hours.

Individual evaluation of statistical parameters for subject 021 - 026

	IONIC REFERENCE (LINEAR)				
	CALIBRATION INTERVAL [hh:mm]				
	1-point-calibrated	00:30	01:00	02:00	03:00
	CALIBRATION POINTS in 24h				
	1	47	24	12	8
System Error (Mean Value) [%]	-23.61	-0.06	0.00	-0.60	-4.51
Values with System Error between -5% and +5% [%]	11.83	83.87	64.52	47.31	38.71
Values with System Error between -10% and +10% [%]	23.66	92.47	83.87	80.65	65.59
%PRESS	28.27	5.82	9.31	11.68	13.91
MODIFIED %PRESS	27.28	5.00	8.33	9.98	11.51
MAD [%]	8.64	0.00	0.10	0.29	0.50
r^2	0.74	0.96	0.90	0.84	0.81
EGA, A & B [%]	100.0%	100.0%	100.0%	100.0%	100.0%
EGA, A [%]	38.7%	98.9%	96.8%	92.5%	90.3%
MARD [%]	23.99	2.63	5.30	7.03	8.68
M2ARD [%]	29.40	0.00	3.24	5.34	7.04

Figure 87: Statistical evaluation for subject 021.

	IONIC REFERENCE (LINEAR)				
	CALIBRATION INTERVAL [hh:mm]				
	1-point-calibrated	00:30	01:00	02:00	03:00
	CALIBRATION POINTS in 24h				
	1	47	24	12	8
System Error (Mean Value) [%]	7.01	0.41	-0.30	-1.17	1.62
Values with System Error between -5% and +5% [%]	15.38	82.05	70.51	47.44	41.03
Values with System Error between -10% and +10% [%]	44.87	92.31	84.62	67.95	58.97
%PRESS	16.14	5.19	8.16	11.29	13.27
MODIFIED %PRESS	15.48	5.83	8.53	12.57	15.70
MAD [%]	1.16	0.00	0.05	0.27	0.58
r^2	0.86	0.96	0.90	0.82	0.74
EGA, A & B [%]	100.0%	100.0%	100.0%	100.0%	100.0%
EGA, A [%]	80.8%	97.4%	93.6%	87.2%	76.9%
MARD [%]	13.07	2.81	4.96	8.81	11.36
M2ARD [%]	10.79	0.00	2.25	5.22	7.59

Figure 88: Statistical evaluation for subject 023.

IONIC REFERENCE (LINEAR)					
	CALIBRATION INTERVAL [hh:mm]				
	1-point-calibrated	00:30	01:00	02:00	03:00
	CALIBRATION POINTS in 24h				
	1	47	24	12	8
System Error (Mean Value) [%]	81.44	0.30	2.64	8.86	1.36
Values with System Error between -5% and +5% [%]	4.26	73.40	46.81	32.98	22.34
Values with System Error between -10% and +10% [%]	4.26	87.23	64.89	43.62	42.55
%PRESS	81.36	8.08	20.74	27.61	29.97
MODIFIED %PRESS	95.03	9.07	20.37	28.72	34.39
MAD [%]	51.73	0.00	0.41	1.98	2.68
r^2	0.23	0.93	0.70	0.53	0.28
EGA, A & B [%]	72.3%	100.0%	98.9%	98.9%	98.9%
EGA, A [%]	5.3%	94.7%	78.7%	66.0%	59.6%
MARD [%]	81.50	4.18	11.87	19.05	23.29
M2ARD [%]	71.92	0.00	6.37	14.09	16.38

Figure 89: Statistical evaluation for subject 024.

IONIC REFERENCE (LINEAR)					
	CALIBRATION INTERVAL [hh:mm]				
	1-point-calibrated	00:30	01:00	02:00	03:00
	CALIBRATION POINTS in 24h				
	1	47	24	12	8
System Error (Mean Value) [%]	11.58	-0.19	-0.37	-0.16	-0.21
Values with System Error between -5% and +5% [%]	26.32	78.95	68.42	52.63	45.26
Values with System Error between -10% and +10% [%]	50.53	92.63	88.42	73.68	64.21
%PRESS	12.82	4.83	7.37	10.83	14.40
MODIFIED %PRESS	17.07	5.85	7.84	11.26	14.86
MAD [%]	0.99	0.00	0.04	0.23	0.32
r^2	0.89	0.97	0.92	0.83	0.71
EGA, A & B [%]	100.0%	100.0%	100.0%	100.0%	100.0%
EGA, A [%]	73.7%	97.9%	94.7%	86.3%	76.8%
MARD [%]	13.12	2.71	4.31	7.45	10.46
M2ARD [%]	9.93	0.00	1.92	4.81	5.64

Figure 90: Statistical evaluation for subject 025.

IONIC REFERENCE (LINEAR)					
	CALIBRATION INTERVAL [hh:mm]				
	1-point-calibrated	00:30	01:00	02:00	03:00
	CALIBRATION POINTS in 24h				
	1	47	24	12	8
System Error (Mean Value) [%]	-5.22	0.39	0.37	-1.58	-1.08
Values with System Error between -5% and +5% [%]	24.10	78.31	65.06	49.40	39.76
Values with System Error between -10% and +10% [%]	55.42	92.77	86.75	71.08	60.24
%PRESS	11.12	6.26	8.38	11.64	13.81
MODIFIED %PRESS	12.26	7.04	8.90	11.38	13.32
MAD [%]	0.80	0.00	0.08	0.29	0.54
r^2	0.88	0.95	0.91	0.83	0.77
EGA, A & B [%]	98.8%	97.6%	97.6%	97.6%	97.6%
EGA, A [%]	91.7%	95.2%	94.0%	91.7%	81.0%
MARD [%]	10.26	3.20	5.19	7.80	9.78
M2ARD [%]	8.97	0.00	2.77	5.34	7.37

Figure 91: Statistical evaluation for subject 026.

Ultrasonic scans

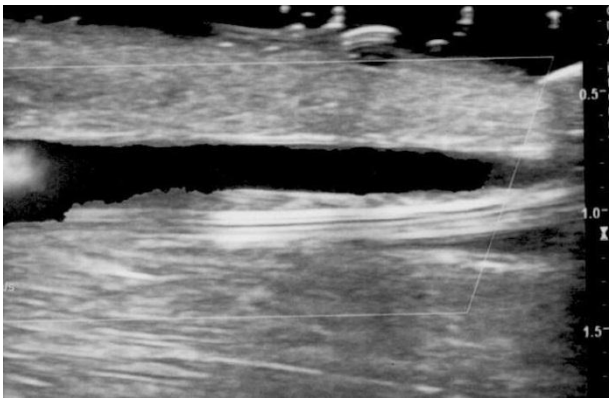

Figure 92A: Ultrasonic scan of Subject 021 showing an increasing thrombus formation from proximal to distal.

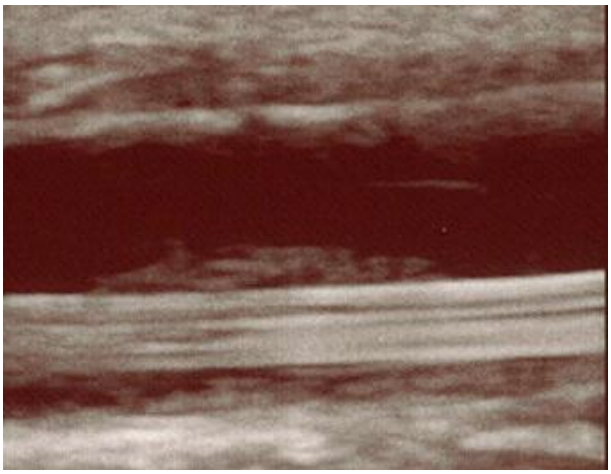

B: Ultrasonic scan of Subject 026 showing a small thrombus on the shaft.

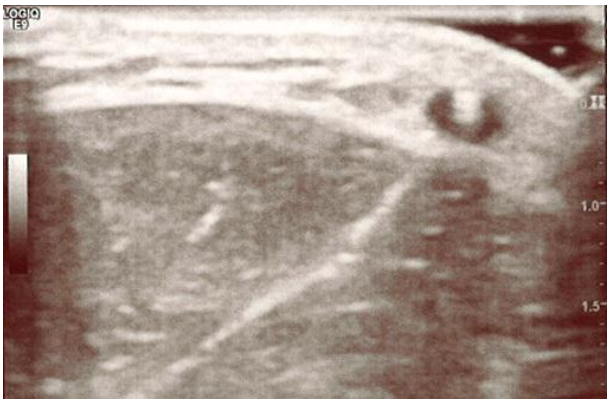

C: Ultrasonic scan of Subject 024 showing no thrombus formation.

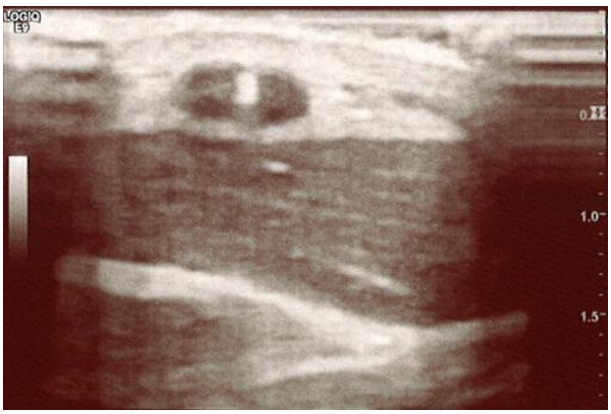

D: Ultrasonic scan of Subject 025 showing no thrombus formation.

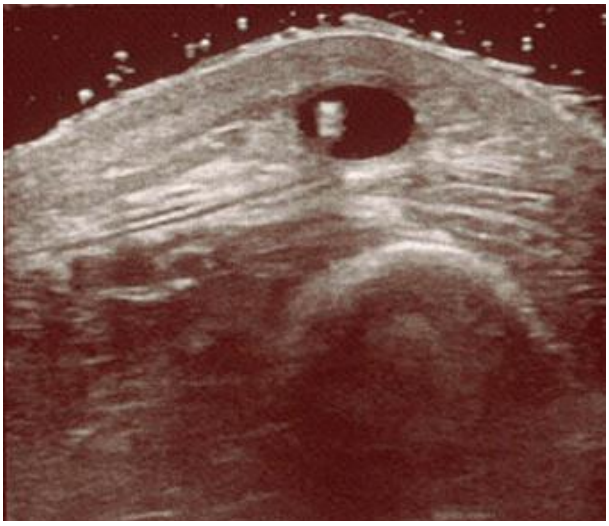

E: Ultrasonic scan of Subject 026showing no thrombus formation.

Pictures of the explanted microdialysis catheters

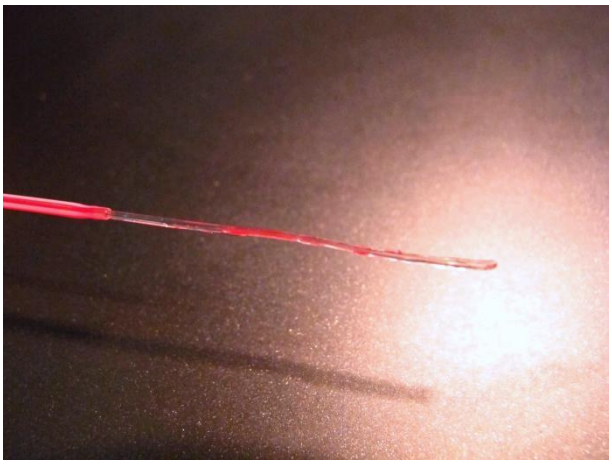

Figure 93A: MD catheter explanted from subject 021.

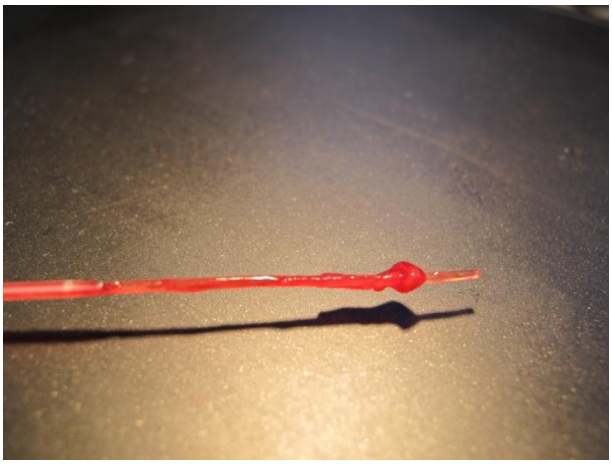

B: MD catheter explanted from subject 023.

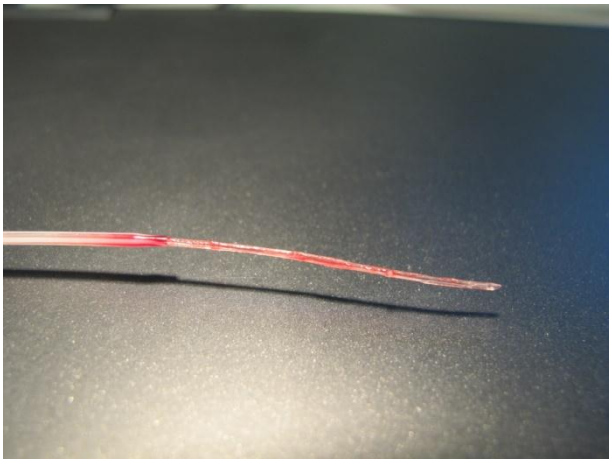

C: MD catheter explanted from subject 024.

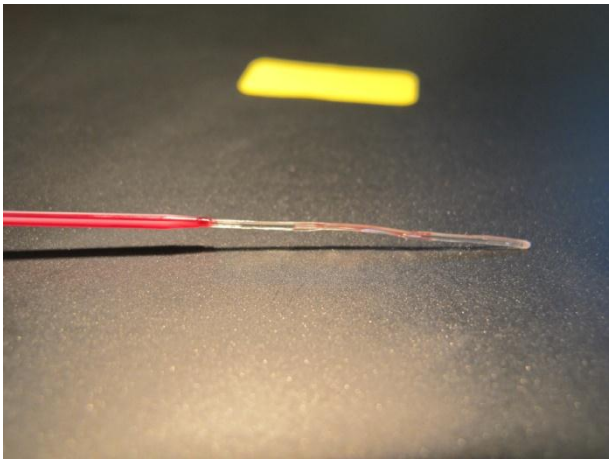

D: MD catheter explanted from subject 025.

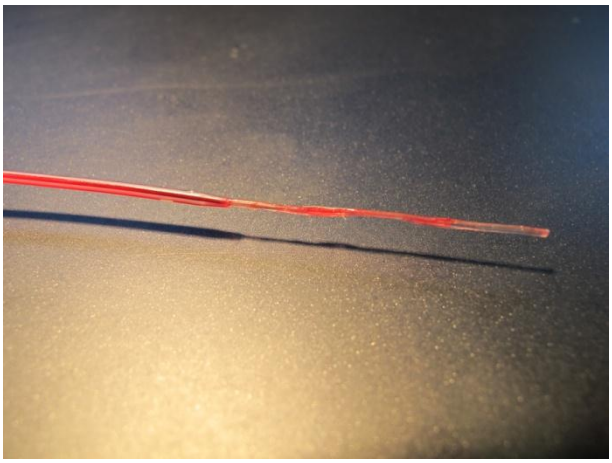

E: MD catheter explanted from subject 026.

ACKNOWLEDGEMENTS

Writing this thesis would not have been possible without the tireless commitment and support of the following people I would like to thank by name:

Dipl.-Ing. Dr.techn. Lukas Schaupp for supervising my work and introducing me into the field of microdialysis;

Dipl.-Ing. Dr.techn. Roland Schaller-Ammann for supervising my work, providing me his manifold input and supporting me throughout my stay at the Medical University of Graz;

Dipl.-Ing. Dr. Martin Hajnsek for introducing me into the field of biosensors;

Dipl.-Ing. Andreas Huber for providing me with his superior preliminary work and for being available for any further questions and explanations at any time;

Assoc.Prof. Mag.rer.nat. Dr.rer.nat. Juliane Gertrude Bogner-Strauß for evaluating my thesis;

and

Fraser Shearer, BSc for his input concerning correct and advanced scientific writing and phrasing.

Furthermore, I would like to thank the following people that made an incident-free, high-quality clinical trial possible and who provided me with advice and support whenever needed:

Andrea Berghofer, Barbara Binder, Martina Brunner, Sigrid Deller, Werner Doll, Martin Gaksch, Janka Gerdova, Madlen Hernach, Harald Kojzar, Stefan Korsatko, Matthias Ladurner, Thomas Limbacher, Thomas Pieber, Joachim Priedl, Sarah Raudner, Werner Regittnig, Mathias Tschaikner, and all student assistants who contributed to the study.

Moreover, I would like to thank all 5 volunteers for participating at the clinical trial.

And last but not least, I would like to thank my family, especially my parents *Dipl.-Ing. Gerhard Greiner, Dipl.-Ing. Heidrun Greiner-Bogensberger* and my sister *Petra Greiner,* for their imperturbable support and faith, as well as all my friends backing me up any time I was struggling with problems or achieving progress.

The EU-CLAMP Project receives funding from the European Union´s Seventh Framework Programme (FP7-SME-2010-1) doing research for the benefit of small and medium enterprises (SMEs) under grant agreement no. [262007] (www.eu-clamp.eu).

REFERENCES

[1] C. Zalpour, Anatomie Physiologie für die Physiotherapie, 2nd ed., URBAN & FISCHER, 2006.

[2] M. Berger, Diabetes Mellitus, Urban & Schwarzenberg, 1995.

[3] D. R. Whiting, L. Guariguata, C. Weil and J. Shaw, “IDF Diabetes Atlas: Global estimates of the prevalence of diabetes for 2011 and 2030,” *Diabetes Research and Clinical Practice,* pp. 311-321, 2011.

[4] World Health Organisation, September 2012. [Online]. Available: http://www.who.int/mediacentre/factsheets/fs312/en/index.html. [Accessed 17th December, 2012].

[5] D. B. Keenan, J. J. Mastrototaro, G. Voskanyan and G. M. Steil, “Delays in Minimally Invasive Continuous Glucose Monitoring Devices: A Review of Current Technology,” *Journal of Diabetes Science and Technology,* vol. 5, pp. 1207-1214, September 2009.

[6] F. G. Banting, C. H. Best, J. B. Collip, W. R. Campbell and A. A. Fletcher, “Pancreatic extracts in the treatment of diabetes mellitus: preliminary report,” *Canadian Medical Association Journal,* vol. 12, no. 3, pp. 141-146, March 1922.

[7] M. Hompesch and K. Rave, “An Analysis of How to Measure Glucose during Glucose Clamps: Are Glucose Meters Ready for Research?,” *Journal of Diabetes Science and Technology,* vol. 2, pp. 896-898, September 2008.

[8] The European Agency for the Evaluation of Medicial Products, „Note for Guidance on Clinical Investigation of Medicinal Products in the Treatment of Diabetes Mellitus. CPMP/EWP/1080/00,“ *Evaluation of Medicines for Human Use,* 2nd May, 2002.

[9] R. A. DeFronzo, J. D. Tobin und R. Andres, „Glucose clamp technique: a method for quantifying insulin secretion and resistance,“ *American Journal of Physiology - Endocrinology and Metabolism,* September 1979.

[10] L. von Wartburg, “What's a Glucose Clamp, Anyway?,” Diabetes Health, 7th November 2007. [Online]. Available: http://www.diabeteshealth.com/read/2007/11/06/5500/whats-a-glucose-clamp-anyway. [Accessed 7th January, 2013].

[11] A. Huber, “Continuous Blood Glucose Monitoring in Humans combining Intravenous Micodialysis and Ionic Reference Technique,” *Graz University of Technology, Institute of Medical Engineering,* 2012.

[12] C. Weller, M. Linder, A. Macaulay, G. Kessler and A. Ferrari, “Continuous in vivo determination of blood glucose in human subjects,” vol. 87, pp. 658-668, July 1960.

[13] E. J. Fogt, L. M. Dodd, E. M. Jenning and A. H. Clemens, “Development and Evaluation of a Glucose Analyzer for a Glucose-Controlled Insulin Infusion System (Biostator),” *Clinical Chemistry,* vol. 24, no. 8, pp. 1366-1372, 1978.

[14] Probe & go Labordiagnostika GmbH, [Online]. Available: http://www.probe-go.de/produkte/glucostator/mappe. [Accessed January, 17th 2013].

[15] E. Kulcu, J. A. Tamada, G. Reach, R. O. Potts and M. J. Lesho, “Physiological Differences Between Interstitial Glucose and Blood Glucose Measured in Human Subjects,” *Diabetes Care,* vol. 8, pp. 2405-2409, August 2003.

[16] O. Rooyackers, C. Blixt, P. Mattsson and J. Wernermann, “Continuous glucose monitoring by intravenous microdialysis,” *Acta Anaesthesiologica Scandinavica,* August 2010.

[17] J. M. Delgado, F. V. DeFeudis, R. H. Roth, D. K. Ryugo and B. M. Mitruka , "Dialytrode for long term intracerebral perfusion in awake monkeys," *Archives internationales de pharmacodynamie thérapie,* 1972.

[18] U. Ungerstedt, "Functional correlates of dopamine neurotransmission," *Bulletin der Schweizerischen Akademie der Medizinischen Wissenschaften,* July 1974.

[19] C. Hage, L. Mellbin, L. Rydén and J. Wernermann, "Glucose Monitoring by Means of an Intravenous Microdialysis Catheter Technique," *Diabetes Technology & Therapeutics,* April 2010.

[20] J. Kehr, "A survey on quantitative microdialysis: theoretical models and practical implementations," *Journal of Neuroscience Methods,* vol. 48, 1993.

[21] L. Schaupp and T. Pieber, "Method for measuring the concentration of substances in living organisms using microdialysis and a device for carrying out said method". United States Patent US 7,022,071 B2, 4th April 2006.

[22] S. J. Updike and G. P. Hicks, "The Enzyme Electrode," *Nature,* pp. 986-988, June 1967.

[23] P.-C. Nien, T.-S. Tung and K.-C. Ho, "Amperometric Glucose Biosensor Based on Entrapment of Glucose Oxidase in a Poly(3,4-ethylenedioxythiophene) Film," *Electroanalysis,* vol. 18, no. 13-14, pp. 1408-1415, 2006.

[24] G. McGarraugh, "The Chemistry of Commercial Continuous Glucose Monitors," *Diabetes Technology & Therapeutics,* vol. 11, pp. 17-24, 2009.

[25] BVT Technologies, s.a., [Online]. Available: http://www.bvt.cz/. [Accessed 29th October, 2012].

[26] Innovative Sensor Technologies GmbH, "I.S.T.," [Online]. Available: http://www.istech.at/. [Accessed 3rd October, 2012].

[27] Dr. Müller Gerätebau GmbH, [Online]. Available: htpp://www.dr-mueller-geraetebau.de/. [Zugriff am 4th October, 2012].

[28] I. M. E. Wenthold, A. A. Hart, J. B. Hoekstra and J. H. Devries, "How to Asses and Compare the Accuracy of Continuous Glucose Monitors?," *Diabetes Technologies & Therapeutics,* vol. 10, pp. 57-68, 2nd Novemer, 2008.

[29] W. L. Clarke, D. Cox, L. A. Gonder-Frederick, W. Carter and S. L. Pohl, "Evaluating Clinical Accuracy of Systems for Self-Monitoring of Blood Glucose," *Diabetes Care,* vol. 10, no. 5, September - October 1987.

[30] Normenausschuss Medizin, *EN ISO 15197:2003,* 2004.

[31] International Organization for Standardization, "ISO 14971 Second Edition; Medical devices - Apllication of risk management to medical devices," 2007. [Online]. Available: http://www.isoert.ru/isoert_iso_14971.pdf. [Accessed 19th November, 2012].

[32] Österreichischer Verband für Elektrotechnik und Österreichisches Normungsinstitut, "ÖVE/ÖNORM EN61025:2006; Fehlzustandsbaumanalyse," 1st September, 2007.

[33] Österreichischer Verband für Elektrotechnik, "ÖVE/ÖNORM EN3100:2009; Risikomanagement - Verfahren zur Risikobeurteilung," 1st December, 2010.

[34] International Electrotechnical Comission, "IEC 60601-1," Genève, Switzerland, 2002.

[35] European Medicines Agency, "ICH Topic E 6 (R1) Guideline for Good Clinical Practice," July 2002. [Online]. Available: www.emea.europa.eu/docs/en_GB/document_library/Scientific_guideline/2009/09/WC500002874.pdf. [Accessed 13th November, 2012].

[36] World Medical Association, "WMA Declaration of Helsinki - Ethical Principles for

Medical Research Involving Human Subjects," October 2008. [Online]. Available: www.wma.net/en/30publications/10policies/b3/. [Accessed 13th November, 2012].

[37] European Committee for Standardization, "Council Directive 93/42/EEC concerning medical devices," 14th June 1993. [Online]. Available: http://www.cen.eu/cen/Sectors/Sectors/Healthcare/Pages/default.aspx. [Accessed 13th February, 2013].

[38] N. Leitgeb, Sicherheit von Medizingeräten: Recht - Risiko - Chancen, Vienna: Springer, 2010.

[39] Palm Instruments BV, „Manual: PSTrace for EmStat USB potentiostat," 2011.